

Aus der Universitätsklinik für Hals-, Nasen- und Ohrenheilkunde  
mit Poliklinik Tübingen

**Stress Hormone-Induced Changes of Auditory Function  
in the Rat**

**Inaugural-Dissertation  
zur Erlangung des Doktorgrades  
der Medizin**

**der Medizinischen Fakultät  
der Eberhard Karls Universität  
zu Tübingen**

**vorgelegt von**

**Armbruster, Philipp Carlos**

**2020**



Dekan: Professor Dr. B. Pichler

1. Berichterstatter: Professorin Dr. M. Knipper-Breer  
2. Berichterstatter: Professor Dr. B. Hirt

Tag der Disputation: 10.12.2020

Meiner Familie

# Table of contents

<b>1</b>	<b>Introduction</b>	<b>9</b>
1.1	<i>Background - The auditory system</i>	10
1.2	<i>Organization of the auditory pathway</i>	13
1.3	<i>What is “stress”?</i>	15
1.4	<i>The HPA axis</i>	16
1.5	<i>The role of steroid receptors</i>	17
1.6	<i>The disrupted auditory system</i>	19
1.6.1	<i>Etiology of noise-induced hearing loss</i>	19
1.6.2	<i>Pathophysiology of acoustic over-stimulation</i>	21
1.7	<i>Aim of this work</i>	22
<b>2</b>	<b>Material and methods</b>	<b>23</b>
2.1	<i>Animals</i>	23
2.2	<i>Drug Treatments</i>	23
2.3	<i>Anesthesia</i>	25
2.4	<i>Acoustic trauma and sham treatment</i>	25
2.5	<i>Hearing measurements</i>	26
2.5.1	<i>Distortion product of otoacoustic emissions</i>	26
2.5.2	<i>Measuring auditory brainstem responses (ABRs)</i>	26
2.5.3	<i>Analysis of auditory brainstem responses (ABRs)</i>	27
2.6	<i>Preparation of animals</i>	29
2.7	<i>Immunohistochemistry and high resolution fluorescence microscopy</i>	29
2.8	<i>Cortisol analysis</i>	30
2.9	<i>Statistical analyses</i>	31
<b>3</b>	<b>Results</b>	<b>33</b>
3.1	<i>The effect of GR and MR activation and attenuation on normal hearing</i>	33
3.1.1	<i>The effect of GR- and MR-potent drugs on c/c ratios</i>	35
3.1.2	<i>GR- and MR-potent drugs display no effect on OHC function</i>	36
3.1.3	<i>GR- and MR-potent drugs display no effect on ABR thresholds</i>	39
3.1.4	<i>GR- and MR-potent drugs display no significant effect on supra-threshold responses to a 16 kHz stimulus</i>	42
3.1.5	<i>GR- and MR-potent drugs display no significant effect on supra-threshold responses to a 32 kHz stimulus</i>	46
3.1.6	<i>GR and MR-potent drugs display no significant effect on the first synapse of the auditory pathway</i>	49
3.1.7	<i>Conclusion</i>	50
3.2	<i>The effect of different corticosterone levels on normal hearing</i>	50
3.2.1	<i>The effect of a continuous treatment with corticosterone on c/c ratio</i>	52
3.2.2	<i>A continuous treatment of corticosterone on OHC function displays no effect on OHC function</i>	53
3.2.3	<i>A continuous treatment with corticosterone displays no effect on ABR thresholds</i>	54

3.2.4	A continuous treatment with corticosterone displays no significant effect on supra-threshold responses to a 32 kHz stimulus	56
3.2.5	A continuous treatment with corticosterone displays no significant effect on the first synapse of the auditory pathway	59
3.2.6	Conclusion	59
3.3	<i>The role of the GR and the MR during excessive noise exposure and subsequent hearing recovery</i>	60
3.3.1	GR blockage with mifepristone (GR antagonist) maintains DPOAE thresholds best after AT	60
3.3.2	GR blockage with mifepristone (GR antagonist) maintains ABR thresholds best 14 days after AT	64
3.3.3	GR blockage with mifepristone (GR antagonist) maintains supra-threshold responses of a 16 kHz stimulus best after AT	69
3.3.4	Mifepristone (GR antagonist) and corticosterone (GR/MR agonist) preserve the first synapse of the auditory pathway best after AT	76
<b>4</b>	<b>Discussion</b>	<b>78</b>
4.1	<i>The role of corticosterone (GR/ MR agonist) on hearing function</i>	79
4.2	<i>The role of spironolactone (MR antagonist) on hearing function</i>	81
4.3	<i>The role of mifepristone (GR antagonist) on hearing function</i>	82
4.4	<i>Summarizing the role of stress on hearing</i>	83
4.5	<i>Perspectives</i>	85
<b>5</b>	<b>Synopsis</b>	<b>86</b>
	<b>Appendix</b>	<b>88</b>
	<b>References</b>	<b>97</b>
	<b>Publication list</b>	<b>107</b>
	<b>Erklärung zum Eigenanteil</b>	<b>107</b>
	<b>Danksagung</b>	<b>108</b>

## List of abbreviations

ABR	AUDITORY BRAINSTEM RESPONSE
AC	AUDITORY CORTEX
ACTH	ADRENOCORTICOTROPIC HORMONE
AN	AUDITORY NERVE
ANF	AUDITORY NERVE FIBER
BLA	BASOLATERAL AMYGDALA
CN	COCHLEAR NUCLEUS
CRH	CORTICOTROPIN-RELEASING HORMONE
DCN	DORSAL PART OF THE COCHLEAR NUCLEUS
DPOAEs	DISTORTION PRODUCT OTOACOUSTIC EMISSIONS
GC	GLUCOCORTICOID
GR	GLUCOCORTICOID RECEPTOR
HPA AXIS	HYPOTHALAMUS-PITUITARY-ADRENAL AXIS
IC	INFERIOR COLLICULUS
IHC	INNER HAIR CELL
LSO	LATERAL SUPERIOR OLIVE
MGB	MEDIAL GENICULATE BODY
MNTB	MEDIAL NUCLEUS OF THE TRAPEZOID BODY
MR	MINERALOCORTICOID RECEPTOR
MSO	MEDIAL SUPERIOR OLIVE
NIHHL	NOISE-INDUCED HIDDEN HEARING LOSS
NIHL	NOISE-INDUCED HEARING LOSS
NKAA3	NA <sup>+</sup> /K <sup>+</sup> -ATPASE SUBUNIT A3
OHC	OUTER HAIR CELL
PTS	PERMANENT THRESHOLD SHIFTS
PVN	PARAVENTRICULAR NUCLEUS OF THE HYPOTHALAMUS
ROS	REACTIVE OXYGEN SPECIES
SAM	SYMPATHOADRENAL MEDULLARY SYSTEM
SOC	SUPERIOR OLIVARY COMPLEX
SPL	SOUND PRESSURE LEVEL
SR	SPONTANEOUS ACTION POTENTIAL DISCHARGE RATE
TTS	TEMPORARY THRESHOLD SHIFTS
VCN	VENTRAL PART OF THE COCHLEAR NUCLEUS

## List of figures

FIGURE 1:	SCHEMATIC OF THE HUMAN EAR.	11
FIGURE 2:	PHASED ZOOM OF THE COCHLEA AND THE ORGAN OF CORTI.	13
FIGURE 3:	SCHEMATIC DEPICTION OF THE ASCENDING AUDITORY PATHWAY.	15
FIGURE 4:	THE SIMPLIFIED HPA AXIS.	18
FIGURE 5:	ABR WAVE PEAKS.	29
FIGURE 6:	IMMUNOSTAINING.	31
FIGURE 7:	EXPERIMENTAL DESIGN OF A SINGLE APPLICATION OF GR- AND MR- POTENT SUBSTANCES FOLLOWED BY SHAM TREATMENT OR EXCESSIVE NOISE EXPOSURE.	35
FIGURE 8:	CORTICOSTERONE/CREATININE RATIO (C/C RATIO) OF URINE SAMPLES.	36
FIGURE 9:	SINGLE APPLICATION OF CORTICOSTERONE, MIFEPRISTONE (MR ANTAGONIST) AND SPIRONOLACTONE (GR ANTAGONIST) EXHIBITS NO CONCLUSIVE INFLUENCE ON OUTER HAIR CELL FUNCTION.	39
FIGURE 10:	SINGLE DRUG APPLICATION EXHIBITS NO INFLUENCE ON HEARING THRESHOLDS.	41
FIGURE 11:	SINGLE DRUG APPLICATION DOES NOT INFLUENCE ABR THRESHOLDS OF 11.3 KHZ, 16 KHZ AND 32 KHZ.	42
FIGURE 12:	SINGLE TREATMENT WITH CORTICOSTERONE, MIFEPRISTONE AND SPIRONOLACTONE EXHIBITS NO STRIKING DIVERGING EFFECT ON EARLY (WAVE I) AND LATE (WAVE IV) SUPRA-THRESHOLD ABR WAVE RESPONSES TO FREQUENCY-SPECIFIC TONE BURST STIMULI AT 16 KHZ.	44
FIGURE 13:	REACH AND SIZE OF SUPRA-THRESHOLD ABR WAVES.	45
FIGURE 14:	TREATMENT WITH CORTICOSTERONE, MIFEPRISTONE OR SPIRONOLACTONE HAS NO IMPACT ON REACH AND RESPONSE SIZE OF ABR WAVES TO 16 KHZ SOUND STIMULI.	46
FIGURE 15:	SINGLE TREATMENT WITH CORTICOSTERONE, MIFEPRISTONE, AND SPIRONOLACTONE EXHIBITS NO STRIKING DIVERGING EFFECT ON EARLY (WAVE I) AND LATE (WAVE IV) SUPRA-THRESHOLD ABR WAVE RESPONSES TO FREQUENCY-SPECIFIC TONE BURST STIMULI AT 32 KHZ.	48
FIGURE 16:	TREATMENT WITH CORTICOSTERONE, MIFEPRISTONE OR SPIRONOLACTONE HAS NO IMPACT ON REACH AND RESPONSE SIZE OF ABRs TO 32 KHZ SOUND STIMULI.	49
FIGURE 17:	IHC RIBBON NUMBER IS NOT INFLUENCED BY SINGLE DRUG APPLICATION OF CORTICOSTERONE, MIFEPRISTONE OR SPIRONOLACTONE.	50
FIGURE 18:	EXPERIMENTAL DESIGN OF REPEATED CORTICOSTERONE APPLICATIONS TO MIMIC CHRONIC STRESS.	52
FIGURE 19:	CORTICOSTERONE/CREATININE RATIO (C/C RATIO) OF URINE SAMPLES.	53
FIGURE 20:	MULTIPLE INJECTIONS OF HIGH CORTICOSTERONE (30 MG/KG) OR LOW CORTICOSTERONE (3 MG/KG) EXHIBIT NO INFLUENCE ON OUTER HAIR CELL FUNCTION.	54



FIGURE 21:	A CONSECUTIVE APPLICATION OF CORTICOSTERONE EXHIBITS NO INFLUENCE ON HEARING THRESHOLDS.	56
FIGURE 22:	CONSECUTIVE APPLICATION OF CORTICOSTERONE DOES NOT INFLUENCE HEARING THRESHOLDS.	57
FIGURE 23:	MULTIPLE INJECTIONS OF DIFFERENT CONCENTRATIONS OF CORTICOSTERONE SHOW NO STRIKING EFFECT ON EARLY (WAVE I) AND LATE (WAVE IV) SUPRA-THRESHOLD ABR WAVE RESPONSES TO FREQUENCY-SPECIFIC TONE BURST STIMULI AT 32 KHZ.	58
FIGURE 24:	CONSECUTIVE TREATMENT WITH 3 MG AND 30 MG CORTICOSTERONE HAS NO IMPACT ON REACH AND RESPONSE SIZE OF ABRS TO 32 KHZ SOUND STIMULI.	59
FIGURE 25:	IHC RIBBON NUMBER IS NOT SIGNIFICANTLY IMPAIRED BY A FIVE-DAY DRUG APPLICATION WITH 3 MG/KG OR 30 MG/KG CORTICOSTERONE.	60
FIGURE 26:	PRE-TREATMENT WITH MIFEPRISTONE BUT NOT CORTICOSTERONE OR SPIRONOLACTONE PRESERVES OHC FUNCTION AFTER ACOUSTIC TRAUMA SIGNIFICANTLY.	64
FIGURE 27:	PRE-TREATMENT WITH MIFEPRISTONE PRESERVES ABR THRESHOLDS BEST AFTER ACOUSTIC TRAUMA.	67
FIGURE 28:	PRE-TREATMENT WITH MIFEPRISTONE MAINTAINS THRESHOLDS AFTER ACOUSTIC TRAUMA BEST.	68
FIGURE 29:	TREATMENT WITH MIFEPRISTONE BUT NOT SPIRONOLACTONE OR CORTICOSTERONE, MAINTAINS EARLY (WAVE I) AND LATE (WAVE IV) ABR AMPLITUDES TO A WIDER RANGE AT 16 KHZ.	71
FIGURE 30:	PRE-TREATMENT WITH MIFEPRISTONE AND CORTICOSTERONE, BUT NOT SPIRONOLACTONE, MAINTAINS THE REACH FOR CODING HIGH STIMULUS LEVELS AND RESPONSE SIZE OF ABRS TO 16 KHZ SOUND STIMULI AFTER AT.73	
FIGURE 31:	PRE-TREATMENT WITH MIFEPRISTONE, BUT NOT SPIRONOLACTONE OR CORTICOSTERONE, MAINTAINS EARLY (WAVE I) AND LATE (WAVE IV) ABR AMPLITUDES TO A WIDER RANGE AT 32 KHZ.	75
FIGURE 32:	PRE-TREATMENT WITH MIFEPRISTONE, BUT NOT CORTICOSTERONE OR SPIRONOLACTONE, MAINTAINS AMPLITUDE REACH AND RESPONSE SIZE OF ABRS TO 32 KHZ AFTER AT.	76
FIGURE 33:	MIFEPRISTONE AND CORTICOSTERONE, BUT NOT SPIRONOLACTONE OR VEHICLE PRE-TREATMENT PREVENTS, IN PART, IHC RIBBON LOSS IN HIGH-FREQUENCY COCHLEAR TURNS.	77

## List of tables

TABLE 1:	OVERVIEW OF PHARMACOLOGICAL GROUPS.	25
SUPP. TABLE 1:	STATISTICAL INFORMATION OF THE RESULTS	98
SUPP. TABLE 2:	CORTISOL AND CREATININE RAW DATA	102

# 1 Introduction

Approximately 70 million people suffer from severe hearing loss worldwide (Shield 2006). Rough estimates reckon this number is going to increase more than tenfold to 900 million by 2050 due to demographic and environmental changes (Vio and Holme 2005). Hearing loss leads to flawed speech understanding and thus decreases the capacity to engage in conversations or social activities. The loss of communication skills results in impaired social mobility and increased difficulty in establishing or maintaining emotional relationships. These factors together lead to social isolation and are mainly responsible for the increasing prevalence of depression in people with impaired hearing (Nelson, Nelson et al. 2005, Mathers, Fat et al. 2008, Mosges, Koberlein et al. 2008, Tikka, Verbeek et al. 2017). Ultimately, hearing loss leads to a decline in perceived life quality and, on a global scale, decreases productivity and raises expenses for medical treatment (Basner, Babisch et al. 2014). Taking these factors together, hearing impairment causes a total estimated loss of 284 billion EUR in Europe alone (Shield 2006).

The etiology of hearing loss is complex as a multitude of pathologies, congenital or acquired, can result in impaired hearing function. However, excessive noise has been isolated to play a key role in hearing impairment, shaping the term noise-induced hearing loss (NIHL). For decades, the mainstay of treatment for NIHL was the application of systemic corticosteroids, as glucocorticoids and stressors were described to be protective against damage associated with noise over-exposure (Sha and Schacht 2017). Conversely, stressors are also risk factors for hearing disorders (Singer, Kasini et al. 2018). How these contradictory effects are related remains elusive. In the present study we aimed to analyze the role of the Hypothalamus-pituitary-adrenal (HPA) axis – the key player in stress response mechanism – on auditory nerve processing and susceptibility to excessive noise in the rat animal model and further discuss related pathophysiology and treatment options.

This work is structured as follows. The anatomy of hearing, the pathophysiology of NIHL and the organization of the HPA axis will be outlined in chapter 1. The drugs and measurement methods used in this experiment will be declared in chapter 2. In chapter 3 the experimental results will be set forth which then will be evaluated and discussed in chapter 4 and finally fit into current literature.

## 1.1 Background - The auditory system

The auditory system is complex and needs to be elucidated to better understand noise-related pathologies.

The main task of the auditory organ is the conversion of acoustic to electric signals which can be processed by the central nervous system. Hearing, the perception of sound, grants mammals the ability to perceive, distinguish, and locate sound sources. The hearing organ is classified into four sections and consists of the outer ear, middle ear, inner ear, and the subsequent auditory pathway.

Briefly, the auricle operates as funnel, directing sound waves to the ear canal. The compression and rarefaction of these waves set the thin tympanic membrane and the subsequent ossicles in motion. The malleus, incus and stapes amplify the signal and transduce vibrations via the oval window to the inner ear (Fig. 1), which consists of two organs, the vestibular system (sense of balance) and the cochlea (sound detection and processing) (Fig. 2).

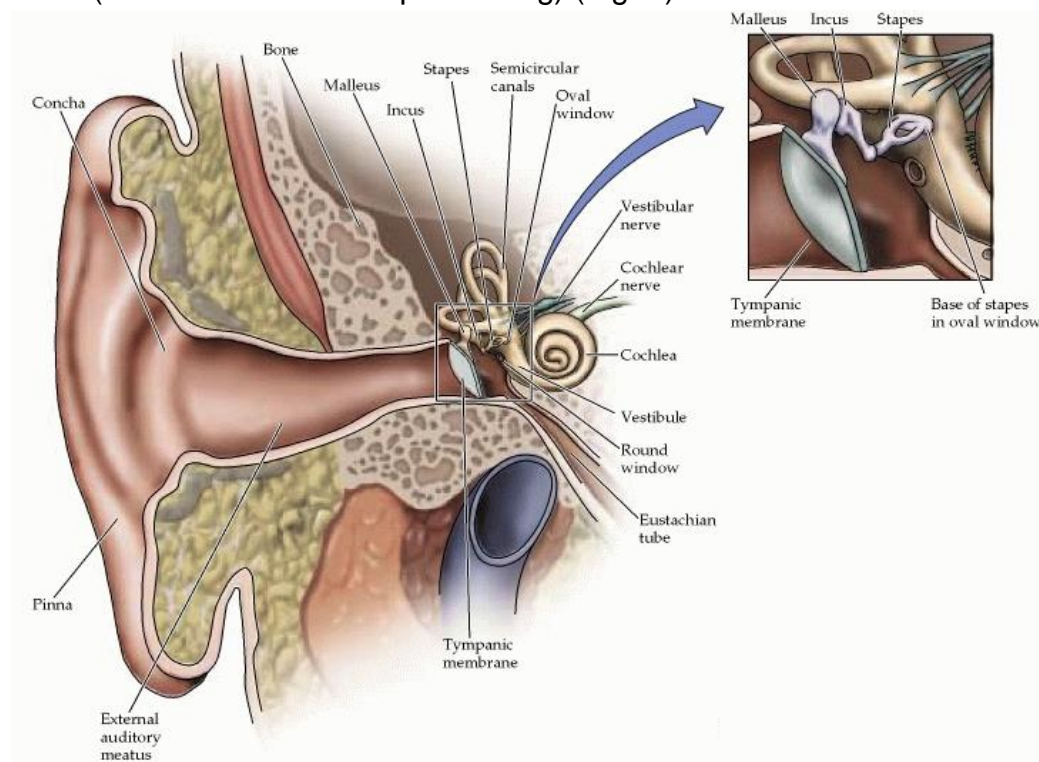


**Figure 1. Schematic of the human ear.** The anatomy of the outer ear, middle ear and inner ear is depicted in a frontal plane cut through the external ear canal. A zoomed-in version of the tympanic cavity shows the chain of the ossicles, connecting the tympanic membrane to the oval window (modified from (Dale Purves 2001)).

Once sound waves enter the bony labyrinth of the cochlea, the impulse is propagated to the fluid-filled cavity and causes the liquid (called perilymph) to move. As sound travels through the perilymph, the thickness and stiffness of the basilar membrane decreases. This membrane is a structural element that supports the organ of Corti, the receptor organ for hearing. The rigidity is highest at the base and becomes less stiff at the apex (the helicotrema). Therefore, travelling sound waves with high frequencies (up to 20 kHz) correspond to areas near the bottom basilar membrane and low-frequency (minimum 20 Hz) waves travel down the tube and cause the apical basilar membrane to vibrate. The frequency and stiffness of the basilar membrane are proportional to each other. This specific structural arrangement of frequency susceptibility is called tonotopy (Ehret 1978).

The sound energy is then conveyed to the Organ of Corti, where the hair cells of the sensory epithelium detect vibrations. The organ of Corti is limited by the tectorial membrane and the basilar membrane and consists of different cell types. The supporting cells act as pillars and provide structural and metabolic support. The hair cells with its mechanoreceptors act as signal detectors and convert movement into electrical signals which are transmitted via synapses to the auditory cortex (Waschke 2015). There are two types of hair cells, the outer hair cells (OHCs) and inner hair cells (IHCs). Both OHCs and IHCs are equipped with stereocilia in the upper part of the hair cells which are responsible for signal transduction (Peter Dallos 1996). When the tectorial membrane is caused to move by sound waves, the stereocilia deflect, causing the mechano-transducer channels to open and potassium ions flow from the surrounding potassium-rich endolymph into the cytosol of hair cells. The shift of ion charge causes the hair cells to open calcium channels and the resulting influx of calcium ions leads to the depolarization of the cellular membrane with subsequent intracellular glutamate release. Simultaneously, the depolarized OHC triggers prestin, a protein located in the lateral cellular membrane, to contract. This response provides mechanical feedback and amplifies the sound signal (Peter Dallos 1996).

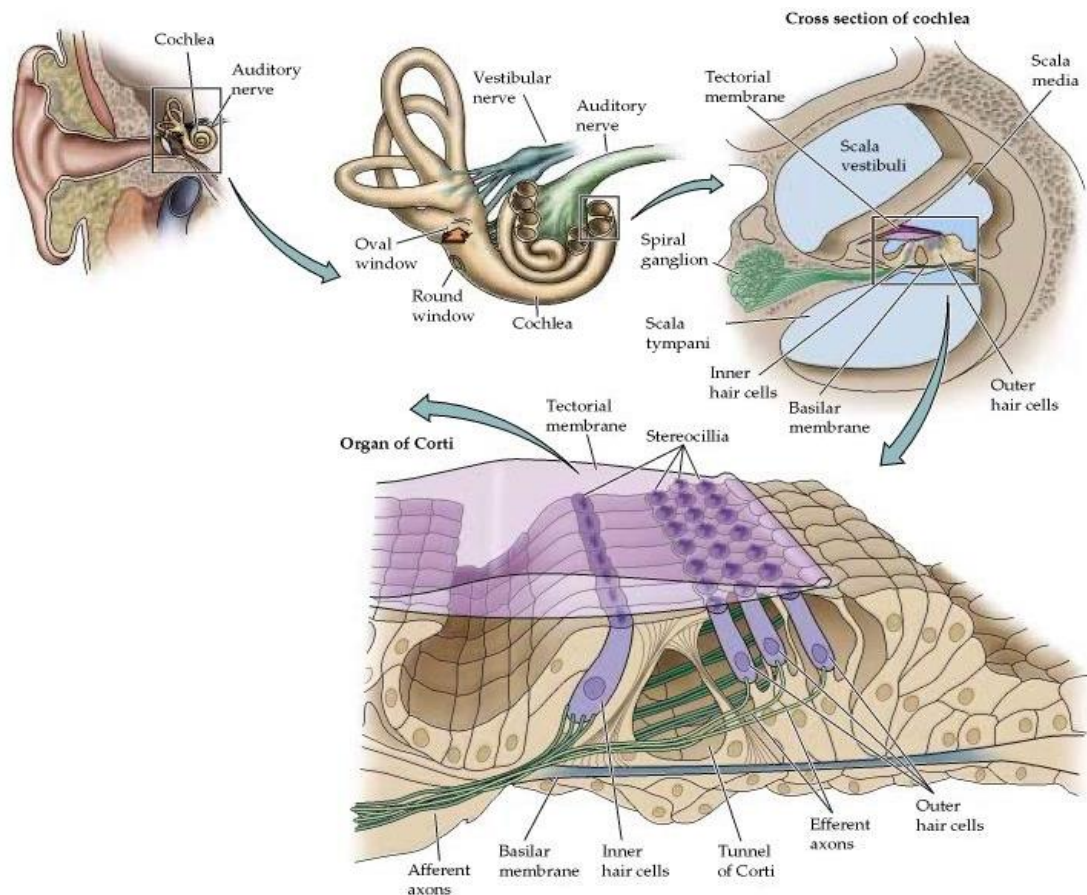


**Figure 2. Phased zoom of the cochlea and the Organ of Corti.** The cochlea is responsible for sound detection. The organ consists of three fluid compartments, the scala vestibuli, scala media and scala tympani which are spiralling towards the apex. The organ of Corti is located in the scala media and holds the outer hair cells (OHCs) and inner hair cells (IHCs) (modified from (Dale Purves 2001)).

The amplified signal is then detected by the actual sensory cells, the IHCs. These neurons are characterized by synapses specialized for sustained, rapid vesicle exocytosis and connect to ca. 95% of afferent fibers in the auditory pathway (Singer, Panford-Walsh et al. 2014). A peculiar feature of this synapse is an organelle called the synaptic ribbon, which tethers a large pool of readily releasable vesicles of neurotransmitters (Matthews and Fuchs 2010) and is able to spike up a few hundred times per second to encode sound intensity by action potential spike frequency in post-synaptic neurons with unprecedented precision (Singer, Panford-Walsh et al. 2014, Wichmann and Moser 2015). The transduced electric signal is then propagated along the ascending auditory pathway.

## 1.2 Organization of the auditory pathway

The auditory pathway transmits acoustic information from the organ of Corti to the auditory cortex and is comprised of ascending and descending fibers. The hair cells form a synaptic connection with the spiral ganglion neurons of the auditory nerve (AN) and mark the beginning of the ascending auditory pathway (Chumak, Rüttiger et al. 2015). The AN consists of fibers with selective sensitivity over different parts of the dynamic range of sound (Bing, Lee et al. 2015). These fibers are categorized according to their spontaneous action potential discharge rate (SR) (Liberman 1978, Heinz and Young 2004, Singer, Panford-Walsh et al. 2014). Fibers with a high-SR are specialized for the detection of low sound pressure levels (<20 dB sound pressure level, SPL), while low-SR fibers respond to much higher sound pressure levels (20-40 dB SPL) (Sachs and Abbas 1974, Yates 1991). Low-SR fibers are crucial to hearing in a noisy environment (Furman, Kujawa et al. 2013). The coded sound signal is then transmitted upstream to the cochlear nuclear (CN) complex, where signals are relayed to different parallel ascending tracts (Singer, Panford-Walsh et al. 2014). Each ascending tract then converges at the level of the midbrain into the inferior colliculus (IC) and finally reaches the auditory cortex (Malmierca, Merchan et al. 2002).

The auditory cortex is interconnected either directly or indirectly with the amygdala and hippocampus, structures of the limbic system that play a central role in emotional processing. The auditory thalamus sends direct neural inputs to the basolateral amygdala (BLA), which shares a connection with the hippocampus. This link becomes apparent when BLA stimulation enhances the number of sound responsive neurons in the AC after sound enrichment (Singer, Panford-Walsh et al. 2014). The amygdala in turn activates the hypothalamus-pituitary-adrenal (HPA) axis (Rooszendaal, Griffith et al. 2003, Wolf 2009, Barry, Murray et al. 2017). This connection allows acoustic stimulation to activate stress responses in the inner ear (Yao and Rarey 1996, Terakado, Kumagami et al. 2011, Singer, Panford-Walsh et al. 2014). These neuronal links and circuits between the auditory circuit, the limbic system and the HPA axis ultimately form a sound-activated network.

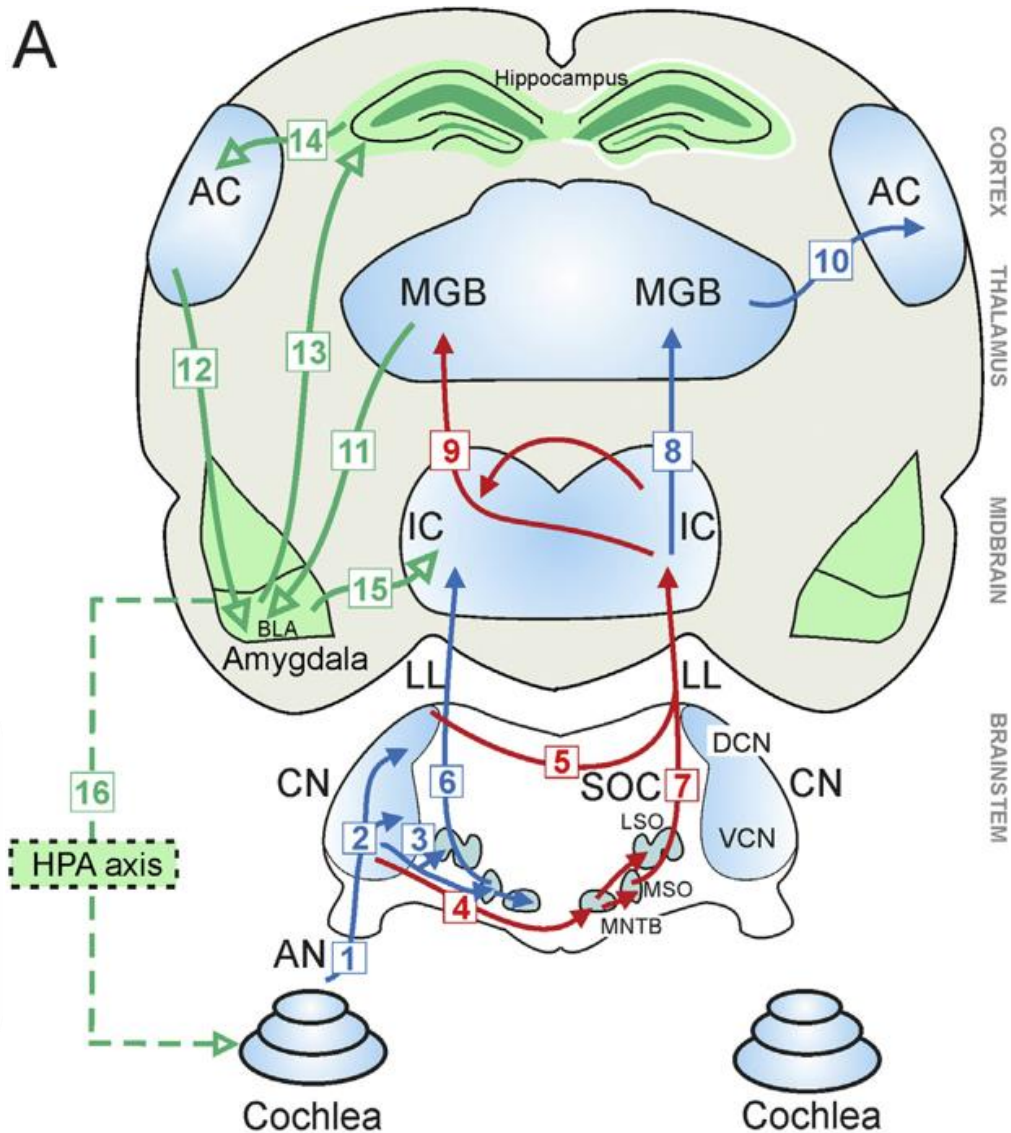


**Figure 3. Schematic illustration of the ascending auditory pathway.** The auditory nerve (AN) projects the transmitted signal coming from the cochlea to the cochlear nucleus complex (CN). Here, the AN fibers connect to the dorsal (DCN) and ventral (VCN) part of the CN. The signal is then transmitted to the ipsilateral (blue) and contralateral (red) lateral (LSO), medial (MSO) superior olive and the medial nucleus of the trapezoid body (MNTB), forming the superior olivary complex (SOC). Efferent fibers emerge from the LSO and MSO that convey information to the hair cells in the cochlea. The DCN transmits ipsilateral (blue) information and the SOC transmits contralateral information (red) to the inferior colliculus (IC). From here, ipsi- and contralateral (green and orange) fibers are interchanged and transmitted to the medial geniculate body (MGB), where both impulses are propagated to the auditory cortex (AC) (Malmierca and Merchan 2004). The MGB contacts the amygdala (green arrows) which simultaneously contacts the hippocampus that in turn shares a connection to the AC (green arrow). Changes of glucocorticoid levels caused by amygdala activity have a great impact on the cochlea (dashed green arrow) (Singer, Panford-Walsh et al. 2014, Chumak, Rüttiger et al. 2015).

### 1.3 What is “stress”?

This sound-activated network and especially the link between the auditory system and the HPA axis, a major player in stress response, is paramount for this work. To better understand the role of the HPA axis, term “stress” has to be defined first. *Stress* originates from the fight-or-flight response described by Walter Cannon (Cannon 1929) and nowadays is commonly defined as “any physical or psychological event that disrupts homeostasis” (Sheriff, Dantzer et al. 2011). Homeostasis is a central concept in biology (Goldstein and Kopin 2007) that describes the process of organisms to maintain equilibrium. This steady state is continuously challenged by internal or external stimuli that cause disruption to homeostasis, so-called *stressors*. The organism’s response to these stressors is called *stress response* (Cannon 1932). Two regulatory systems in the human body with the goal to maintain equilibrium have been isolated: The sympathoadrenal medullary system (SAM) and the hypothalamus-pituitary-adrenal (HPA) axis. Where the SAM reacts within seconds after encountering a stressor, the HPA pathway takes 3-5 minutes to obtain a measurable increase of stress hormone concentration (so-called *glucocorticoids*, GCs) in the blood (Sheriff, Dantzer et al. 2011).

Thus, the SAM axis is responsible for the short-term fight-or-flight response mediated through the sympathetic nervous system which reacts to acutely stressful situations and directly accelerates metabolic turnover to adapt to the new challenging situation. The HPA axis in turn initiates a prolonged stress response by modulating GC-responsive systems.



## 1.4 The HPA axis

The HPA axis is comprising three organs that create a network of mutual influence and feedback interactions. This system orchestrates a variety of stress responses that ultimately regulate bodily functions such as the metabolic system, the reproductive system, the immune system and the central nervous system.

In detail, the paraventricular nucleus of the hypothalamus (PVN) is the motor of the HPA axis and builds together with the anterior lobe of the pituitary gland and the suprarenal gland the HPA circuit (Bao and Swaab 2010). Activation of PVN neurons is regulated by afferent fibers originating from the limbic circuit. Stressors but also exertion, illness and the circadian rhythm prompt the neuroendocrine neurons of the PVN to release corticotropin-releasing hormone (CRH) and vasopressin. These hormones synergistically stimulate the secretion of adrenocorticotrophic hormone (ACTH) in the hypophyseal portal system of the pituitary gland. ACTH in turn acutely triggers the GC biosynthesis by shifting cholesterol into the mitochondria of adrenocortical cells and causes GC levels to rise (Gomez-Sanchez and Gomez-Sanchez 2014). The increased GCs act as second messenger on the glucocorticoid receptors and mineralocorticoid receptors, which in turn initiate the stress response in the peripheral tissue. At the same time, GCs provide feedback control by suppressing the upstream endocrine activity of the hypothalamus and the pituitary gland (Fig. 4) (Han, Ozawa et al. 2007). This feedback response of the HPA axis is mainly mediated by MR-related corticosteroid activation (Cole, Kalman et al. 2000). Throughout the day, the HPA axis triggers pulsatile GC releases from suprarenal glands that occur every 60-120 minutes with one secretory episode lasting approximately 20 minutes. In humans, the release pattern follows a distinct diurnal cycle with low GC concentrations during nights and peak production just before awakening. During the course of the day, GC levels slowly decrease and finally reach its minimum value again during the night. In nocturnal rodents, this cycle is inverse with low GC concentration during days and peak production in the evening hours. This rhythm is important to consider when analyzing GC values in experimental settings (Young, Abelson et al. 2004, Fries, Dettenborn et al. 2009)

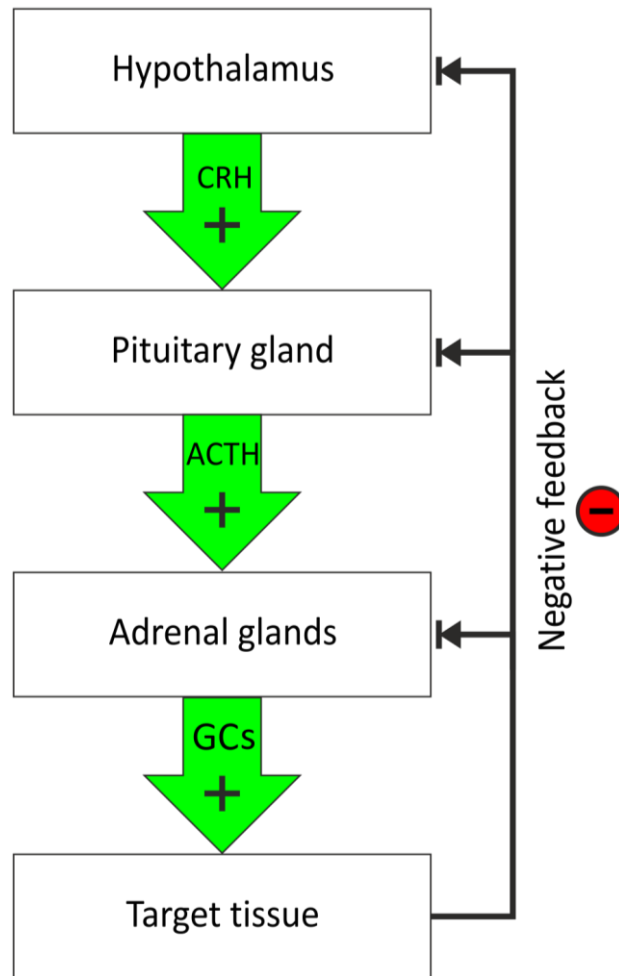


**Figure 4. The simplified HPA axis.** The hypothalamic paraventricular nucleus in the hypothalamus produces corticotropin-releasing hormone (CRH) stimulates the release of adrenocorticotrophic hormone (ACTH) in the hypophyseal portal system of the pituitary gland. ACTH prompts glucocorticoid (GC) synthesis and release in the adrenal gland which eventually carries out genomic and non-genomic effects within target tissues. The rise of GCs triggers a negative feedback loop that stops the release of CRH, ACTH and GC and thereby slackens the HPA axis response.

## 1.5 The role of steroid receptors

Ultimately, the output of the HPA axis are the hormones corticosterone (main GC in rodents) and cortisol (main GC in the human body). Both messengers are ligands for the glucocorticoid receptor (GR) and the mineralocorticoid receptor (MR) and coordinate cellular activities. GRs and MRs initiate rapid effects through secondary cell signalling pathways within the plasma membrane as well as genomic effects via gene transcription for proteins in the nucleus (Gomez-Sanchez and Gomez-Sanchez 2014).

MR and GR are cognate steroid receptors of ligand activated transcription factors and their expression often co-occurs in the same cell. Additionally, many transcriptional events depend on certain ratios of activated GR and MR. Both receptors compete for the same ligands, share many chaperones (a protein that promotes protein folding), and bind the same target location at the DNA (Gomez-Sanchez and Gomez-Sanchez 2014).

Prominent MR functions are ion homeostasis, osmotic regulation and adjustments on bodily hemodynamics. In neuronal tissue, MR activity regulates membrane excitability and significant neuronal responses during memory formation, learning and stress (Gomez-Sanchez and Gomez-Sanchez 2012, Gomez-Sanchez and Gomez-Sanchez 2014). In the auditory system, MRs increase the turnover of the Na<sup>+</sup>/K<sup>+</sup>-ATPase pump which is paramount in ion homeostasis of the scala media in the inner ear (Agarwal and Mirshahi 1999).

However, an excessive activation of MRs results in an increase of reactive oxygen species (ROS) and inflammation (Gilbert and Brown 2010, Zhu, Manning et al. 2011, Gomez-Sanchez and Gomez-Sanchez 2012). This is important to mention as free radicals accumulate in hair cells shortly after being exposed to excessive noise.

Prominent GR functions are the regulation of energy supply and the mediation of stress reactions. The role of GR on inflammation is considered contrary to MR function and dampens MR-mediated inflammatory responses (Gomez-Sanchez and Gomez-Sanchez 2012). Although the affinity of GRs for corticosterone and cortisol is ten times lower than for MRs (Reul and de Kloet 1985, Arriza, Simerly et al. 1988), during the pinnacle of GC concentration or during stress exposure, GRs are activated by ligands.

When activated, GRs and MRs are transported into the nucleus, where homodimers (GR:GR, MR:MR) or heterodimers (GR:MR) are formed and co-transcription factors stabilize promotor binding of specific genes at the hormone responsive element (HRE) (Savory, Prefontaine et al. 2001). After gene transcription, an export signal moves the receptor out of the nucleus and back into cellular cytosol (Fejes-Toth, Pearce et al. 1998, Nishi, Ogawa et al. 2001, Pascual-Le Tallec and Lombes 2005, Gomez-Sanchez and Gomez-Sanchez 2012).

Homodimers of MR and GR act differently at the same HRE and exhibit diverse transcriptional efficiencies when compared to heterodimers (Viengchareun, Le

Menuet et al. 2007, Ackermann, Gresko et al. 2010, Gomez-Sanchez and Gomez-Sanchez 2014). The formation of MR:GR heterodimers is controlled by GR secretion as MR homodimers predominate at low GC concentrations. The highest MR:GR heterodimer formation occurs during stress. Recent studies suggest that these heterodimers are most efficient in gene transcription (Ackermann, Gresko et al. 2010). This finding is crucial for brain functionality and hearing function as MR and GR expression is high in neuronal tissue and in the inner ear, showing that both systems are important effector organs for stress adaptation (De Kloet 2004, Terakado, Kumagami et al. 2011, Gomez-Sanchez and Gomez-Sanchez 2014).

The multi-layered nature of GRs and MRs and the intricacy of the cellular stress response in the brain and the inner ear as presented here makes it difficult to pinpoint GR and MR functions. This makes steroid receptors unique in complexity and facilitates interactions in both synergy and opposition. To explore the specific role of both receptors in the cochlea and on the first synapse of the auditory nerve is the subject of this work.

## **1.6 The disrupted auditory system**

Any type of damage that is inflicted upon the sensitive auditory system can impair hearing function and consecutively cause hearing loss. The etiology and pathophysiology of disrupted auditory functionality and related pathways interfering with the vulnerability and recovery of the auditory system will be discussed in the following.

### **1.6.1 Etiology of noise-induced hearing loss**

Although the pathogenesis of noise-induced hearing loss (NIHL) is a complex and multifactorial disease that emerges from underlying genetic interactions and environmental factors (Le, Straatman et al. 2017), the main risk factor for NIHL is excessive noise (Kujawa and Liberman 2006). NIHL prevalence started to rapidly increase with the introduction of the industrial revolution. Occupational noise exposure paired with a more recent increase of social noise exposure, such as through personal music players, may add to the rise in NIHL prevalence (Basner, Babisch et al. 2014).

Noise is omnipresent in our everyday lives and can affect both body and psyche, resulting in a variety of auditory and non-auditory health effects (Basner, Babisch et al. 2014). Today, approximately 5% of the world's population is reportedly affected by impaired hearing (Sha and Schacht 2017), rendering NIHL one of the most common diseases in modern times.

Chronic sound exposure can lead to sensorineural hearing loss, which is associated with irreversible damage to the sensory epithelium located in the organ of Corti (Nadol 1993). The duration of noise exposure and its intensity define different types and different pathological patterns of noise-related hearing loss.

The human auditory system allows us to process a large dynamic range of sound pressure levels. Our perception of sound intensity approximates a logarithmic scale, making the dB scale a useful measure. For reference, human hearing ranges from -9 dB SPL at 3 kHz (a faint whisper) to 140 dB SPL (a gunshot). A normal human conversation is usually held around 60 dB SPL. The *equal-energy principle* (equal energy will cause equal damage, creates a continuum of acoustic over-stimulation ranging from a short time interval of high-level sound exposure to a long time interval of low-level sound exposure (Suvorov, Denisov et al. 2001, Le, Straatman et al. 2017). NIHL can result from both sudden noise exposure (acoustic trauma, AT) and long-term noise exposure (environmental exposure). Typically, sudden high impulse exposures to noise are more damaging to the ear than steady state low impulses (Suvorov, Denisov et al. 2001, Le, Straatman et al. 2017). The resulting diversity of hearing loss led to two types injury:

(A) Temporary threshold shifts (TTS) with a transient loss of acuity but no hair cell loss (usually lasting 24-48h followed by a return to baseline hearing threshold levels).

(B) Permanent threshold shifts (PTS) with permanent hearing impairment and concomitant hair cell loss (Le, Straatman et al. 2017).

However, recent evidence suggests that decline in hearing acuity caused by early acoustic over-exposure resulting in TTS may continue long after the acoustic over-stimulation has stopped, even at frequencies outside the original NIHL. These findings hint that ears with a history of acoustic trauma are substantially different from those without (Gates, Schmid et al. 2000) and accelerate age-related hearing loss (Kujawa and Liberman 2006).

### 1.6.2 Pathophysiology of acoustic over-stimulation

Extreme noise intensities or long-term sound exposures beyond 80 dB carry an increased risk of (A) structural or (B) metabolic damage to the organ of Corti (Le, Straatman et al. 2017, Sha and Schacht 2017, Tikka, Verbeek et al. 2017).

(A) *Structural damage* is inflicted when sound intensities above 130 dB SPL impinge the cochlea, leading to a disruption of the organ of Corti from the basilar membrane and subsequently to a mixing of peri- and endolymph as well as a disconnection of cell junctions (Henderson and Hamernik 1986, Le, Straatman et al. 2017). Sound intensities less than 130 dB SPL may still cause a detachment of the OHC stereocilia from the tectorial membrane, although this is theorized to be transient and therefore subject to TTS (Nordmann, Bohne et al. 2000).

(B) *Metabolic decompensation* involves stereocilia disruption and an additional reduction of synaptic vesicles at the presynaptic membrane (Kim, Park et al. 2014). Postsynaptic over-stimulation can cause an excessive amount of glutamate which triggers inflammatory swelling of cell bodies and dendrites (Spoendlin 1971, Robertson 1983). This process is commonly referred to as glutamate excitotoxicity (Le, Straatman et al. 2017). It is theorized that the co-occurrence of both excessive glutamatergic postsynaptic stimulation at the hair cell level and the formation of free radicals (ROS) during over-exposure to noise stimuli promote hair cell death (Yamane, Nakai et al. 1995). ROS are important initiators and mediators of cell death (Dixon and Stockwell 2014) and continue to form until a maximum concentration of ROS is reached 7-10 days after trauma (Yamashita, Jiang et al. 2004), spreading from the basal end to the apex of the cochlea (Henderson, Bielefeld et al. 2006).

Even after a full recovery of hearing thresholds after acoustic trauma, the first synapse of the auditory system can be damaged considerably, resulting in a loss of synaptic connections between IHCs and type I afferent auditory nerve fibers (ANFs) (Kujawa and Liberman 2009, Shi, Chang et al. 2016). Therefore, noise exposures that only cause reversible threshold shifts with no hair cell loss (TTS) still provoke a permanent loss of >50% of the first synaptic connection in the organ of Corti (Liberman 2017, Sha and Schacht 2017). This synaptopathy occurs imminently after acoustic trauma and most likely is also caused by glutamate excitotoxicity injuring the post-synaptic terminals (Shi, Chang et al. 2016). The neurons of the spiral ganglion cells may survive

during the following months and years but eventually also perish as a consequence of synaptic loss (Liberman 2017).

The noise-induced synaptopathy with sustained pure-tone thresholds, as in TTS, appears in functional hearing analysis as amplitude loss of supra-threshold ABR waves. Here, the reduction of dynamic range is attributed to the selective loss of auditory nerve fibers (ANFs) with low-spontaneous rates (low-SR) and high thresholds (Furman, Kujawa et al. 2013, Rance and Starr 2015). These fibers are known for signal coding in noisy background and are considered vital for speech understanding in difficult listening environments and may explain the reduced speech perception in individuals with noise-induced synaptopathy (Shi, Chang et al. 2016, Le, Straatman et al. 2017).

These new insights on TTS caused a change of paradigm and suggested that not the hair cells but the synapse between hair cells and cochlear nerve is the most vulnerable element in the inner ear (Liberman, Epstein et al. 2016). As a consequence, the hearing organ compensates for the loss of synaptic function with a reversible central gain increase and shifts balance between excitatory and inhibitory midbrain responses. This reaction may play an important role in associated hyperacusis and tinnitus (Heeringa and van Dijk 2014).

## **1.7 Aim of this work**

As shown here, the pathophysiology of hearing loss is complex and sparks controversial discussions of the definite role of stress in respect to hearing vulnerability and the recovery of hearing after acoustic trauma. Hence, aim of the present study was to further explore the influence of GRs and MRs on the organ of Corti, the auditory nerve fiber, and central auditory processing to better understand the impact of stress signaling on the pathogenesis of noise-induced hearing loss.

In brief: How does stress influence hearing? Adding a piece to the puzzle.

## 2 Material and methods

### 2.1 Animals

A total of 55 female Wistar rats were used for this work. Animal care, treatments, procedures and the experimental protocol followed the guidelines of the EU Directive 2010/63/EU for animal experiments and were reviewed and approved by the University of Tübingen, the Veterinary Care Unit and the Animal Care and Ethics Committee of the regional board of the Federal State Government of Baden-Württemberg (approval number HN1/14). Animals were provided by Charles River Laboratories (Research Models and Services, Germany GmbH, Kißlegg, Germany). See also (Singer, Kasini et al. 2018).

Rats were 6 to 8 weeks old and weighed between 200 g and 300 g. Food and water was supplied ad libitum. The rats were housed in groups of four under an artificial 12/12-hour light/dark cycle, where noise levels did not exceed 60 dB sound pressure level. The suffering of animals in this experiment was minimized not only by limiting measurement duration and frequency, selecting measurement periods at time points where changes are bound to happen, but also by keeping animals in social groups (3-4 animals / cage) to ensure normal interaction. Also, animals underwent anesthesia to minimize pain during measurements and urine collections. Doing so, discomfort was reduced to a minimum which in turn diminished the animals' stress response and ultimately prevented interference with the experimental setup and endpoints.

### 2.2 Drug Treatments

To study the influence of stress on hearing function and hearing recovery, a total of three GR- and MR-potent substances were tested for effect in the following experimental design and compared to a control substance.

**1. Corticosterone** (Sigma-Aldrich, St. Louis, USA), the main glucocorticoid in rodents, is the drug of choice to act as pharmacologically induced stress component. Corticosterone was injected at a concentration of 3 or 30 mg/kg bodyweight.



**2. Mifepristone** (RU-486, Sigma-Aldrich, St. Louis, USA) is a specific glucocorticoid receptor antagonist with no affinity for the mineralocorticoid receptor (Trune and Kempton 2009). RU-486 was injected at a concentration of 100 mg/kg bodyweight.

**3. Spironolactone** (Sigma-Aldrich, St. Louis, USA), is a specific mineralocorticoid receptor (Delyani 2000). Spironolactone was injected at a concentration of 75 mg/kg body weight.

**4. Vehicle** was used as negative control for drug application. The vehicle was injected at a concentration of 2 ml/kg BW.

**Table 1. Overview of pharmacological groups.** Each group received either spironolactone, mifepristone, corticosterone, or vehicle substance intraperitoneally.

<b>Group</b>	<b>Solution</b>
Spironolactone (spir)	30 mg Spironolactone + 720 µl PEG + 80 µl EtOH (37,5 mg/ml Spironolactone)
Mifepristone (mif)	30 mg RU-486 + 540 µl PEG + 60 µl EtOH (50 mg/ml RU-486)
Corticosterone (cort)	20 mg Corticosterone + 1200 µl PEG + 133,33 µl EtOH (15 mg/ml Corticosterone)
Vehicle	540 µl PEG + 60 µl EtOH

All substances were dissolved in polyethylenglycole (Sigma-Aldrich, St. Louis, USA) and subsequently diluted with ethanol (1:10) directly before use. For better solubility, substances were put in a 60 C water bath for 30 minutes and subsequently put in an ultrasonic cleaner for 15 minutes. Drugs were injected intraperitoneally. All injections were done during the morning hours to prevent bias caused by circadian variation of internal corticosterone (Buijs, van Eden et al. 2003, Tahera, Meltser et al. 2006). After injection, rats were returned to their cages.

## **2.3 Anesthesia**

During noise exposure and ABR measurements, animals were anesthetized with an intraperitoneal injection of xylazine hydrochloride (5 mg/kg body mass; Rompun® 2%, Bayer HealthCare, Leverkusen) and ketamine hydrochloride (75 mg/kg body mass; Ketavet®, Pfizer Pharm. GmbH, Karlsruhe). Foot-withdrawal reflexes were checked regularly to adjust the level of anesthesia and additional doses of anesthetics were administered up to a third of initial dose if necessary.

During anesthesia, core body temperature was monitored via a rectal digital thermometer and maintained at 35,5 °C - 38°C by cooling pads or heating lamps to avoid overheating or hypothermia.

To ensure adequate moisturizing of the rat's eyes, polyacrylacid eye gel (Vidisic®, Bausch&Lomb GmbH, Dr. Mann Pharma, Berlin) was administered.

## **2.4 Acoustic trauma and sham treatment**

After being anesthetized, animals were put on a rotating disc in a reverberating box inside an acoustic chamber which was previously pre-warmed with a red-light lamp. The direction of the rotation was changed at the 30-minute mark. For acoustic trauma induction, animals were binaurally exposed to a sinusoidal free field tone (10 kHz, 116 dB SPL RMS for 60 minutes). To deliver sound, a reverberating chamber with tilted, non-parallel walls was equipped with seven loudspeakers (1x Visaton, DR 45 N, Haan, Germany and 6x Piezeo Horn 335835, Conrad Electronic, Hirschau, Germany) to achieve a mostly homogeneous sound field as described in previous experiments (Rüttiger, Singer et al. 2013). The Visaton DR 45 N was used as central top speaker. The other six speakers were mounted at the top (2 speakers) and sidewalls (4 speakers) of the chamber.

The sine tone was controlled and analyzed by microphone and computer reading was performed by a fast Fourier transform (FFT) program.

Animals treated with sham exposure followed same protocol with sound device and speaker switched off. Doing so, confounders were limited to a minimum and ensured that possible changes between sham treated and noise exposed groups are only attributable to the pharmacological effect.

## 2.5 Hearing measurements

### 2.5.1 Distortion product of otoacoustic emissions

The measurement and analysis of distortion products of otoacoustic emissions (DPOAE) is a widely used method to determine the activity of the outer hair cells (OHC) that function as a non-linear amplifier of the cochlea (Sha and Schacht 2017). DPOAE originate from an active contraction of OHC which can be detected with a sensitive microphone. For this measurement, a phasis II System (Esaotebiomedica, Italy) was used to generate acoustic stimuli and to subsequently record evoked potentials (Knipper, Zinn et al. 2000).

Pure-tone continuous sound signals were generated and used as stimuli. Sound signals were amplified, filtered (0,2-5 kHz 6-pole Butterworth filter, Wulf Elektronik) and averaged across 64-256 repetitions (Rüttiger, Singer et al. 2013). Sound levels were subsequently assessed using a probe microphone and a measuring amplifier.

Cubic distortion products were measured at the frequency  $2f_1-f_2$ . For each frequency  $f_1$ , the best ratio  $f_2/f_1$  was determined using an intermediate sound level (60 dB) (Knipper, Zinn et al. 2000). Frequency pairs of tones were between  $f_2 = 4$  kHz and  $f_2 = 32$  kHz (Chumak, Rüttiger et al. 2015). Sound levels of  $f_1$  were always kept 10 dB louder than  $f_2$  levels. Subsequently, sound levels were gradually increased in steps of 5 dB. In order to decrease the background noise to a minimum (at least 10 dB below the level of emission), recording windows were averaged as described in previous experiments (Knipper, Zinn et al. 2000). Animals were under anesthesia during the duration of the measurements.

### 2.5.2 Measuring auditory brainstem responses (ABRs)

Acoustic stimuli create an electromagnetic potential in the inner ear that gets transduced along the ascending auditory pathway, as described in chapter 1.2. This electromagnetic signal can be measured to assess the summed neuronal potential of the auditory pathway after sound stimulus presentation (Knipper, Van Dijk et al. 2013, Rüttiger, Singer et al. 2013) and is commonly referred to as auditory brainstem response (ABR). With this electrophysiological method, the signal pathway can be objectively investigated from the first synapse in the AN to higher cortical regions.

ABR waves were measured after short click, noise, or frequency-specific tone bursts. The click stimulus was a broadband stimulus with a center frequency at 4,9 kHz. For the noise burst a random phase with a duration of 1 ms was generated. Pure-tone stimuli had a duration of 3 ms with 1 ms cosine squared rise/fall times and frequencies ranging from 1.41 to 32 kHz. Sound pressure was gradually increased in 5 dB steps (maximal 105 dB SPL). For more detailed threshold analysis and supra-threshold ABR wave analysis, certain frequencies, spanning from 4 to 32 kHz, were recorded with a 2 dB sound pressure increment (Rüttiger, Singer et al. 2013). In this experiment, the pure-tone records of 16 and 32 kHz were used to analyze supra-threshold ABR waves. Generated sound stimuli were subsequently delivered to the rat's ear by a loudspeaker (DT-911, Beyerdynamic, Heilbronn, Germany) which was placed at 3 cm lateral to the animal's pinna (Rüttiger, Singer et al. 2013). During measurements, rats were positioned in a soundproof chamber (IAC 400-A, Industrial Acoustics Company GmbH, Niederkrüchten, Germany) (Knipper, Van Dijk et al. 2013). Evoked potentials then were recorded at the ear (positive, active), the vertex (negative, reference) and the back of the rat (ground) with subcutaneous silver wire electrodes (Rüttiger, Singer et al. 2013). The electric signal was amplified, band-pass filtered (200 Hz to 2kHz), and averaged over 500 repetitions. Hearing thresholds were assessed by determining the minimal sound pressure that produced a visually evoked potential in the expected time window of the recorded signal (Engel, Braig et al. 2006, Chumak, Rüttiger et al. 2015). ABRs were recorded during stimulus presentation and polarity was alternated to eliminate artefacts (compression and rarefaction) (Rüttiger, Singer et al. 2013).

### **2.5.3 Analysis of auditory brainstem responses (ABRs)**

Each ABR threshold to click and noise stimuli was analyzed for each ear separately. ABR waveforms to pure-tone stimuli and its input-output function (peak I/O) were measured and assessed on the ear with lower click thresholds. The ABR wave functions were averaged and smoothed out by a moving zero-phase Gaussian filter with a window length of 5 data points (0.5 ms) (Chumak, Rüttiger et al. 2015).

For all groups, the ABR wave data for 16 or 32 kHz stimuli was analyzed for peak and amplitude by customized computer programs. Wave amplitudes were defined as peak-to-peak amplitude of a negative peak followed by a positive peak (Rüttiger, Singer et al. 2013). The resulting peak amplitudes of ABR waves are directly correlated to certain

activity of the ascending auditory pathway and were clustered into two groups: early and late ABRs.

The first measurable response (wave I) was interpreted as the sum of the first stimulus-related potential and attributed to signal transduction within the auditory nerve (Rüttiger, Singer et al. 2013). These early signals were peaks ranging between 0.9 and 2 ms. Late peaks (4 – 6 ms) qualify as signals of central processing and fall into the time range of neural processing in the inferior colliculus and thalamic activation (see Fig. 5) (Rüttiger, Singer et al. 2013, Singer, Panford-Walsh et al. 2014). Based on these definitions, settings were adjusted to extract ABR peaks (Chumak, Rüttiger et al. 2015). ABR peak-to-peak (wave amplitude) growth functions were then constructed for each individual rat and calculated for increasing stimulus levels with reference to the ABR thresholds (from -15 to a maximum of 85 dB above threshold), whereas stimulus levels never exceeded 110 dB SPL (Singer, Kasini et al. 2018). When damaged, the cochlear nerve loses its connection to the IHCs, which is reflected in a decline of amplitude of ABRs (Fig. 5).

Figure 5

ABR wave peaks

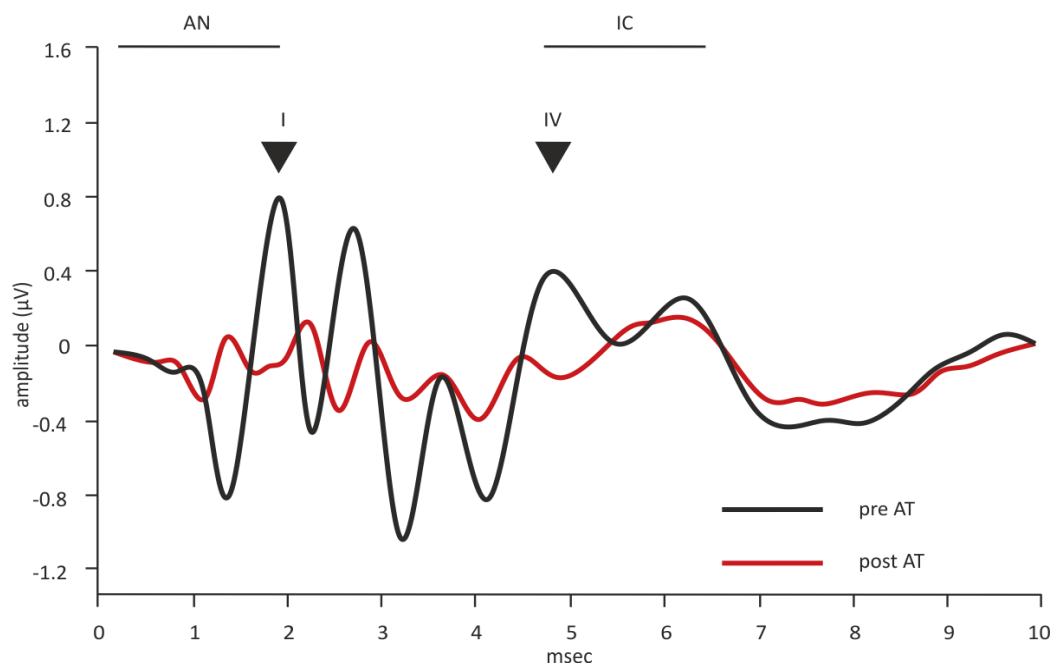


**Figure 5. ABR wave peaks.** When measured, the usual ABR wave shows five prominent peaks occurring within the first 10 ms after sound stimuli presentation. Since the peaks represent the delay of neural processing, the waves can be attributed to different stations of the ascending auditory pathway. Wave I represents the summed potential of the auditory nerve, whereas the subsequent waves receive contributions from more than one anatomical structure. Wave IV accounts for the activity of the inferior colliculus and thalamic region. If an acoustic trauma injures the inner ear of the rat (post AT, red), all amplitudes of ABR waves are reduced when compared to un-traumatized control animals (pre AT, black) (Knipper, Van Dijk et al. 2013, Bing, Lee et al. 2015). **AN** Auditory nerve, **IC** inferior colliculus, **AT** acoustic trauma, **I** wave I, **IV** wave IV.

## 2.6 Preparation of animals

After finishing with the experiments, animals were deeply anaesthetized with carbon dioxide and consecutively sacrificed through decapitation. The auditory bulla was exposed via a dorsolateral approach and cochleae were rapidly isolated, dissected and fixed by immersion in 2% paraformaldehyde (PFA), 125 mM sucrose in 100 mM phosphate-buffered saline (PBS), pH 7.4, for 2 h (Knipper, Zinn et al. 2000, Bing, Lee et al. 2015). Cochleae were decalcified using rapid decalcifier (RDO; Apex Engineer Product Corporation, Aurora, IL, USA). Afterwards samples were embedded in Tissue Tek (optimum cutting temperature compound; Thermo Fisher Scientific, Waltham, MA, USA), followed by an overnight incubation in 25% sucrose and Hanks' buffered saline (HBS) and stored at -80°C (Chumak, Rüttiger et al. 2015, Singer, Kasini et al. 2018). Samples were cryosectioned parallel to the modiolus in 10 µm sections with a Cryostat (Leica Cryostat 1720 Digital Leica, Wetzlar, Germany), mounted on microscope slides (SuperFrost Plus, Thermo Fisher Scientific, Waltham, MA, USA) and stored at -20°C in a freezer as described in earlier works (Muller 1991, Tan, Ruttiger et al. 2007, Singer, Zuccotti et al. 2013).

The auditory cortex, hippocampus and inferior colliculus were identified with a rat atlas (Paxinos and Watson, 1998). Brain tissue was extracted with a small forceps, frozen with liquid nitrogen and stored at -80°C.

## 2.7 Immunohistochemistry and high-resolution fluorescence microscopy

Slides were thawed and permeabilized with 0,5 % Triton X-100 (Sigma-Aldrich, St. Louis, USA) in PBS for 10 minutes at room temperature. To block unspecific bindings, normal goat serum (NGS) was applied for 30 minutes and slides were put in a wet chamber. Cochleae were stained using monoclonal mouse antibodies against CtPB2/RIBEYE (1:50 concentration, Cell applications, San Diego, CA, USA) and Na<sup>+</sup>/K<sup>+</sup>-ATPase subunit  $\alpha$ 3 (NKAA $\alpha$ 3) (McLean, Smith et al. 2009). Primary antibodies were diluted in 2% NaCl, 0,1% Triton X-100, PBS and 1% NGS. Both antibodies were added at the same time (100 µl) and incubated overnight at 4°C in a wet chamber. Sections were then rinsed and mounted in Vectashield (Knipper, Zinn et al. 2000,

Singer, Kasini et al. 2018).

For image acquisition and CtBP2/RIBEYE-immunopositive spot counting, an Olympus BX61 microscope equipped with an X-Cite Lamp (Olympus, Tokyo, Japan) for epifluorescence illumination and a z-axis motor was used for histological examination (Singer, Kasini et al. 2018). Pictures of inner hair cells were acquired using an Olympus XM10 CCD monochrome camera. For ribbon counts, cryosectioned cochleae were visualized over a distance of 8  $\mu\text{m}$ , covering the entire inner hair cell nucleus, synapses and areas beyond it in an image stack along the z-axis (z-stack) (Singer, Geisler et al. 2016). One image stack along the z-axis consisted of 30 layers with a z-increment of 0.28  $\mu\text{m}$  (Rüttiger, Singer et al. 2013). For each layer and each fluorochrome, one image was generated to display spatial protein distribution (Heidrych, Zimmermann et al. 2009). Z-stacks were three-dimensionally deconvoluted using cellSens Dimensions ADVML Algorithm (OSIS; Olympus, Hamburg, Germany). This algorithm helps to erase flare light, display the examined object with increased resolution, and sharpen the image.

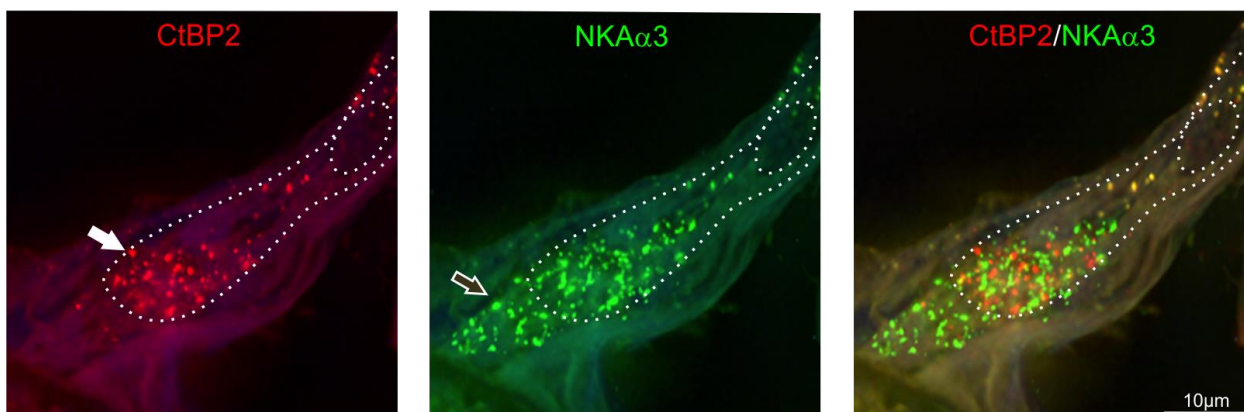


**Figure 6.** Immunohistochemical staining of IHC ribbons with CtBP2/RIBEYE (arrows, red dots) and NKA $\alpha$ 3 (open arrows, green). Nuclear staining with DAPI (blue). Dashed lines represent the IHC boundaries and cell nuclei, (Singer, Kasini et al. 2018). Scale bars = 10 $\mu\text{m}$ .

## 2.8 Cortisol analysis

Urine analysis was performed as previously described (Singer, Kasini et al. 2018). In brief, urine was collected each time hearing measurements were carried out and during noise exposure or sham treatment, respectively. Collected probes were analyzed for cortisol levels by IDEXX (Vet Med Labor, Ludwigsburg, Germany), using the chemiluminescence immunoassay Immulite 2000 Cortisol (Siemens Healthcare

Diagnostics, Tarrytown, NY, USA). To rule out major influences due to the circadian rhythm, all experiments were conducted in the morning (8-12 a.m.) and the trauma induction of each experimental group was evenly distributed throughout the day.

To eliminate bias caused by fluctuations in urine dilution, urine concentration was assessed by analyzing probes for creatinine levels as well. Raw data contained different units of measurement (cortisol in  $\mu\text{g/l}$ ; creatinine  $\text{mg/dl}$ ), so cortisol was multiplied with a factor of 2.76 and creatinine with a factor of 88.4 to convert values into SI units. These values were put in a ratio (see below) and labelled as cortisol/creatinine ratio (*c/c*, with cortisol in  $\text{nmol/l}$  and creatinine in  $\mu\text{mol/l}$ ). Raw data of IDEXX analysis is attached as supplemental data (Supplementary Table 2).

$$\text{Cortisol} - \text{Creatinine} - \text{Ratio} \left( \frac{c}{c} \text{ratio} \right) = \frac{\left( [\text{CORT}] \text{ in } \frac{\text{nmol}}{\text{l}} \right) * 2.76}{\left( [\text{CREA}] \text{ in } \mu \frac{\text{mol}}{\text{l}} \right) * 88.4}$$

According to the manufacturer, this immunoassay shares a cross-reactivity of 1.2% with corticosterone, the primary glucocorticoid in rats. In this study, the cortisol/creatinine (*c/c*) ratio was used to estimate the corticosterone levels in female Wistar rats as a strong correlation between serum cortisol and corticosterone has been observed (Gong, Miao et al. 2015). Therefore, *c/c ratio* is also referred to as corticosterone-creatinine ratio in the following (Singer, Kasini et al. 2018).

## 2.9 Statistical analyses

For cortisol analysis and maximal DPOAE amplitude, 1-way ANOVA with Tukey's multiple comparison test (GraphPad Prism) was used.

DPOAE threshold analysis was compared by using 2-way ANOVA, followed by Tukey's or Bonferroni's (for delta analysis) multiple comparison test.

For the click and noise analysis, 1-way ANOVA and post-hoc Tukey's multi comparison test was calculated.

The DPOAE I/O function was checked by a 2-way matched, repeated-measures ANOVA (0/10/20 - 65 dB SPL) to determine significance.

For frequency dependent ABR, 2-way ANOVA followed by Tukey's (each data set is compared to every other data set) or Bonferroni's (data sets are compared to vehicle), multiple comparison test was performed.



The frequency specific ABR threshold analysis of 4, 11.3, 16 and 32 kHz was checked by 1-way ANOVA and followed by post-hoc Tukey's multiple comparison test.

No statistical analysis was performed with growth function data of ABR wave I and IV amplitude in Fig. 8, 10, 18, 24 and 26 as statistical comparisons for same values were carried out in Fig. 9, 11, 19, 25 and 27 and checked with 1-way ANOVA, followed by Tukey's multiple comparison test.

Counts for CtBP2 immunopositive ribbons were compared by using 1-way ANOVA with Dunnett's multiple comparisons test (Singer, Kasini et al. 2018).

If both ANOVA and post-hoc test reached significance for pairwise comparisons, it is indicated by asterisks (\*  $p < 0.05$ , \*\*  $p < 0.01$ , \*\*\*  $p < 0.001$ , \*\*\*\*  $p < 0.0001$ ). n.s. denotes non-significant results ( $p > 0.05$ ). If not otherwise denoted, no asterisks mean no significance between values. Detailed information about the statistical analyses is given in Supplementary Table 1.

### **3 Results**

Goal of this work was to elucidate the incoherent and elusive relationship between stress and the auditory system. Therefore, the primary glucocorticoid (GC) in rats (corticosterone) and its target receptors, the glucocorticoid (GR) and mineralocorticoid (MR) receptor were the focus of this research.

In order to break the complexity of this interaction, three questions were formulated.

**Chapter 3.1: Does activation or attenuation of GRs and MRs alter normal hearing?**

**Chapter 3.2: Do different levels of corticosterone affect normal hearing?**

**Chapter 3.3: Does activation or attenuation of GRs and MRs after excessive noise exposure improve or corrupt hearing recovery?**






Different experimental layouts were designed to answer these questions and each question will be addressed individually in the following chapters.

#### **3.1 The effect of GR and MR activation and attenuation on normal hearing**

In a first experiment, animals were randomly assigned to four treatment groups, each consisting of eight animals. Pre-test measurements were conducted, evaluating auditory brainstem responses (ABRs), distortion product otoacoustic emissions (DPOAEs) and urinary cortisol/creatinine ratios (c/c).

Animals then received a single intraperitoneal injection of either vehicle, corticosterone (GR-/MR-agonist), mifepristone (GR-antagonist) or spironolactone (MR-antagonist) depending on their group's allocation. 90 minutes after drug injection, rats either underwent sham treatment or were exposed to a 10 kHz sine tone at 116 dB SPL for 60 minutes. Follow-up measurements were conducted at 150 mins, 3d, 7d and 14d before sacrificing rats at 15 days after drug injection (Fig. 7).

The impact of different GR- and MR-potent drugs on normal hearing function and on c/c ratios in sham exposed rats will be addressed in chapter 3.1. The impact of GR- and MR-potent drugs on animals after excessive noise exposure will be outlined in chapter 3.3.

drug agent	c/c value		→	activation or blockage of receptors	
	via drug injection	endog. level		GR	MR
① vehicle		+ 		—	—
② Corticosterone 30 mg/kg		+ 		✓	✓
③ Mifepristone 100mg/kg		+ 		✗	—
④ Spironolactone 100mg/kg		+ 		—	✗

**B**

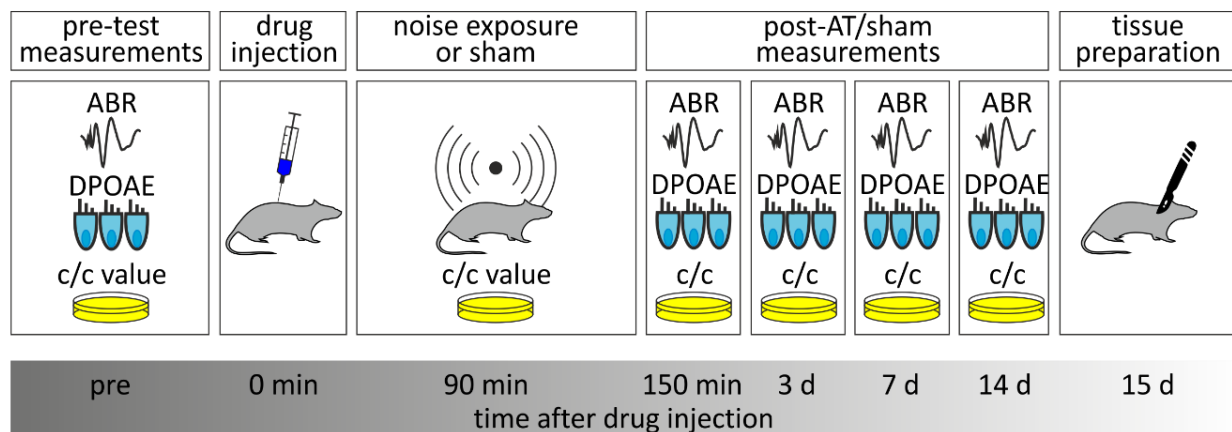


**Figure 7. Experimental design of a single application of GR- and MR-potent substance followed by sham treatment or excessive noise exposure.** **A.** Four different treatment options indicated by ① - ④. The drug effect on a cellular level is illustrated as check mark for GR/ MR activation, as red cross for GR/ MR blockage, or as a blue hyphen for receptor activity not exceeding baseline conditions. The anticipated effect of the drug agents on the rats' metabolic system is characterized as c/c value (corticosterone/ creatinine value) **B.** Time scale of the experiments. Animals either received noise exposure or sham treatment, depending on their group assignment.

### 3.1.1 The effect of GR- and MR-potent drugs on c/c ratios

At first, the c/c ratios of rats were analyzed at different time points to evaluate the impact of selected drugs on stress hormone balance. The c/c ratio thereby acted as a parameter to quantify stress levels of the rats.

No statistical relevant difference of c/c ratios between groups was noted prior to the experiment. Likewise, application with mifepristone and spironolactone did not exhibit a significant impact on c/c ratios at any given time.

However, corticosterone caused the c/c ratio to peak 150 minutes after drug application (Fig. 8, labelled as *day 0*), reaching statistical significance when compared to vehicle, mifepristone and spironolactone.

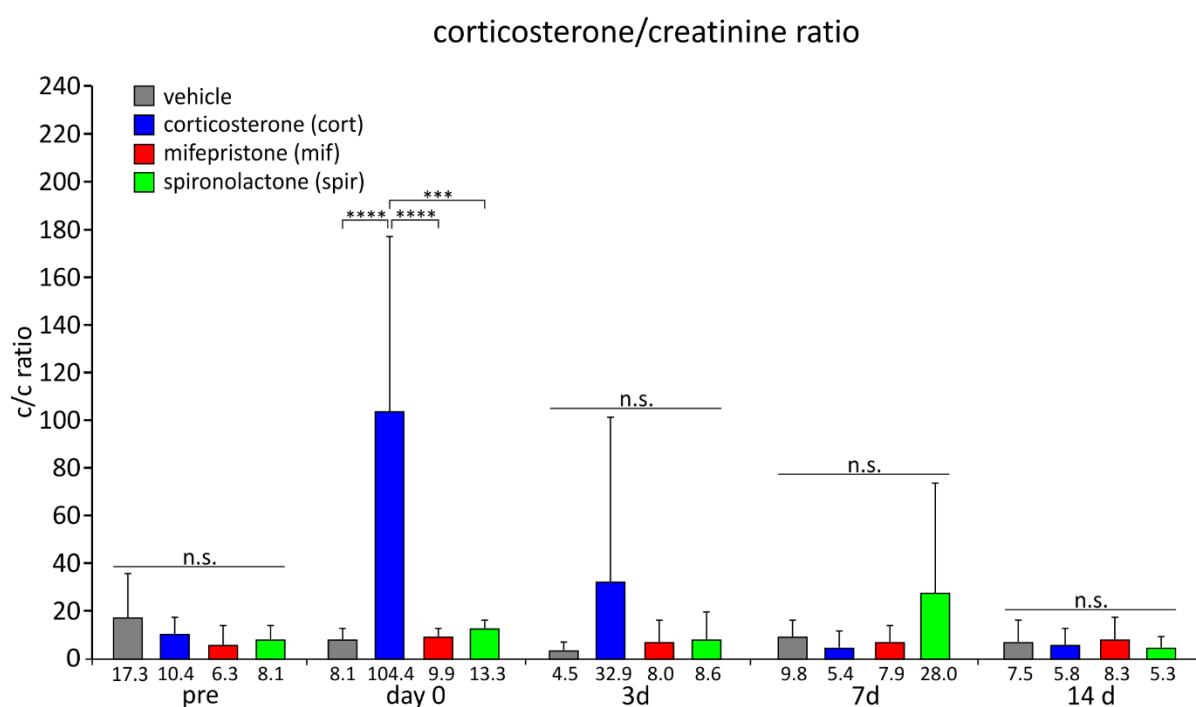


**Figure 8. Corticosterone/creatinine ratio (c/c ratio) of urine samples.** Urine samples were collected during each measurement period. C/c ratios are shown for each individual group. There was no significant difference between c/c ratios before the experiment. Right after drug application, c/c ratios peaked in the corticosterone group (blue bars) significantly. No effect was observed for pre-treatment with mifepristone (GR antagonist, red bars) or spironolactone (MR antagonist, green bars). Three days after drug application and thereafter, differences between groups were no longer significant, although a non-significant surge of c/c levels 7 days after spironolactone application was noted. Error bars represent SD (n = 6-8 animals); n.s., not significant. \*\*\* P < 0.001, \*\*\*\* P < 0.0001. For details of statistical analyses, see Supplemental Table 1.

This finding supports the presumption that only the application of corticosterone affects the endogenous stress hormone levels (c/c ratios) significantly (see Fig. 3 A). On the days following injection, the corticosterone-treated cohort recovered to normal, non-significant values. However, a surge of spironolactone-treated animals was prominent seven days after drug application. This increase of blood corticosterone did not reach significance due to high variance within the spironolactone group.

Taken together, this finding illustrates the great short-term impact of corticosterone on c/c ratios and reveals its lack of long-term effects due to its quick metabolization. On top of that, the sudden surge of stress hormone within the spironolactone group may hint a long-term MR-related effect on c/c ratios.

### **3.1.2 GR- and MR-potent drugs display no effect on OHC function**

DPOAE measurements quantify OHC electro-motility and therefore work as a great tool to evaluate OHC function and their capacity to amplify sound signals. DPOAEs of drug-treated animals were recorded, analyzed and results were displayed in Fig. 9.

In the first panel (Fig. 9A), the maximum DPOAE amplitude of each group was determined before drug treatments to look for variations between groups. No statistical relevant differences were noted at that point in time. Follow-up DPOAE analyses were done on days 3, 7, and 14 with no significant changes over this time period. Therefore, it can be inferred that a single drug application of corticosterone, mifepristone or spironolactone does not affect DPOAE maximal response amplitudes.

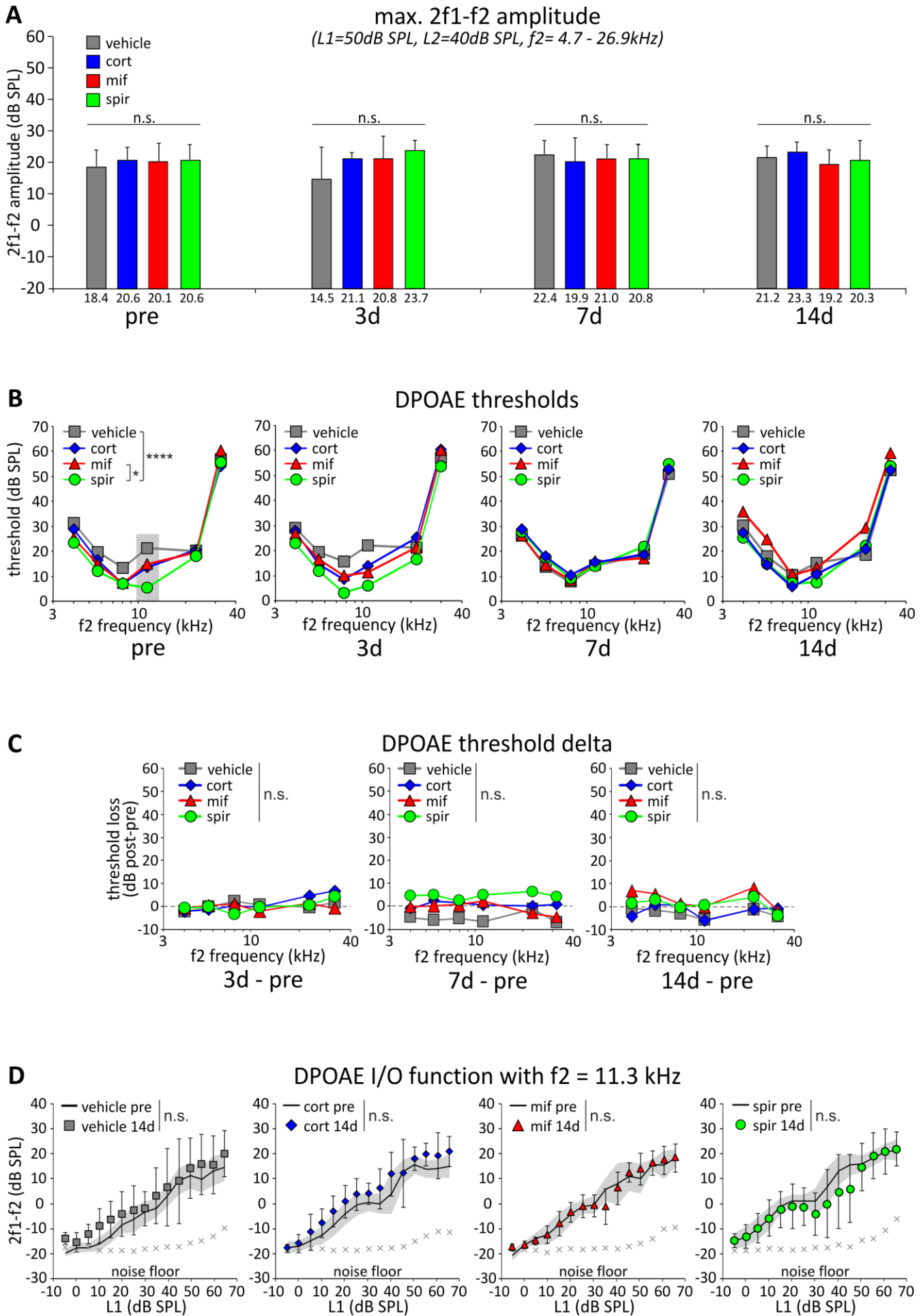
In a second step, DPOAE thresholds were analyzed (Fig. 9B). Pre-treatment DPOAE thresholds differed greatly at 11.3 kHz, therefore pre-existing inter-group differences were eliminated by calculating threshold delta values between the time point of measurement and pre-value. The result is displayed in Fig. 9C, showing no effect of the treatment regimens of GR- or MR-potent drugs on DPOAE thresholds at day 3, 7, or 14 after drug application.

Lastly, the growth function of the distortion product is shown in Fig. 9D, where amplitude strength of 2f1-f2 is plotted against stimulus intensity (L1 in dB SPL). When comparing data generated 14 days after the experiment to pre-test values, no significant differences in terms of slope, reach or strength of the I/O growth function were found.

Together, these data provide conclusive evidence that a single application of GR- or MR-potent drugs poses no short- or long-term influence on OHC sensitivity, response characteristics or other electromechanical properties.

---

**Figure 9. Single application of corticosterone, mifepristone (MR antagonist) and spironolactone (GR antagonist) exhibits no conclusive influence on outer hair cell function.** **A.** Treatment with corticosterone, mifepristone or spironolactone did not influence DPOAE amplitude at any time point of the experiment. 1-way ANOVA. **B, C.** DPOAE thresholds for frequency-specific tones before drug application (pre) differed significantly, therefore delta values were calculated, and statistical analysis was focused to C. No drug effect on delta values of vehicle, corticosterone-, mifepristone-, or spironolactone-treated animals was observed. Delta values were calculated as the difference between the time point of measurement minus pre-value. 2-way ANOVA. **D.** Drug treatment had no effect on I/O-growth function. Data generated for 11.3 kHz before drug application (black line with grey shadow as SD) and at 14d post treatment (colored symbols with whiskers). Noise floor is visualized with grey crosses. 2-way matched RM ANOVA (ranging from 10 - 65 dB SPL). Whiskers represent SD (n = 8-16 ears/ 4-8 animals per group); n.s., not significant. \* P < 0.05, \*\*\*\* P < 0.0001. For details of statistical analyses, see Supplemental Table 1.



### 3.1.3 GR- and MR-potent drugs display no effect on ABR thresholds

To further evaluate the influence of GR- and MR-potent substances on auditory thresholds, anesthetized rats were exposed to a variety of sound stimuli during ABR recordings. Free field click and noise burst stimuli contain different frequency clusters to estimate general hearing performance in low and high frequencies (Fig. 10 A, B). Here, individual groups did not differ significantly before the experiment. 150 minutes after treatment, thresholds displayed no significant pharmacological influence either as no effect between groups was obtained. This finding stays consistent throughout subsequent measurements (day 3, 7, 14).

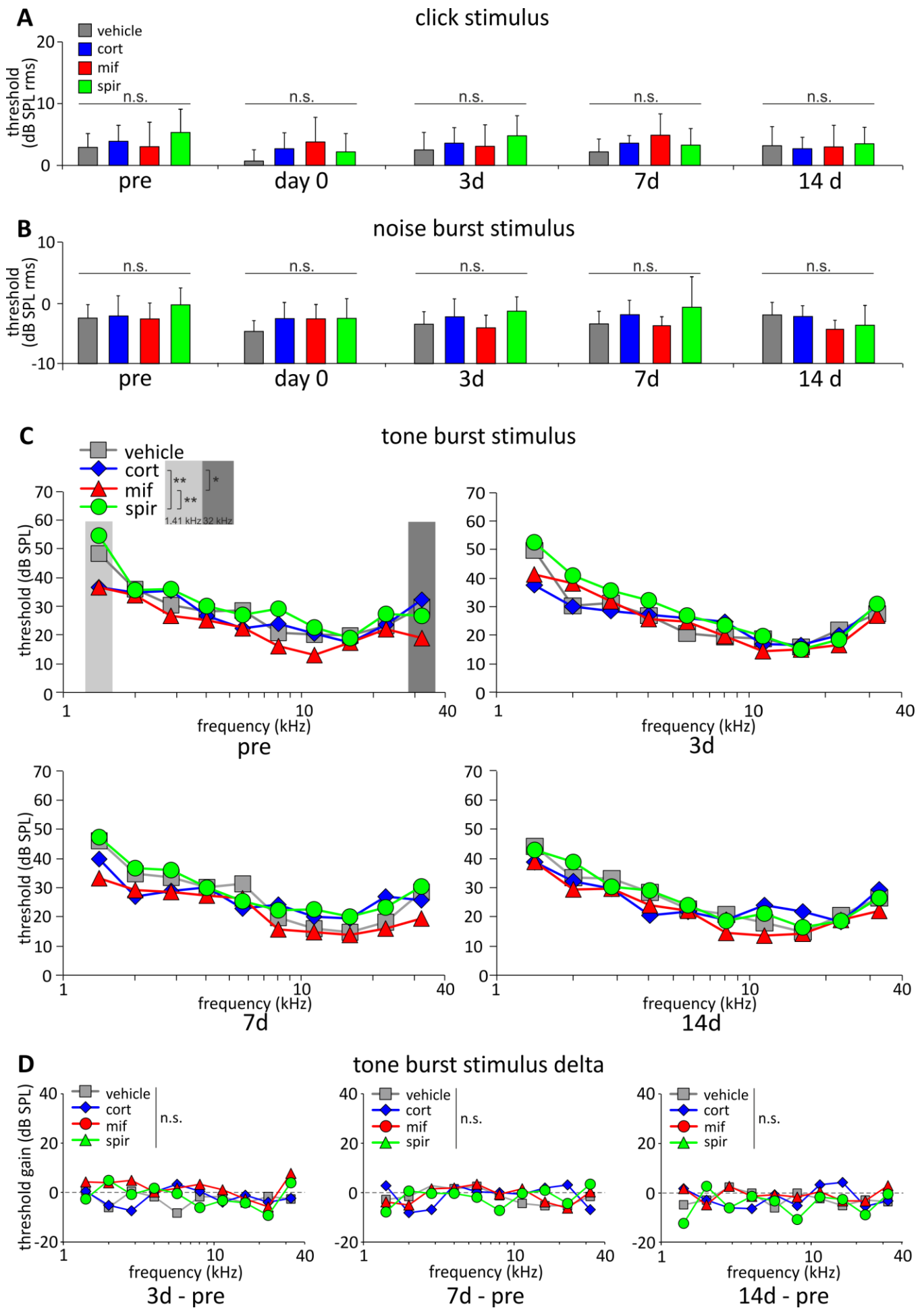
A more specific analysis about hearing thresholds offers the frequency-specific pure tone ABR analysis. In pre-test measurements, a typical U-shaped graph was obtained with lowest threshold at around 10 kHz (Fig. 10 C). As there was a statistically significant difference in pre-measurements at 1.41 kHz and 32 kHz, delta values between post measurements and pre-test values were calculated to exclude pre-existing bias (Fig. 10D). Consequently, statistical analyses of calculated delta values revealed no significant changes throughout the experiment.

To also detect small differences in the best-hearing frequency to high frequency range of the rats, frequency-specific stimuli were re-recorded and analyzed for 11.3 kHz- (Fig. 11A), 16 kHz- (Fig. 11B) and 32 kHz-stimuli (Fig. 11C) with a 2 dB sound pressure increment. In pre-test data sets and at 3, 7, or 14 days after drug injection, drug treatments did not affect hearing thresholds. This result is consistent with the overall ABR assessments and let us conclude that a single injection of corticosterone, mifepristone, or spironolactone has no short- or long-term influence on ABR thresholds. This accounts for click and noise stimuli as well as for frequency-specific ABR threshold analysis ranging between 1.41 and 32 kHz.

---

**Figure 10. Single drug application exhibits no influence on hearing thresholds. A, B.** Drug application of corticosterone (blue bars), mifepristone (red bars) and spironolactone (green bars) had no effect on click or noise-burst stimulus-evoked ABRs compared with vehicle (grey bars) at any given time point (Singer, Kasini et al. 2018). 1-way ANOVA. **C, D.** ABR thresholds for frequency-specific tones before drug application (pre) differed in low (1.41 kHz) and high (32 kHz) frequencies significantly, therefore delta values were calculated and further statistical analysis was limited to D. Throughout the experiment, no systematic drug effect on frequency-specific thresholds of vehicle-, corticosterone-, mifepristone-, or spironolactone-treated animals was noted. Delta values were calculated as difference between the time point of measurement and pre-value. 2-way ANOVA. Error bars represent SD (n = 8-16 ears/ 4-8 animals per group); n.s., not significant. \* P < 0.05, \*\* P < 0.01. For details of statistical analyses, see Supplemental Table 1.





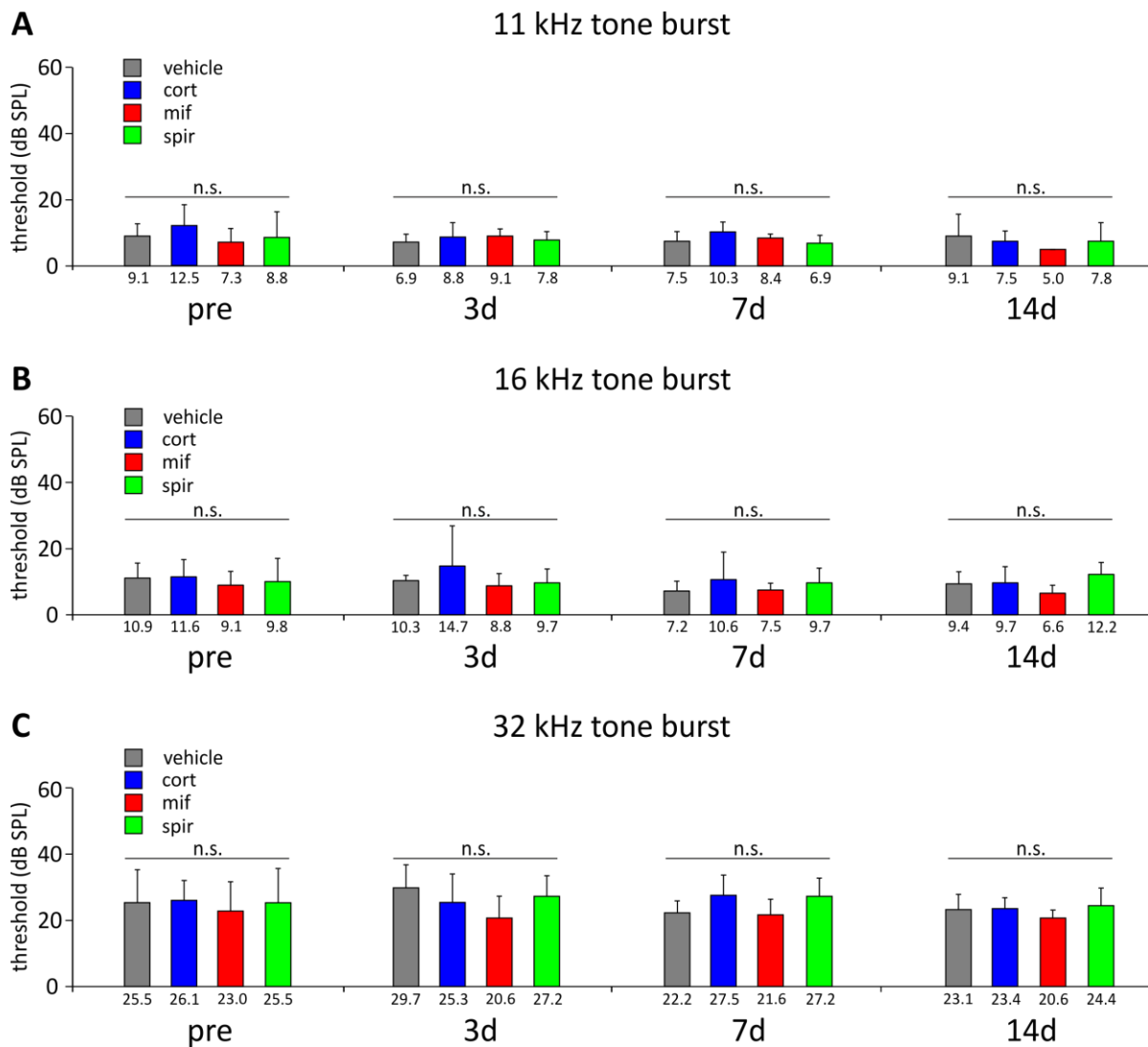


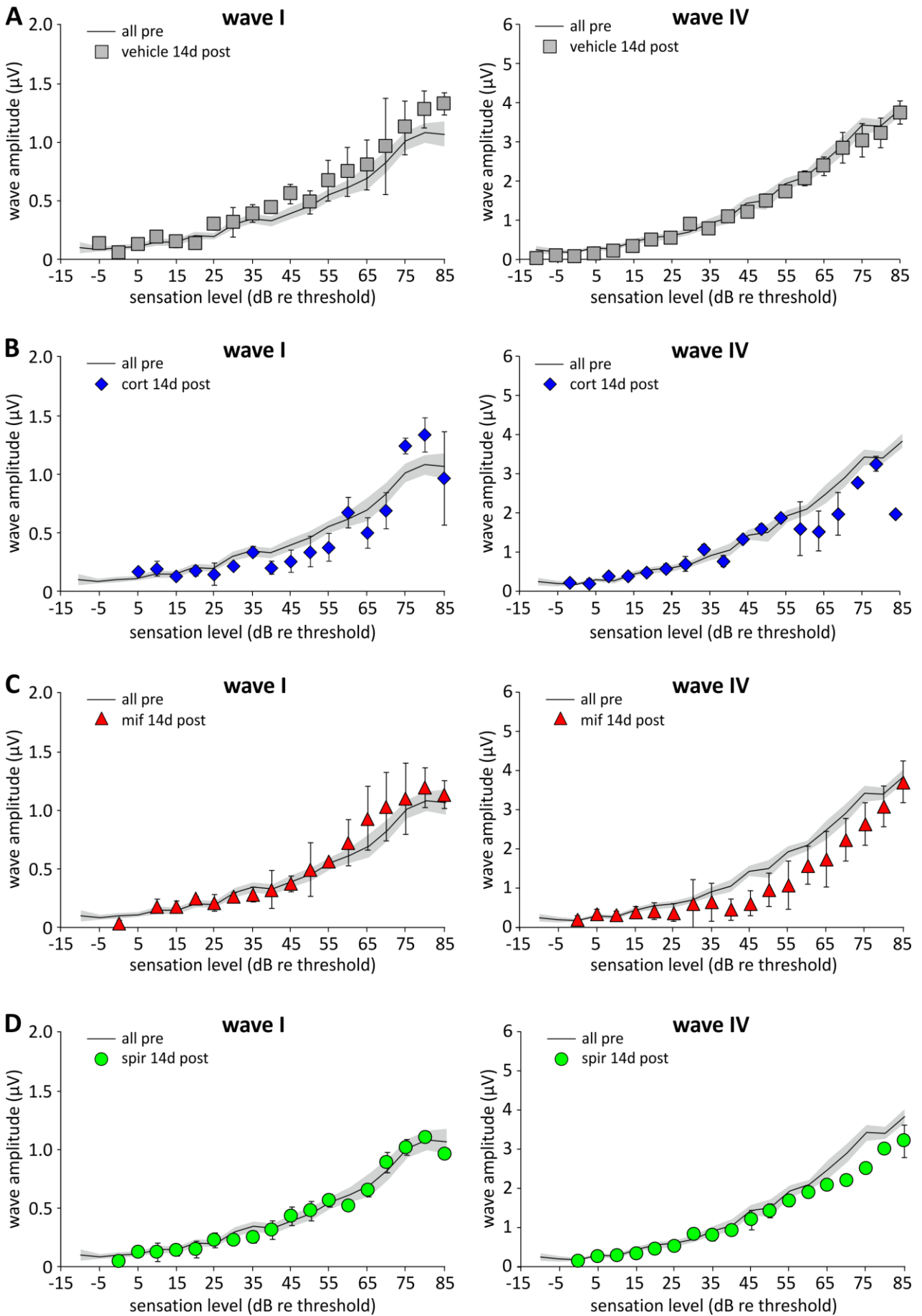
**Figure 11. Single drug application does not influence ABR thresholds of 11.3 kHz, 16 kHz and 32 kHz. A-C.** Thresholds after treatment with corticosterone (blue bars), mifepristone (red bars) and spironolactone (green bars) are not significantly altered when compared to vehicle treatment (grey bars). Thresholds have been evaluated for 11.3 kHz, 16 kHz and 32 kHz. Values below graph depict mean thresholds in dB SPL for each group and time point. 1-way ANOVA. Error bars represent SD (n = 4-8 ears/ 4-8 animals per group); n.s., not significant. For details of statistical analyses, see Supplemental Table 1.

### **3.1.4 GR- and MR-potent drugs display no significant effect on supra-threshold responses to a 16 kHz stimulus**

As described in chapter 1.2, threshold measurements displayed in Fig. 10 and 11 allow us to assess the sensitivity of low-threshold auditory fibers with a high spontaneous rate, which is a marker for hearing sensitivity. However, a more detailed insight into speech processing and hearing in noisy environments is achieved by analyzing supra-threshold hearing, which is greatly dependent on high-threshold, low-spontaneous rate fibers. To get a better understanding of the latter, the amplitude growth of early (wave I) and late (wave IV) threshold-normalized ABRs was plotted to a 16 kHz stimulus against increasing stimulus intensities in Fig. 12. The resulting two ABR slopes exhibit the response to a 16 kHz pure-tone burst stimulus on different levels of the auditory pathway to reveal possible drug effects on the first synapse (auditory nerve: wave I) and the subsequent ascending auditory pathway (inferior colliculus: wave IV). Therefore, ABR wave amplitude growth functions were calculated before and 14 days after drug application (Singer, Kasini et al. 2018). Each treated group was compared to an averaged *all pre* group, containing data of pre-test measurements. The same rationale was applied in Fig. 15.

The data presentation in Fig. 12 allow us to detect great variations between groups and overviews the impact of each treatment. However, although there are slight variations between pre- and 14d-post values, no striking systemic drug effect was apparent. Here, no statistical analysis for significances was performed due to data structure and statistical testing was limited to Fig. 14.

16 kHz tone burst stimulus



To perform statistical analyses between groups and to quantify drug effects on dynamic range and amplitude of supra-threshold ABR waves, the maximum amplitude *size* (Fig. 13 A, C) and the dynamic response *reach* (Fig. 13 B, D) were plotted against dB sensation level for wave I and wave IV. In detail, the reach of the response range is defined as the stimulus level at the maximum response of the wave amplitude. The amplitude of said stimulus level is declared as *size* (Fig. 13) (Singer, Kasini et al. 2018). Since the wave amplitude is greatly influenced by the reliability of the discharge rate and synchronicity of firing events of auditory nerve fibers, breaking it down to two values simplifies the complexity of the wave growth function and helps to evaluate the statistical significances (Singer, Kasini et al. 2018).

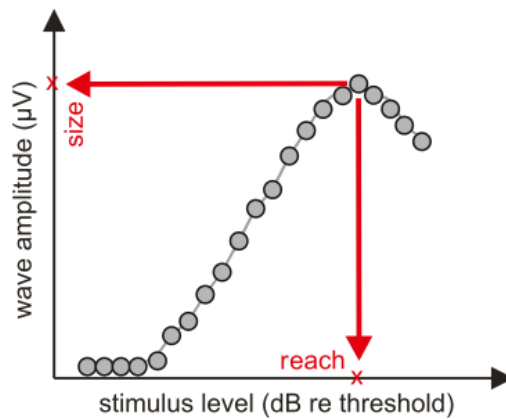


**Figure 13. Reach and size of supra-threshold ABR waves.** The reach of the response range that can be measured is set as the stimulus level at maximum response of the wave amplitude. The amplitude of said data point is declared as *size*. See also (Singer, Kasini et al. 2018).

←

**Figure 12. Single treatment with corticosterone, mifepristone and spironolactone exhibits no striking diverging effect on early (wave I) and late (wave IV) supra-threshold ABR wave responses to frequency-specific tone burst stimuli at 16 kHz. A-D.** Animals were pre-treated with vehicle (grey squares), corticosterone (blue diamonds), mifepristone (red triangles) or spironolactone (green dots) (Singer, Kasini et al. 2018). Baseline responses before drug application (*all pre*) are displayed as mean with shaded areas (SEM). The ABR slope displays the response to a 16 kHz pure-tone burst stimulus on the auditory nerve (wave I) or the inferior colliculus (wave IV) 14 days after drug application. Data are displayed as threshold normalized. SL = sensation level. Error bars indicate SEM (2-4 ears/ 2-4 animals per group).

dynamic range 16 kHz

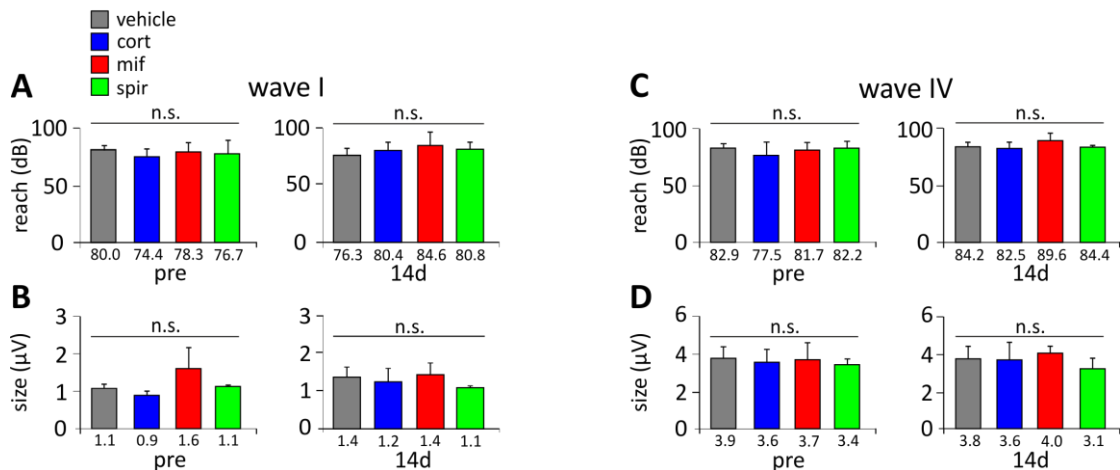


**Figure 14. Treatment with corticosterone, mifepristone or spironolactone has no impact on reach and response size of ABR waves to 16 kHz sound stimuli.** The size of response is defined as the maximum wave amplitude and the reach is defined as the stimulus level at the maximal response of the wave amplitude. **A, B.** ABR wave I reach and size for 16 kHz stimuli at 14d after drug treatment. Animals were treated with vehicle (gray bars), mifepristone (red bars), or spironolactone (green bars) (Singer, Kasini et al. 2018). Drug treatment had no impact on reach or size compared to vehicle. 1-way ANOVA. **C, D.** ABR wave IV reach and size for 16 kHz stimuli at 14d after drug treatment. Drug agents show no effect on reach and size when compared to vehicle. Data are calculated from threshold-normalized growth functions. 1-way ANOVA. Error bars represent SD ( $n = 3-4$  ears/ 3-4 animals per group); n.s., not significant. For details of statistical analyses, see Supplemental Table 1.

As anticipated in Fig. 12, all groups maintained their response size and response reach for early (wave I) as well as for late ABR (wave IV) waves to 16 kHz stimuli two weeks after treatment and no significant differences of supra-threshold analysis were noted between treatment regimens (Fig. 14).

Therefore, it can be concluded that a single treatment with either corticosterone, mifepristone, or spironolactone did not affect supra-threshold behavior of early (auditory nerve, wave I) or late (the inferior colliculus, wave IV) ABRs in response to a 16 kHz pure-tone stimulus.

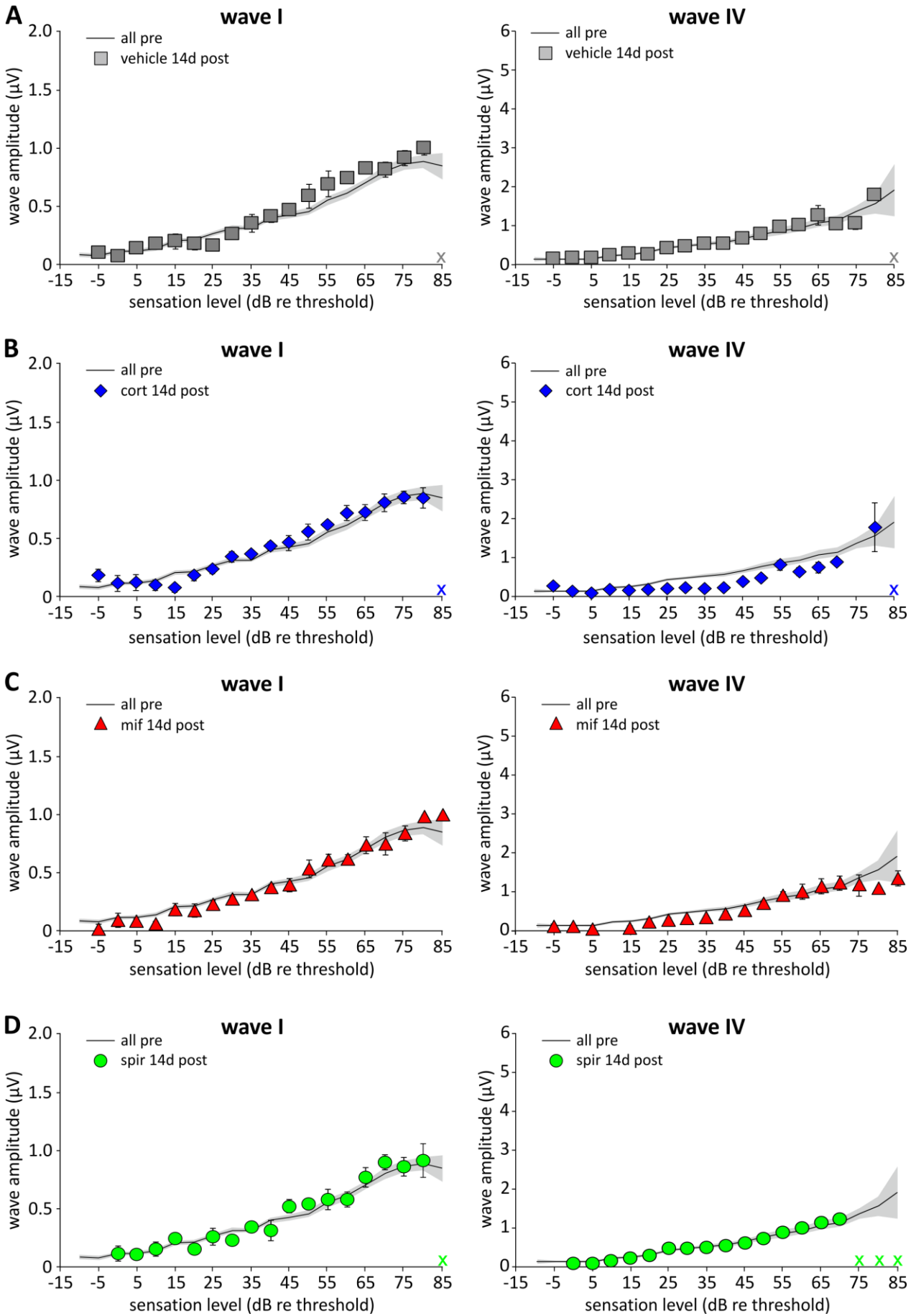
### 3.1.5 GR- and MR-potent drugs display no significant effect on supra-threshold responses to a 32 kHz stimulus

To analyze GR- and MR-potent substances for their influence on high frequency supra-threshold ABRs, early (wave I) and late (wave IV) ABR waves of a 32-kHz-evoked pure-tone stimulus were plotted against stimulus intensity in Fig. 15. ABR wave amplitude growth functions were calculated 14 days after drug treatment and compared to a common pre-test value (Singer, Kasini et al. 2018).

Upon close examination of the slope of each treatment regimen and comparing them to *all pre* values, no drug exhibited a great impact on supra-threshold ABR wave responses. However, wave I and wave IV reach were slightly impaired for vehicle- and corticosterone-treated animals when compared to *all pre*. Animals with spironolactone treatment seemingly displayed a reduced wave I reach and a reduced wave IV reach and size when compared to vehicle. Animals pre-treated with mifepristone presumably maintained reach best among treatments. As demonstrated for Fig. 12, this data display overviews the impact of treatment. To quantify the presumed drug effects and for statistical analyses, the dynamic response *reach* and the maximum amplitude *size* of 32 kHz supra-threshold ABR waves were calculated and the result for wave I and wave IV was plotted in Fig. 16. The above-noted slight differences between treatment groups were still mirrored, yet significant levels were not reached.

Summarizing all information gathered about supra-threshold performance of 16 and 32 kHz, it can be concluded that a single injection of GR- and MR-potent agents (corticosterone, mifepristone and spironolactone) had no significant effect on early or late wave responses and therefore displays no influence on high-threshold, low-spontaneous rate fibers.

32 kHz tone burst stimulus





dynamic range 32 kHz

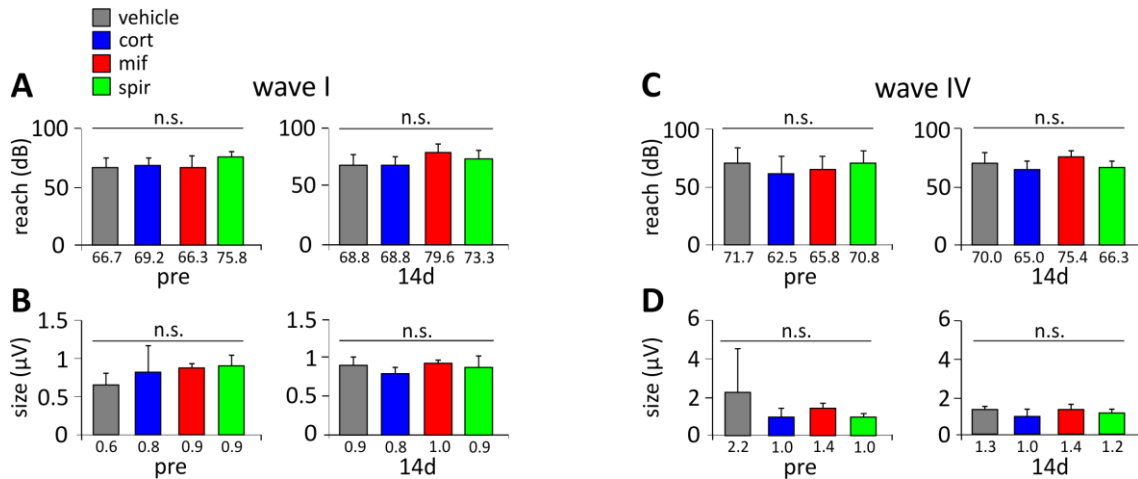


**Figure 16. Treatment with corticosterone, mifepristone or spironolactone has no impact on reach and response size of ABRs to 32 kHz sound stimuli.** The reach of the response range that can be coded is defined as the stimulus level at the maximum response of the wave amplitude. The maximum size of response is defined as the maximal wave amplitude. **A, B.** ABR wave I reach and size for 32 kHz stimuli at 14d after drug treatment. Animals were treated with vehicle (gray bars), corticosterone (blue bars), mifepristone (red bars), or spironolactone (green bars) (Singer, Kasini et al. 2018). Different drug applications have no impact on reach or size compared to vehicle. 1-way ANOVA. **C, D.** ABR wave IV reach and size for 32 kHz stimuli at 14d after drug treatment. Drug agents show no effect on reach and size when compared to vehicle. 1-way ANOVA. Data are calculated from threshold-normalized growth functions. Error bars represent SD (n = 3-4 ears/ 3-4 animals per group); n.s., not significant. For details of statistical analyses, see Supplemental Table 1.

**Figure 15. Single treatment with corticosterone, mifepristone, and spironolactone exhibits no striking diverging effect on early (wave I) and late (wave IV) supra-threshold ABR wave responses to frequency-specific tone burst stimuli at 32 kHz.** **A-D.** Animals were pre-treated with vehicle (grey squares), corticosterone (blue diamonds), mifepristone (red triangles) or spironolactone (green dots). Baseline responses before drug application (*all pre*) are displayed as mean with shaded area (SEM). The ABR slope displays the response to a 32 kHz pure-tone burst stimulus on different levels of the auditory pathway (auditory nerve: wave I, inferior colliculus: wave IV) 14 days after drug application. Small crosses above the x-axis mark the stimulus levels surpassing the limits of stimulation levels (usually 110 dB SL). Data are displayed as threshold normalized. SL = sensation level. Error bars represent SEM. (2-4 ears/ 2-4 animals per group).

### 3.1.6 GR and MR-potent drugs display no significant effect on the first synapse of the auditory pathway

The inner hair cell (IHC) synaptic ribbons maintain a readily releasable vesicle pool of neurotransmitter vesicles. The amplitude size of auditory fiber responses is critically dependent on stable and reliable synaptic vesicle release and the synchronicity of postsynaptic firing events of nerve fibers (Singer, Kasini et al. 2018). IHC ribbons were counted in different tonotopic regions of the cochlea 14 days after drug injection. They were immunohistochemically stained with CtBP2/RIBEYE and subsequently counted.

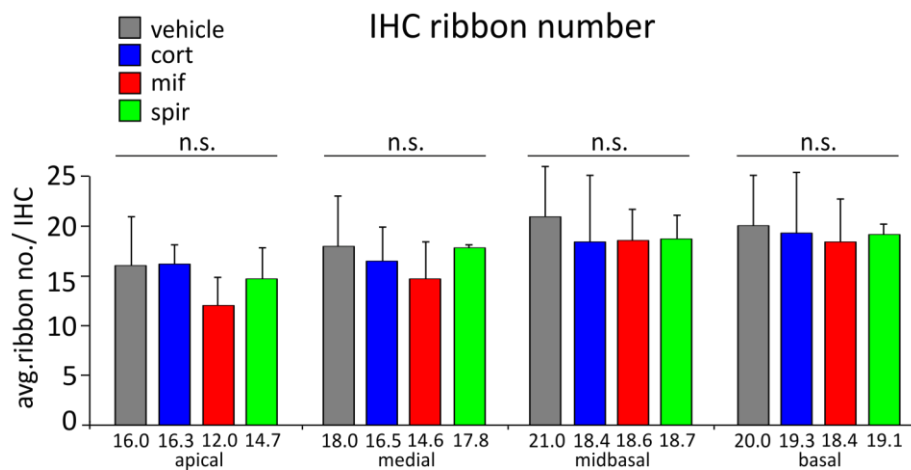


**Figure 17. IHC ribbon number is not influenced by single drug application of corticosterone, mifepristone or spironolactone.** Treatment with vehicle (gray bars), corticosterone (blue bars), mifepristone (red bars), or spironolactone (green bars) has no enhancing or destructive effect on IHC ribbon number in apical, medial, midbasal or basal turns (Singer, Kasini et al. 2018). Y-axis depicts the averaged ribbon number per inner hair cell. Error bars represent SD (n = 2-4 ears/ 2-4 animals per group); 1-way ANOVA. For details of statistical analyses see Supplemental Table 1.

As shown in Fig. 17, there was no statistically significant difference along the tonotopic axis, particularly in midbasal and basal ribbon number, which represent high frequency areas including 16 and 32 kHz (see Fig. 12 - 16).






This result complements the overall performance of the rats' hearing function and let us conclude that single drug application with corticosterone, mifepristone or spironolactone had no influence on threshold, OHC function, supra-threshold ABRs, or on the first synapse of the auditory system.

### **3.1.7 Conclusion**

The measurements presented here contain the assessment of OHC, IHC, and the ascending auditory pathway. The analysis of these data demonstrate consistently that a single treatment with mifepristone, corticosterone or spironolactone had no influence on the unimpaired, native hearing of the rat.

## **3.2 The effect of different corticosterone levels on normal hearing**

A single injection of 30 mg/kg corticosterone highly affects *c/c* levels in rats shortly after application (Fig. 8, *c/c* ratio). The drug then gets quickly metabolized and subsequently *c/c* ratios return to baseline. Yet, a single injection of corticosterone does not influence the electromechanical properties of hair cells (Fig. 9), its ABR thresholds (Fig. 10 – 11), growth functions (Fig. 12 – 16) or the inner hair cell ribbon number (Fig. 17). The experimental design of a single drug application mimics the physiological state of an acute stress response but neglects any given effects of a prolonged stress reaction, known as *chronic stress*. As a consequence, another experiment was performed to further investigate the effect of corticosterone application over time and to better understand the effect of chronic stress on the hearing function of the rat.

drug agent	c/c value		activation or blockage of receptors		
	via drug injection	endog. level	GR	MR	
① vehicle	—	+ 	→	—	—
② Corticosterone 3 mg/kg		+ 	→	✓	✓
③ Corticosterone 30 mg/kg		+ 	→	✓	✓

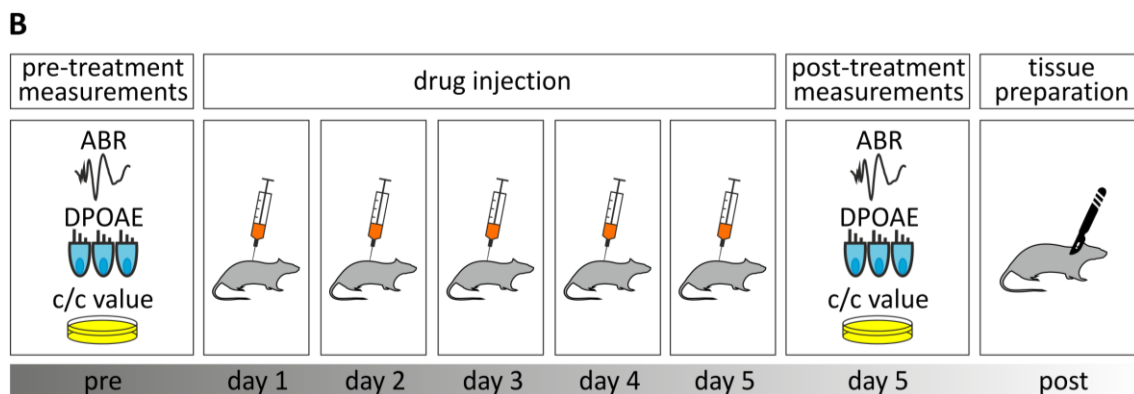


**Figure 18. Experimental design of repeated corticosterone applications to mimic chronic stress.** **A.** Three different treatment groups indicated by ① - ③. Corticosterone acts as GR- and MR-agonist as illustrated with a check mark for GR-/ MR-activation. A blue hyphen stands for receptor activity not exceeding baseline conditions. Vehicle substance is marked as “no effect”. **B.** Time scale of the experiments.

Animals were randomly assigned into three groups that received different concentrations of corticosterone (3 mg/kg or 30mg/kg) or a vehicle substance for five consecutive days. Each group contained six animals. The drug effect of the corticosterone injection on the rats’ metabolic system was measured as urinary c/c ratio. Pre-test measurements (ABR, DPOAE and c/c analysis of urine samples) have been conducted before drug injection. After five days of consecutive drug injections, follow-up measurements were conducted before sacrificing rats for tissue preparation (Fig. 18).

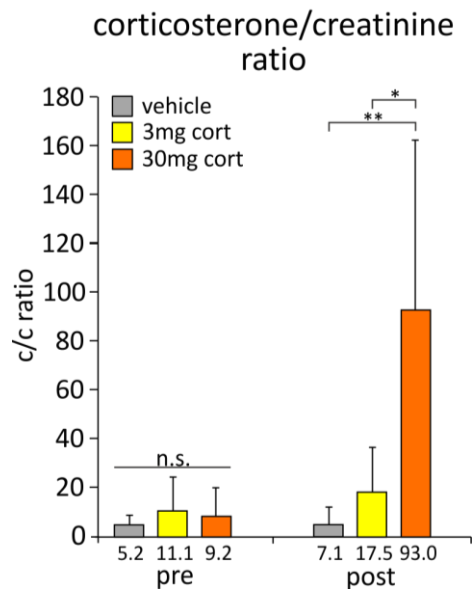
### 3.2.1 The effect of a continuous treatment with corticosterone on c/c ratio

In Figure 19, c/c ratios are shown for pre-test and post-test rat urine. Whereas no significant difference between groups was noted before the experiment (labelled as *pre*), after drug injections (labelled as *post*) c/c ratios significantly peaked in the high-corticosterone group (30 mg/kg) when compared to low-corticosterone and vehicle. The low-corticosterone group (3 mg/kg) experienced a slight increase in c/c ratio yet did not reach significance when compared to vehicle. Taking the findings in chapter 3.1 into account, it can be concluded that repeated application of highly concentrated corticosterone (30mg/kg) increases c/c ratios significantly over the period of the experiment, whereas a lower concentration of corticosterone (3 mg/kg) does not.

**Figure 19. Corticosterone/creatinine ratio (c/c ratio) of urine samples.**

Changes in the c/c ratio are shown for each individual group before the experiment and after five days of continuous drug application, measured with ELISA. There was no significant difference between groups before the experiment. After the pharmacological treatment, c/c ratios peaked in the 30 mg/kg corticosterone group (orange bars) significantly when comparing to vehicle and to the 3 mg/kg corticosterone regimen.

1-way ANOVA. Error bars represent SD (n = 6 animals per group); n.s., not significant. \*P < 0.05, \*\*P < 0.01. Cort = corticosterone. For details of statistical analyses, see Supplemental Table 1.



### 3.2.2 A continuous treatment of corticosterone on OHC function displays no effect on OHC function

Analysis of outer hair cell function of treated rats was executed in the same way as the experiment with GR- and MR-potent pharmaceuticals in chapter 3.1. Results are displayed in Fig. 20. The maximum of the 2f1-f2 amplitude did not differ before the experiment (*pre*) and no effect of corticosterone was visible after the drug application of corticosterone over five days (*post*, Fig. 20A). In a next step, DP thresholds were analyzed and plotted against frequencies (Fig. 20B). Again, no significant effect between treatment groups was noted neither before nor after the course of the experiment.

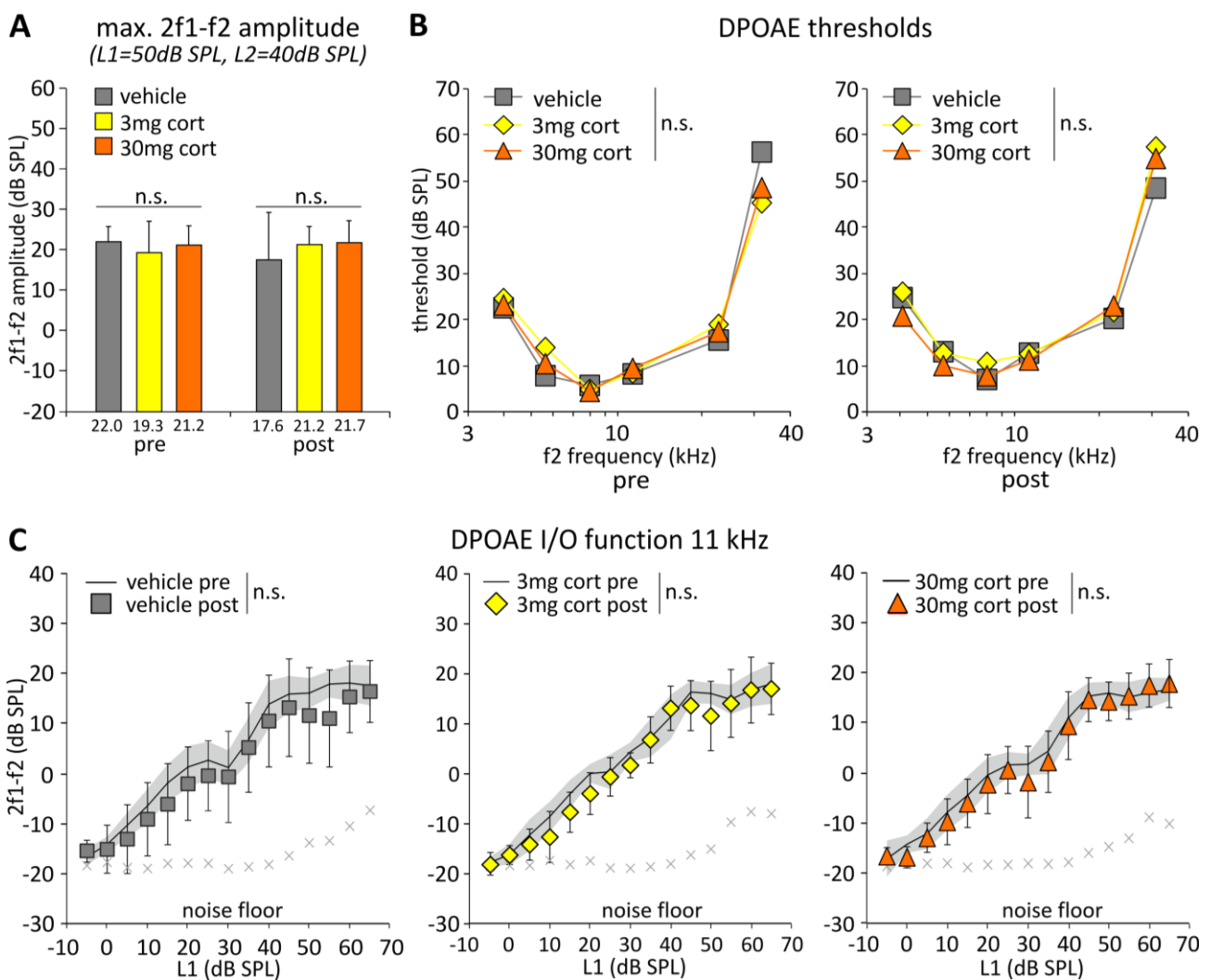


**Figure 20. Multiple injections of high corticosterone (30 mg/kg) or low corticosterone (3 mg/kg) exhibit no influence on outer hair cell function.** **A.** Different concentrations of corticosterone display no effect on DPOAE amplitude before (*pre*) and after drug application (*post*). Also, no effect over time was noted. 1-way ANOVA, two-tailed paired t-test. **B.** DPOAE thresholds for frequency-specific tones before drug application (*pre*) and after drug application (*post*). No changes were noted between groups. 2-way ANOVA. **C.** Treatment had no impact on input-output growth function before drug application (black line with grey shadow as SD) and at 5d post treatment (colored symbols with SD as antenna). Noise floor visualized with grey crosses. Significances were checked with 2-way matched RM ANOVA (ranging from 0 - 65 dB SPL). Error bars represent SD ( $n = 9-14$  ears/ 6 animals per group); n.s., not significant. For details of statistical analyses, see Supplemental Table 1.

In Fig. 20C, growth functions of the distortion product of  $f_2 = 11.3$  kHz were calculated in dependence of stimulus intensity (L1 in dB SPL). To best see differences between treatments, pre-test values of each group were plotted with post-treatment data points of same group. Resulting variations regarding slope, reach or strength of the input/output function remained marginal within treatment groups and statistical analysis showed no significant difference of neither treatment.

Taken together, consecutive drug injection of corticosterone over the course of five days, mimicking chronic stress with significantly elevated c/c ratios, does not alter OHC sensitivity or supra-threshold OHC behavior.

### **3.2.3 A continuous treatment with corticosterone displays no effect on ABR thresholds**

To evaluate the influence of corticosterone on auditory brainstem responses, ABR thresholds were analyzed in Fig. 21 and 22. Click and noise stimuli were recorded before and after pharmacological treatment (Fig. 21 A, B). Before the experiment, no difference between groups was noted. After the corticosterone injections, values remained unaltered and did not significantly differ when compared to vehicle.

The pure-tone evoked ABRs allow the analysis of more detailed, frequency-specific hearing (Fig. 21 C). Whereas before the experiment no difference between groups was noted, after drug injections, thresholds differed significantly at 5.66 kHz between the high corticosterone group (30 mg/kg) and vehicle. To certify this finding, the presumed pharmacological effect within the 30 mg/kg corticosterone group was tested over time. Interestingly, no significant divergence between pre- and post-values were found, although statistical power should be even higher for paired observations, rendering this finding negligible (data not shown. For more information, see Supplemental Table 1). The remaining frequencies (1.41 kHz – 32 kHz) remained unaffected by the corticosterone treatment.

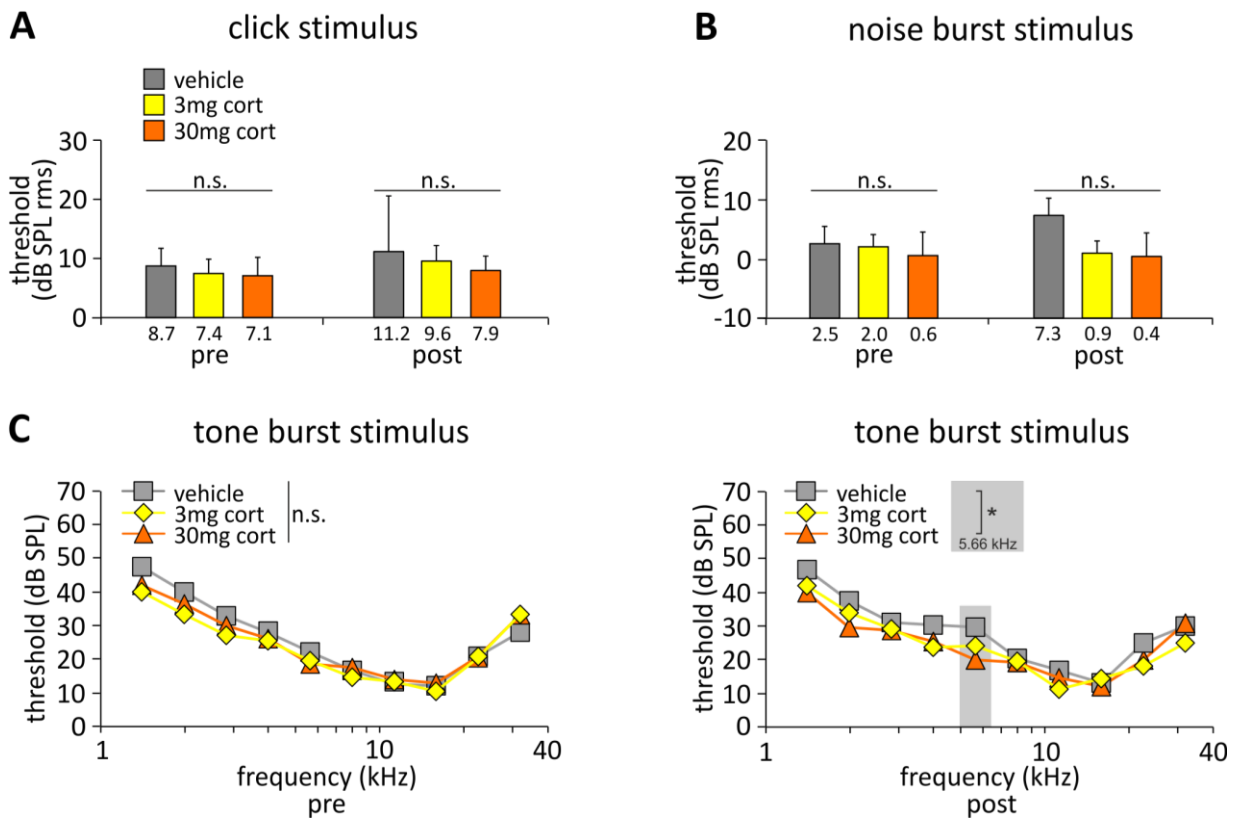


**Figure 21. A consecutive application of corticosterone exhibits no influence on hearing thresholds.** **A, B.** Application of 3 mg/ kg (yellow bars) and 30 mg/ kg corticosterone (orange bars) show no effect on click or noise-burst stimulus-evoked ABR thresholds compared to vehicle (grey bars) after treatment. Threshold in dB SPL rms (root mean square). 1-way ANOVA. **C.** ABR thresholds for frequency-specific tones before drug application (pre) showed no differences before the experiment. After drug application, a significant difference between high corticosterone and vehicle group was noted for 5.66 kHz. 2-way ANOVA.  $P = 0.0045$  Error bars represent SD ( $n = 3-12$  ears/ 3-6 animals per group); n.s., not significant. \*  $P < 0.05$ . For details of statistical analyses, see Supplemental Table 1.

Frequency-specific stimuli had been re-recorded and analyzed for 4 kHz (Fig. 22A), 11.3 kHz (Fig. 22B) and 32 kHz (Fig. 22C) with a lower increment of sound intensity to be able to detect even small differences between thresholds. Before the experiment, pre-test values displayed no significant difference between groups. After drug application, thresholds remained unaffected and even the observed drug effect for 30 mg/ kg corticosterone for a 5.66 kHz tone burst stimulus (Fig. 21 D) could not be reproduced with a 4 kHz tone burst stimulus. Taken together, these findings suggest that multiple drug applications with different corticosterone concentrations did not alter ABR thresholds significantly for click and noise stimuli as well as for frequency-specific ABR threshold analysis between 1.41 and 32 kHz.



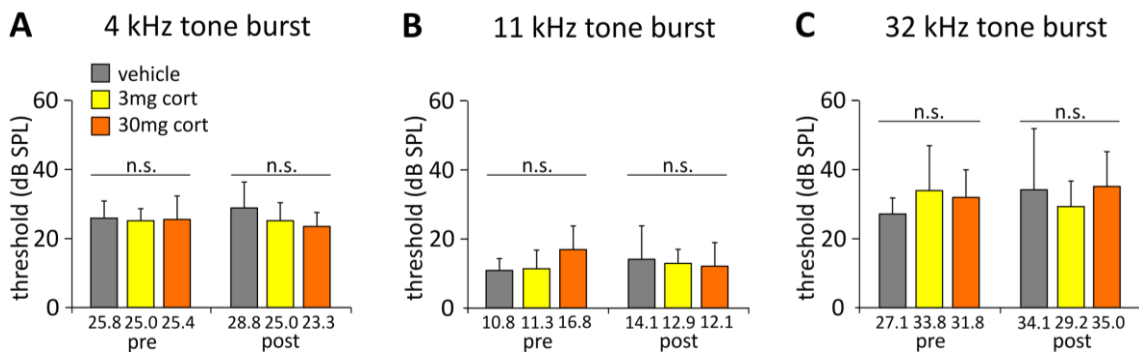


**Figure 22. Consecutive application of corticosterone does not influence hearing thresholds.** A-C. Thresholds upon treatment with 3 mg/kg corticosterone (yellow bars) and 30 mg/kg corticosterone (orange bars) were not significantly altered after drug application when compared to vehicle treatment (grey bars). Thresholds have been evaluated for low (4 kHz), medium (11.3 kHz) and high (32 kHz) frequencies. 1-way ANOVA, two-tailed paired t-test. Error bars represent SD (n = 6-8 ears/ 6 animals per group); n.s., not significant. For details of statistical analyses, see Supplemental Table 1.

### 3.2.4 A continuous treatment with corticosterone displays no significant effect on supra-threshold responses to a 32 kHz stimulus

To be able to analyze supra-threshold hearing, the amplitude growth of early (wave I) and late (wave IV) threshold-normalized ABRs of a 32 kHz stimulus was plotted against increasing stimulus intensities in Fig. 23. The ABR wave amplitude growth was calculated before and 5 days after drug application to reveal possible effects on the auditory nerve (wave I) and the inferior colliculus (wave IV). Each treated group was plotted against an averaged *all pre* group, containing data of pre-test measurements.

When analyzing the resulting supra-threshold responses in Fig. 23, no striking effect but slight aberrations between *all pre*- and post-values of low corticosterone (3 mg/kg) and vehicle group could be noted. To certify these findings and to be able to perform statistical analyses, the maximum amplitude size (Fig. 24 A, C) and maximum dynamic response *reach* (Fig. 24 B, D) for wave I and wave IV were plotted against dB stimulus level with the reach of the response defined as the stimulus level at maximum response and size defined as maximum amplitude of said data point (for details see chapter 3.1).

32 kHz tone burst stimulus

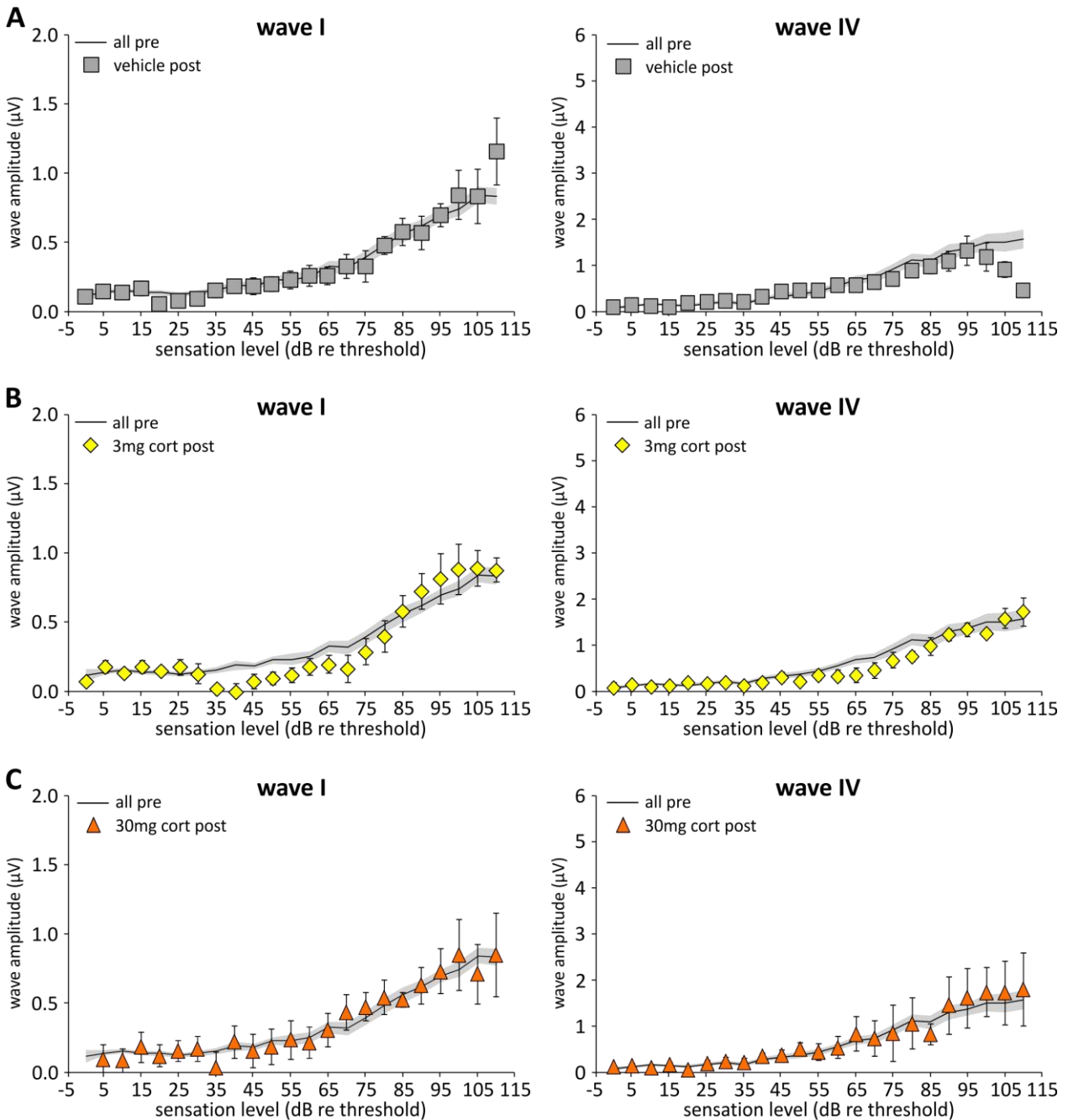


**Figure 23. Multiple injections of different concentrations of corticosterone show no striking effect on early (wave I) and late (wave IV) supra-threshold ABR wave responses to frequency-specific tone burst stimuli at 32 kHz. A-C.** Animals were treated with vehicle (grey squares), 3 mg/kg corticosterone (yellow diamonds) and 30 mg/kg corticosterone (orange triangles). Baseline responses before drug application (*all pre*) are shown as grey line (mean) with shadow (SEM). The ABR slope displays the response to a 32 kHz pure-tone burst stimulus on different levels of the auditory pathway (auditory nerve: wave I, inferior colliculus: wave IV) five days after continuous drug application. Data are displayed threshold normalized. Error bars indicate SEM (n = 4-6 ears / 4-6 animals per group).

dynamic range 32 kHz

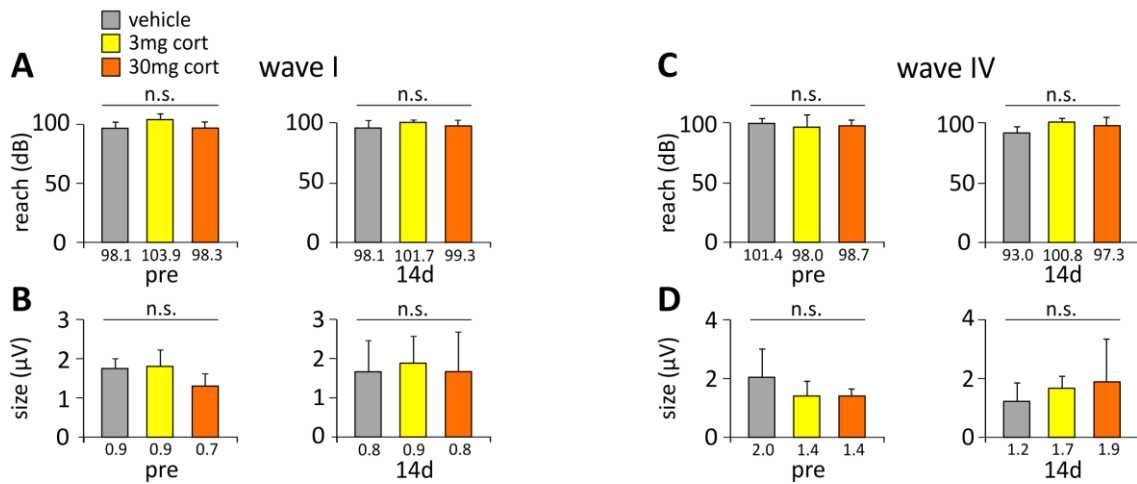


**Figure 24. Consecutive treatment with 3 mg and 30 mg corticosterone has no impact on reach and response size of ABRs to 32 kHz sound stimuli.** The reach of the response range represents the stimulus level at the maximum response of the wave amplitude. The size is defined as the wave amplitude of said response. See also (Singer, Kasini et al. 2018). **A, B.** ABR wave I reach and size for 32 kHz stimuli five days after consecutive drug application. Animals were treated with vehicle (grey bars), 3 mg/kg corticosterone (yellow bars), or 30 mg/kg corticosterone (orange bars). No significant differences were found between groups. 1-way ANOVA. **C, D.** ABR wave IV reach and size for 32 kHz stimuli after five days of treatment. Again, no significant effect of treatment regimens on reach and size of ABRs was found. 1-way ANOVA. Data are displayed threshold normalized. Error bars represent SD (n = 3-6 ears/ 3-6 animals per group). n.s., not significant. Numbers below x-axis indicate wave size and reach in  $\mu\text{V}$ . For details of statistical analyses, see Supplemental Table 1.

Despite slight variations in amplitude size and slope in Fig. 23 after treatment, all groups maintained their response size and response reach for early (wave I) as well as for late ABR (wave IV) waves to a 32 kHz stimulus in Fig. 24 with no significant differences between groups being noted. It can therefore be concluded that a five-day-treatment with 3 mg/kg corticosterone or 30 mg/kg corticosterone has no significant effect on supra-threshold ABRs to 32 kHz sound stimuli.

### 3.2.5 A continuous treatment with corticosterone displays no significant effect on the first synapse of the auditory pathway

As active release sites, synaptic ribbons contribute to the precision of the firing rate of auditory fibers. Therefore, the influence of a consecutive treatment with corticosterone on the IHC synaptic ribbons was investigated in Fig. 25. IHC ribbons were counted in different tonotopic regions to assess the integrity of the first synapse of the auditory pathway for different frequency ranges. Interestingly, application of corticosterone seems to reduce the averaged ribbon number and consecutively impair signal transduction in apical and medial turns, albeit not reaching significant levels. Here, a higher corticosterone concentration leads to a greater reduction of the ribbon count than lower corticosterone concentrations.

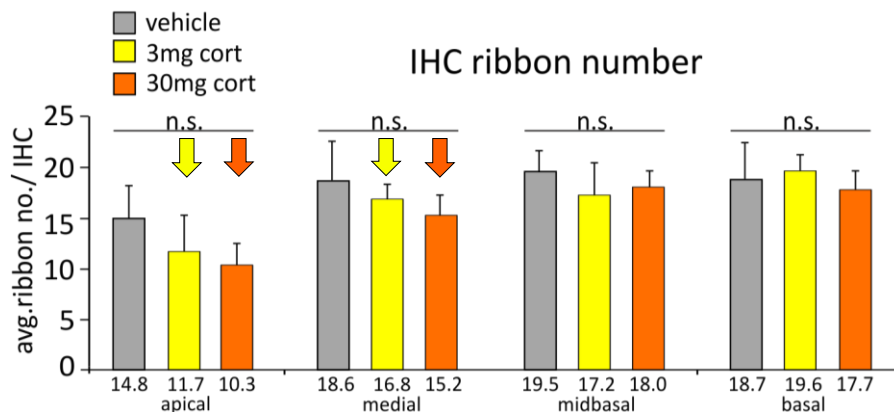


**Figure 25. IHC ribbon number is not significantly impaired by a five-day drug application with 3 mg/kg or 30 mg/kg corticosterone.** Treatment with 3 and 30 mg/kg corticosterone (orange bars) slightly decreases ribbon count in apical and medial turns of the cochlea, albeit not significant (indicated with arrows). Y-axis depicts the averaged ribbon number per IHC. Numbers below x-axis depict average ribbon number per IHC. Error bars represent SD. n.s., not significant. For details of statistical analyses see Supplemental Table 1.

### 3.2.6 Conclusion

After carefully assessing function and properties of OHC, IHC, and the ascending auditory pathway as presented, it can be concluded that a continuous treatment with low-dose corticosterone (3 mg/kg) or high-dose corticosterone (30 mg/kg) has no significant influence on the native hearing sensitivity and supra-threshold behavior of the rat. However, treatment may slightly influence subcellular ribbon structures. Taken together, neither single drug application (*acute stress*, chapter 3.1), nor a continuous drug application of corticosterone over five days (*chronic stress*) affects the hearing function in the rat significantly.

### **3.3 The role of the GR and the MR during excessive noise exposure and subsequent hearing recovery**

As shown in chapter 3.1, a single treatment with mifepristone, corticosterone or spironolactone had no significant effect on ABR thresholds, OHC function, supra-threshold ABRs, or the first synapse of the auditory pathway. Same findings were obtained for a consecutive treatment with different corticosterone concentrations (chapter 3.2). Thus, it can be concluded that activation and attenuation of GR- and MR-receptors does not affect normal hearing.

To further investigate the role of distinct GRs on noise vulnerability and hearing recovery, GRs and MRs were either stimulated or blocked before acoustic trauma with corticosterone (GR-/MR-agonist), mifepristone (GR antagonist) or spironolactone (MR antagonist). The experiment was rolled out according to the design in chapter 3.1 (Fig. 7) and sham treatment was replaced with acoustically traumatizing exposure, leading to acoustic trauma (AT). Hearing assessment consisted of pre-test recordings of ABRs and DPOAEs and follow-up measurements at four different time points. See also (Singer, Kasini et al. 2018).

#### **3.3.1 GR blockage with mifepristone (GR antagonist) maintains DPOAE thresholds best after AT**

OHC function was analyzed and results are displayed in Fig. 26. The maximum amplitude of DOPAEs is shown for each pharmacological group and compared to an *all pre* group, containing pre-test measurement data of all animals to serve as reference (Fig. 26A). Significant differences between values within the *all pre* group have been ruled out by statistical testing before being merged.

No significant differences between treatment groups and *all pre* were noted before the experiment. Three days after noise exposure, the maximal DPOAE responses of all noise-exposed animals were significantly lower when compared to *all pre*. However, animals treated with corticosterone and mifepristone displayed higher remaining signal levels than animals treated with vehicle and

spironolactone when compared to *all pre*, albeit not significant. Over the course of the experiment, the maximum response returned to almost normal levels, with animals treated with spironolactone showing best amplitude recovery after major initial amplitude loss. 14 days after acoustic trauma, only the vehicle-treated group displayed a significant permanent amplitude loss when compared to *all pre*.

In Fig. 26B, DPOAE thresholds are displayed at four different time points throughout the experiment. Again, before the experiment no significant differences between groups were noted. Three days after acoustic trauma however, thresholds increased for all noise-treated groups with great variations between treatment regimens. The mifepristone-treated group (GR-antagonist) showed best preserved thresholds, followed by animals treated with corticosterone (GR- and MR-agonist). Interestingly, pre-treatment with mifepristone preserved frequencies significantly around the bandwidth of the AT when compared to vehicle (8 kHz, 11.3 kHz), whereas lower and higher frequencies only displayed insignificant changes after AT. This inter-group difference is then lost 7 and 14 days after noise treatment. Over time, thresholds recovered within every group and again, spironolactone-treated animals displayed best threshold recovery over time. The *all pre* reference group in Fig. 26 B was excluded from statistics for factor 'drug effect'.

To be able to tell long-lasting drug effects apart from short-term drug effects, thresholds of sham-treated animals and noise-exposed animals 14 days after noise exposure were plotted for each individual treatment in Fig. 26C. Significant threshold losses were found for animals treated with vehicle substance (at 8 kHz, 11.3 kHz, and 22.6 kHz), corticosterone (at 22.6 kHz), and spironolactone (at 11.3 kHz), whereas treatment with mifepristone did not alter thresholds significantly.

Lastly, the DPOAE growth function for a 11.3 kHz stimulus is displayed in Fig. 26D, where amplitude strength ( $2f_1-f_2$ ) is plotted against stimulus intensity (L1 in dB SPL) for each individual drug treatment 14 days after sham treatment or noise exposure respectively. Each noise-treated group presented noticeable amplitude loss 14 days after exposure when compared to sham groups. However, animals

treated with spironolactone and mifepristone maintained slightly better signal strength when compared to treatment with corticosterone and vehicle substance, albeit not statistically significant.

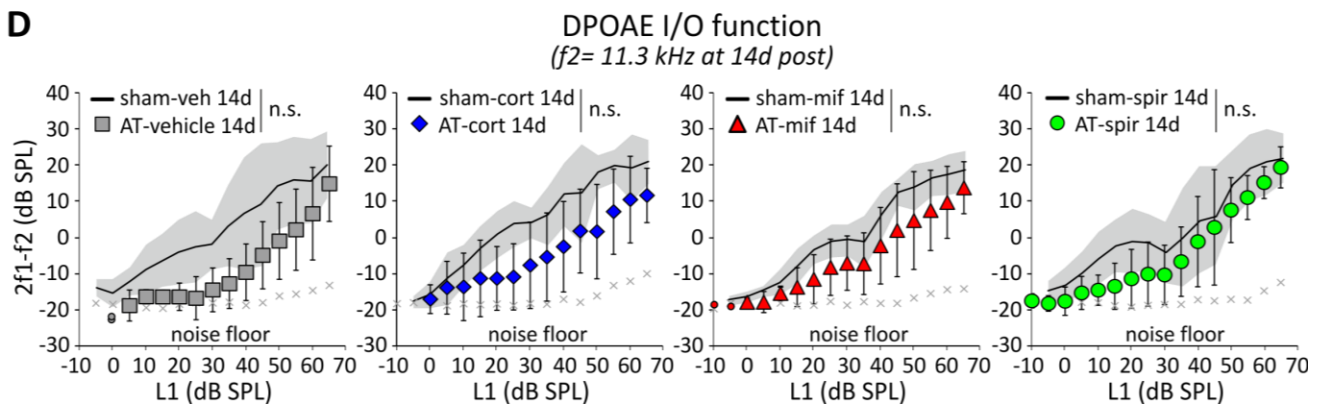
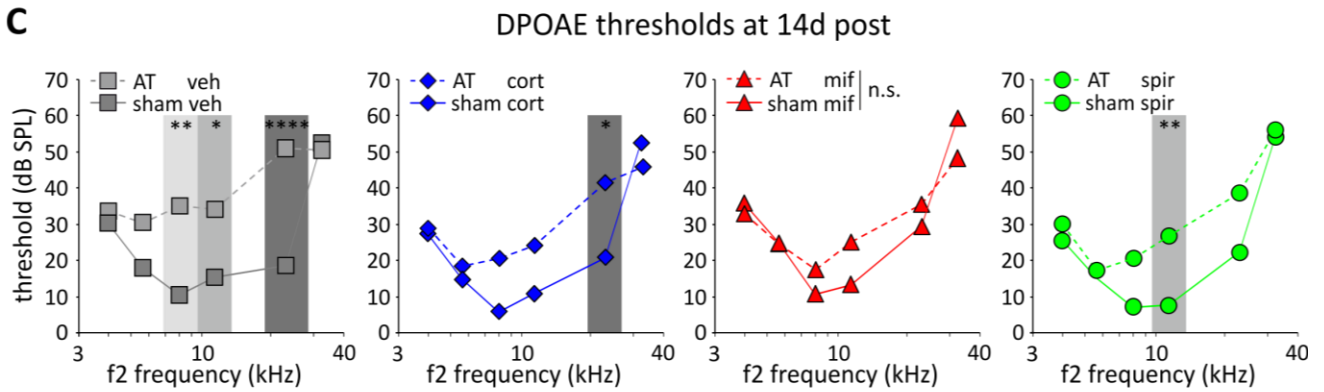
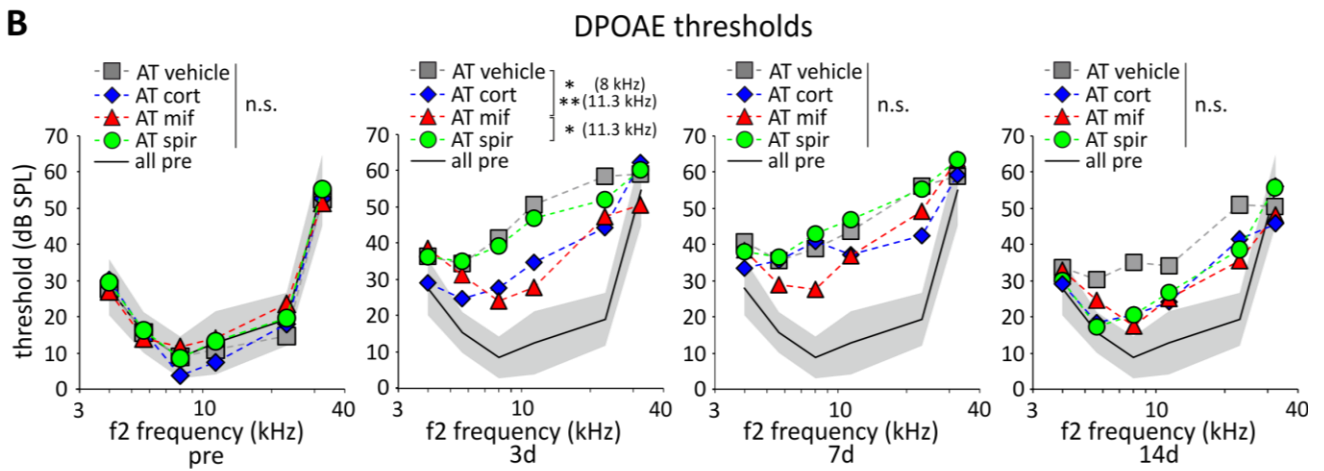
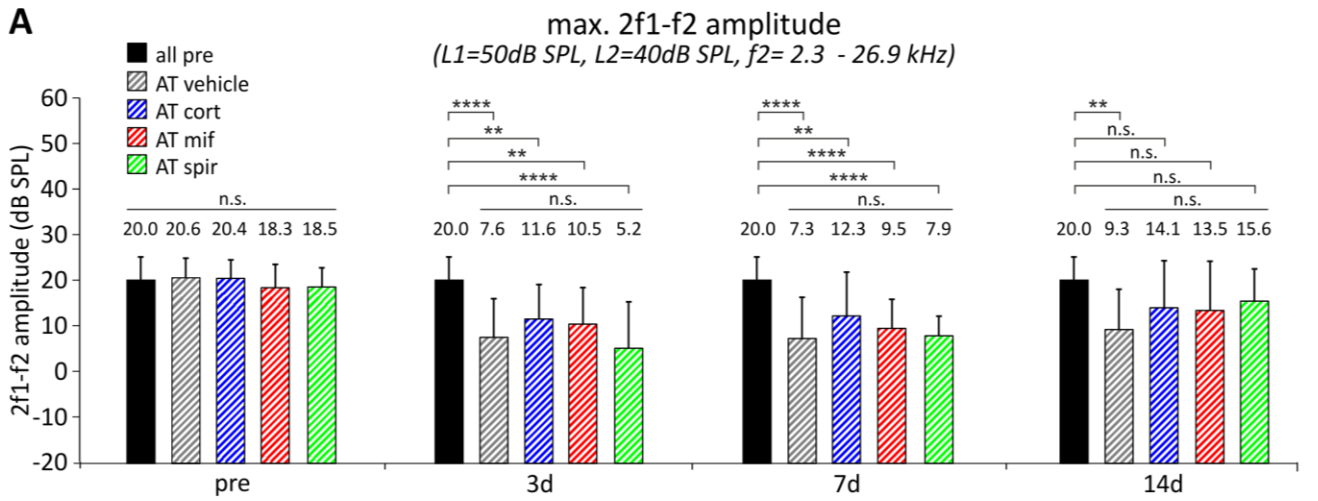
*Summarizing GR and MR function on OHC vulnerability*

Excessive noise significantly impaired DPOAE amplitude and increased DP thresholds, especially shortly after acoustic trauma.

GR blockage with mifepristone maintained DPOAE thresholds significantly better than treatment with corticosterone, spironolactone or vehicle substance (Fig. 26 B). This finding can be either the result of decreased OHC vulnerability during noise exposure or due to an ample threshold recovery shortly after acoustic insult exerted through GR blockage.

MR blockage with spironolactone slightly aggravated OHC vulnerability shortly after AT when compared to vehicle group with an ensuing substantial recovery of DPOAE thresholds and amplitudes underlining the importance of MR receptors during disruptive acoustic overexposure.

Subsequently, this discovery may reveal a disruptive role of GR mediated molecular responses and suggest that the corticosterone-related effect (GR-/MR-agonist) of DPOAE threshold and amplitude preservation after excessive noise (Fig. 26 A, B), albeit being non-significant, may be exerted through MRs.





### 3.3.2 GR blockage with mifepristone (GR antagonist) maintains ABR thresholds best 14 days after AT

In the next step, ABR thresholds to a click stimulus (Fig. 27A) and noise band stimulus (Fig. 27B) were assessed at five different time points. Individual groups did not differ significantly before the experiment. However, thresholds increased drastically 60 minutes after traumatizing noise (labelled as *day 0*). ABR thresholds of vehicle-treated animals escalated shortly after AT, followed by corticosterone-, mifepristone-, and spironolactone-treated animals. In contrast with DPOAE data, spironolactone here displays a threshold-preserving feature shortly after AT in click stimulus recordings. 14 days after AT, thresholds of traumatized groups recovered, yet with still significant permanent threshold loss when compared to *all pre*. Between the pharmacological regimens, no statistically significant differences were noted 14 days after noise exposure (Fig. 27 A).

---

**Figure 26. Pre-treatment with mifepristone but not corticosterone or spironolactone preserves OHC function after acoustic trauma significantly.** **A.** Pre-values of experimental groups did not exhibit differences before being exposed to acoustic trauma (AT). Three days after acoustic trauma, AT-animals (grey bars) displayed a significantly smaller amplitude of DPOAE function. Spironolactone- and vehicle-treated animals exhibited severe initial amplitude losses, although DPOAE amplitude was partly regained 14d after acoustic trauma. Vehicle group maintained a significant amplitude loss when compared to *all pre* 14 days after AT. 1-way ANOVA. Tukey's multiple comparison test. **B.** Treatment with mifepristone (GR-antagonist, red) and corticosterone (GR-/MR-agonist, blue) exhibited a threshold-protecting feature 3d after AT that cannot be found in groups treated with vehicle or spironolactone (MR antagonist, green). *All pre* values are depicted as black line with shadow as SD. After 7 and 14 days, thresholds were regained throughout all groups and became insignificant between treatments. 2-way ANOVA. Tukey's multiple comparison test. **C.** To further investigate long term effects of treatments after AT, DPOAE threshold losses were displayed individually for each group and noise exposed animals were plotted against their sham treatment 14 days after AT (replotted from Fig. 9). Vehicle-, corticosterone- and spironolactone-pre-treated animals displayed a permanent threshold loss that reached significant levels between 8 kHz and 22.6 kHz. Mifepristone-treated animals displayed an ample threshold recovery. 2-way ANOVA. Bonferroni's multiple comparison test. **D.** Drug treatment (color symbols) had no significant effect on input-output growth function when compared to sham-exposed pre-treated animals (black line with grey shadow as SD) at 11.3 kHz. Noise floor visualized with grey crosses. The *all pre* group was excluded from statistics. Significances were checked with 2-way matched RM ANOVA (ranging from 20 - 65 dB SPL). Error bars represent SD (n = 3-64 ears/ 3-32 animals); n.s., not significant. \* P < 0.05, \*\* P < 0.01, \*\*\*\* P < 0.0001. For details of statistical analyses, see Supplemental Table 1.

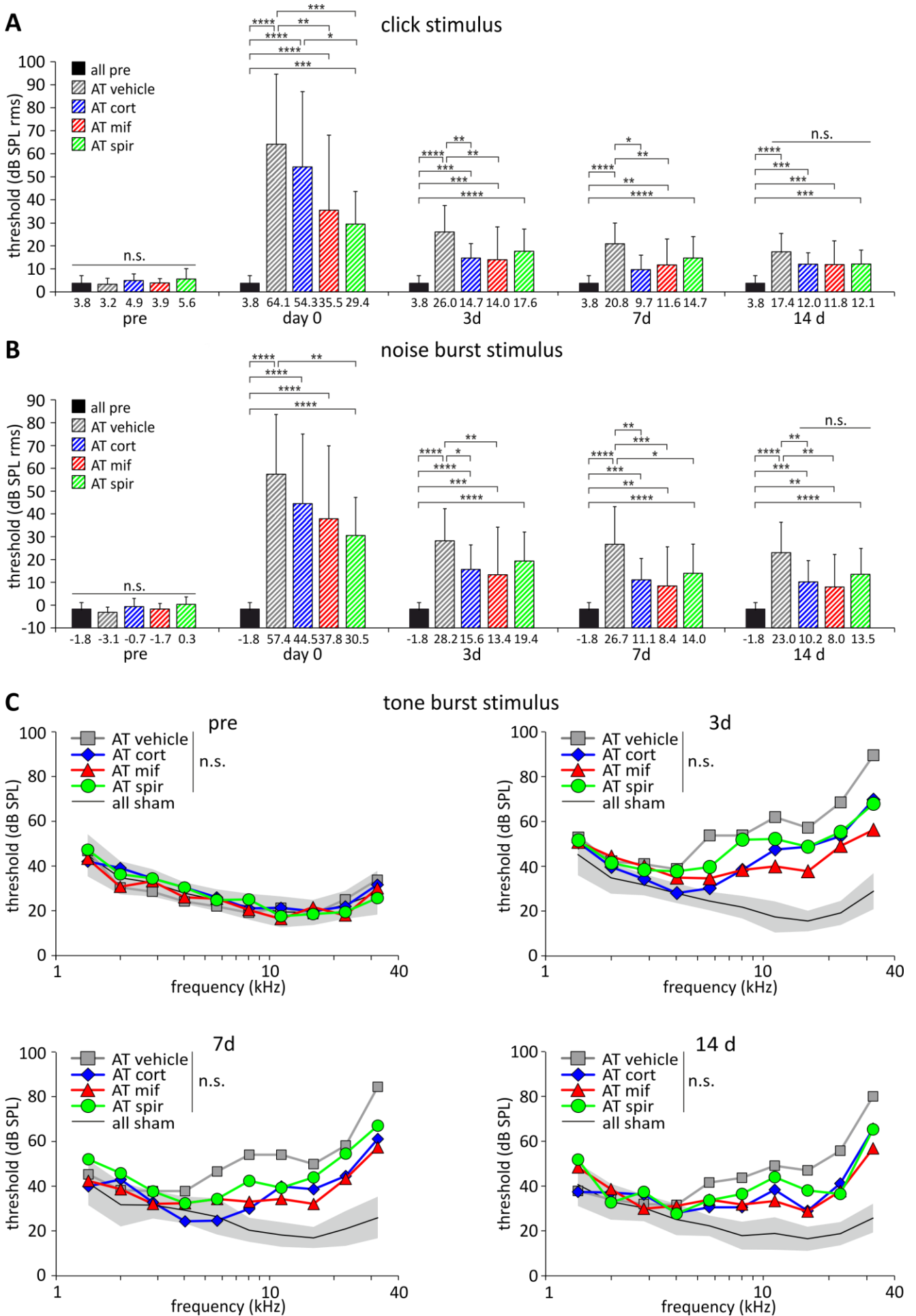
When assessing ABRs to higher frequencies with a noise band stimulus (Fig. 27 B), similar findings as in Fig. 27 A were observed. This time, even 14 days post noise exposure, pre-treatment with corticosterone and mifepristone maintained thresholds significantly better when compared to pre-treatment with vehicle.

In Fig 27C, frequency-specific thresholds were analyzed between 1.41 kHz and 32 kHz. For reference, averaged thresholds of all sham-treated animals (labelled as *all sham*) were added to the graph. The *all sham* group contains data from chapter 3.1, where significant differences between the pharmacological treatment regimens of corticosterone, mifepristone and spironolactone were being ruled out before being merged into one group.

Thresholds did not differ in pre-treatment measurements. Yet, 3 days after AT, threshold loss occurred for all noise-treated groups between 5.66 kHz and 32 kHz. Again, vehicle group was leading in threshold loss, followed by spironolactone, corticosterone and lastly mifepristone. Although thresholds recovered over time, this specific ranking is maintained throughout the experiment and shows the consistency of threshold loss within one group, similar to Fig. 27 A and B.

---

**Figure 27. Pre-treatment with mifepristone preserves ABR thresholds best after acoustic trauma. A, B.** Spironolactone (green bars) maintains click and noise thresholds after acoustic trauma better than mifepristone- (red bars) and corticosterone-treated animals (blue bars) when compared to vehicle-group (grey bars). Thresholds of all groups recover 14 days after acoustic trauma and subsequently, differences between noise-treated groups lose significance in click stimulus-evoked ABRs. However, pre-treatment with corticosterone and mifepristone maintained thresholds of noise-burst stimulus-evoked ABRs significantly better 14 days after AT when compared to pre-treatment with vehicle. Threshold in dB SPL rms (root mean square). 1-way ANOVA. **C, D.** Pre-treatment with mifepristone more than corticosterone or spironolactone maintains thresholds for frequency-specific tones after AT when compared to vehicle. Threshold loss for all groups occurs between 5.66 kHz and 32 kHz. All sham group added for reference. 2-way ANOVA. Error bars represent SD; n.s., not significant. \* P < 0.05, \*\* P < 0.01, \*\*\* P < 0.001, \*\*\*\* P < 0.0001. For details of statistical analyses, see Supplemental Table 1.

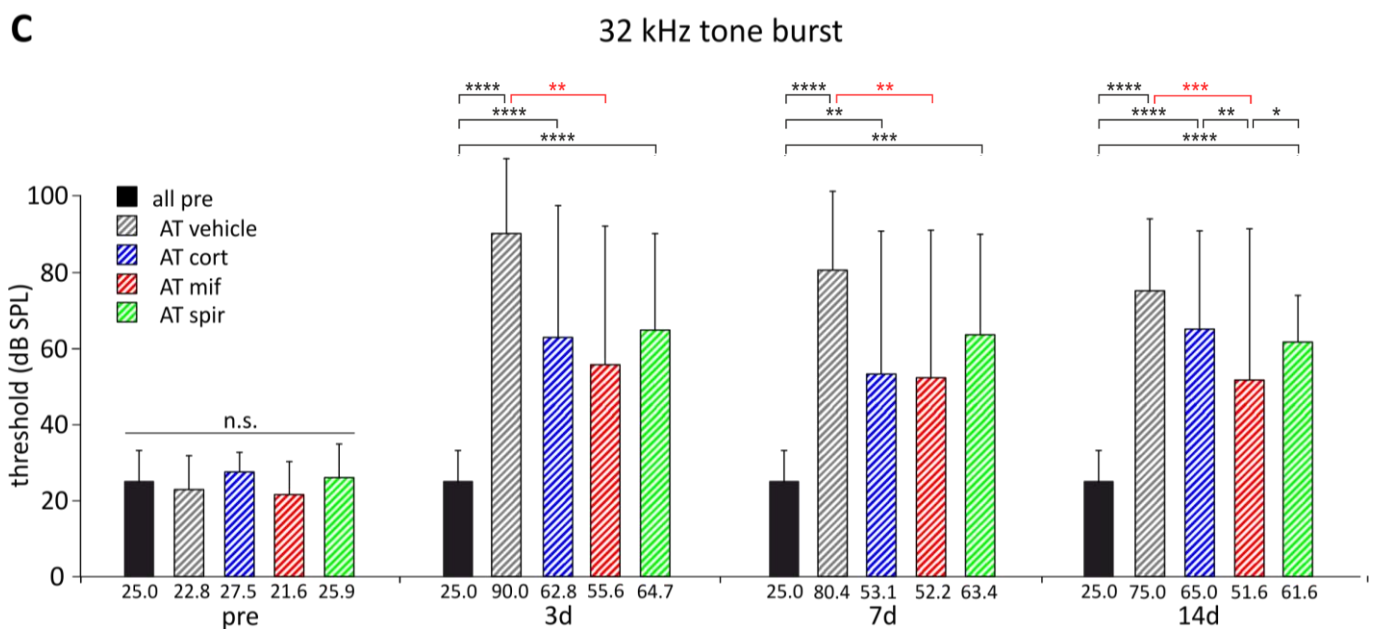
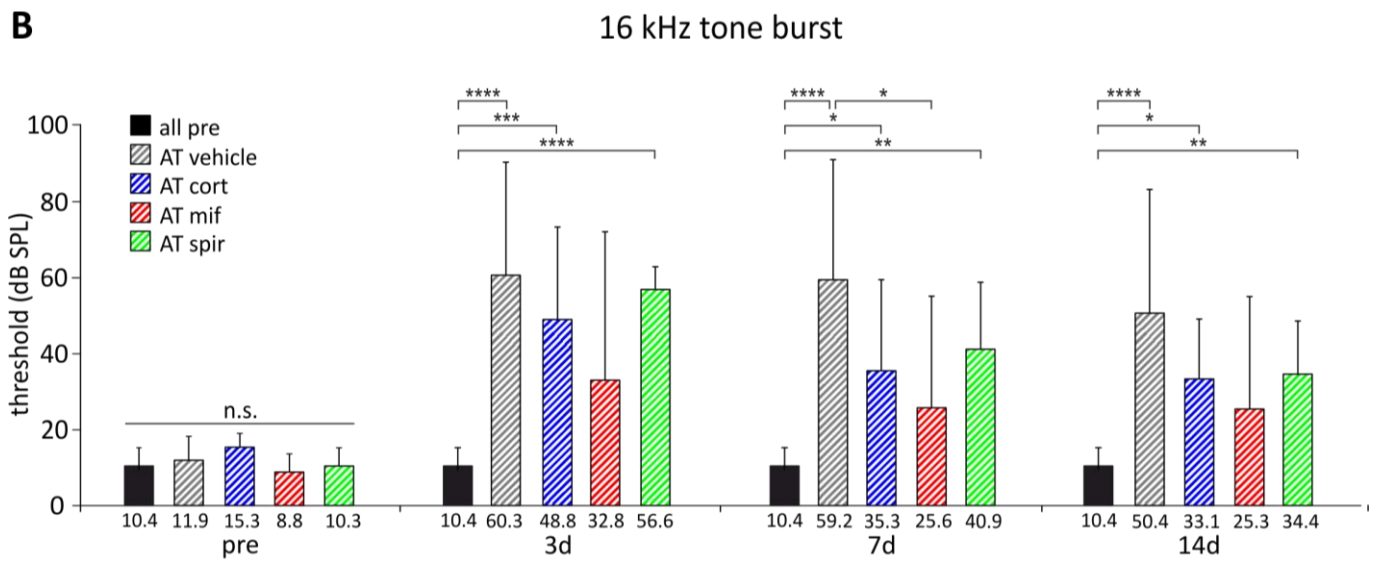
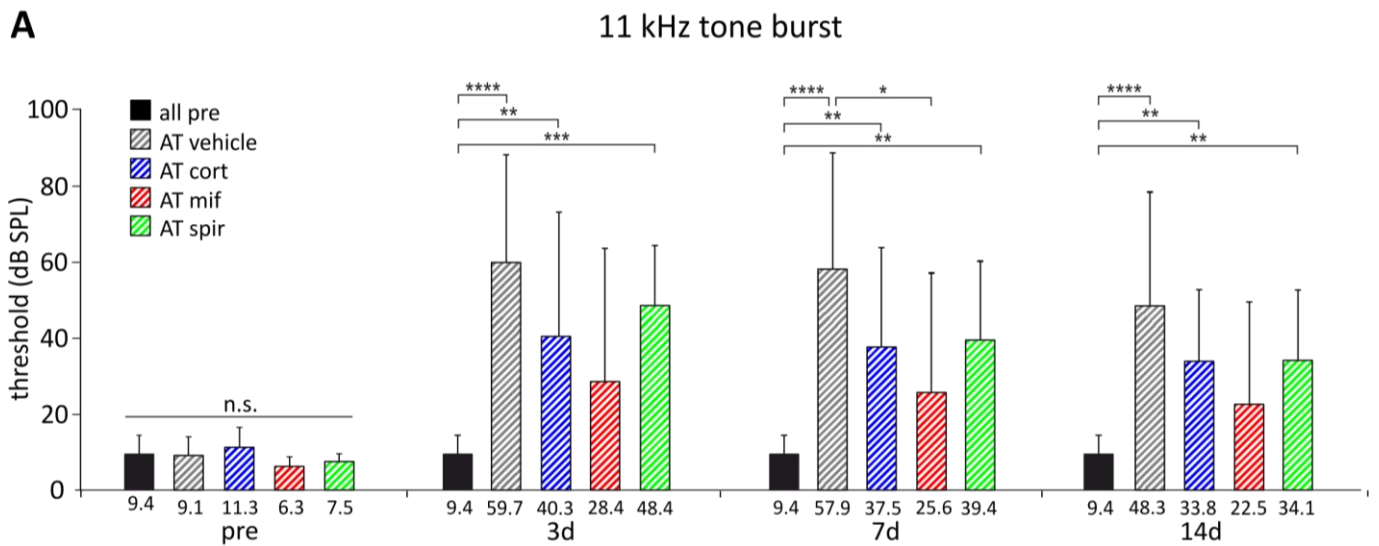


In Fig. 28, depicted frequencies (11.3 kHz, 16 kHz and 32 kHz) were recorded with more repetitions than in Fig. 27 to be able to better distinguish threshold losses between groups. The results confirm the findings in Fig. 27. No differences between groups were striking during pre-test measurements, whereas three days after AT, threshold loss occurred for all groups with vehicle-treated animals displaying highest and mifepristone-treated animals displaying lowest threshold losses. Again, this pattern stays consistent within all frequencies (Fig. 28 A-C) and over time (3d – 14d after AT). At any given time, vehicle-treated animals display the worst outcome when comparing threshold loss, whereas mifepristone-treated groups exhibit best short- and long-term threshold-preserving qualities. The mifepristone group exclusively displays significantly lower thresholds than the vehicle group (Fig. 28 C, highlighted in red) and no significant threshold loss when compared to the *all pre* group. Matching with data shown in Fig. 27 C, higher frequencies were affected more by acoustic trauma (Fig, 28 C, 32 kHz) than medium frequencies (Fig. 28 A and B, 11 and 16 kHz).

Over the course of the experiment, thresholds of all groups recovered and corresponding to earlier findings (OHC behavior after AT, Fig. 26), spironolactone-treated animals displayed best threshold recovery after considerable initial threshold loss when compared to corticosterone and mifepristone.

---

**Figure 28. Pre-treatment with mifepristone maintains thresholds after acoustic trauma best. A-C.** Thresholds before acoustic trauma did not differ significantly. Three days after acoustic trauma, thresholds of corticosterone- (cort, blue bars), spironolactone- (spir, green bars) and vehicle-treated animals (grey bars) differed significantly at 11.3 kHz, 16 kHz and 32 kHz from *all pre* values. At 32 kHz, only mifepristone-treated animals (mif) displayed significantly lower thresholds when compared to vehicle-treated groups (highlighted in red). At no point during the experiment, mifepristone-treated animals exhibited significant threshold loss when compared to *all pre*. These effects are consistent throughout the experiment and are also visible 14d post noise exposure. 1-way ANOVA. Error bars represent SD; n.s., not significant. \* P < 0.05, \*\* P < 0.01, \*\*\* P < 0.001, \*\*\*\* P < 0.0001. For details of statistical analyses, see Supplemental Table 1.



### *Summarizing MR and GR function on ABRs in traumatized animals*

By GR and MR stimulation, corticosterone reduced ABR threshold loss and enhanced threshold recovery, especially in lower frequencies (click and noise stimuli) when compared to vehicle.

GR-blockage with mifepristone attenuates transient as well as permanent threshold losses in all frequencies, yet most effectively in high frequencies.

By blocking MR with spironolactone, substantial threshold losses were found especially in higher frequencies, with subsequent ample recovery.

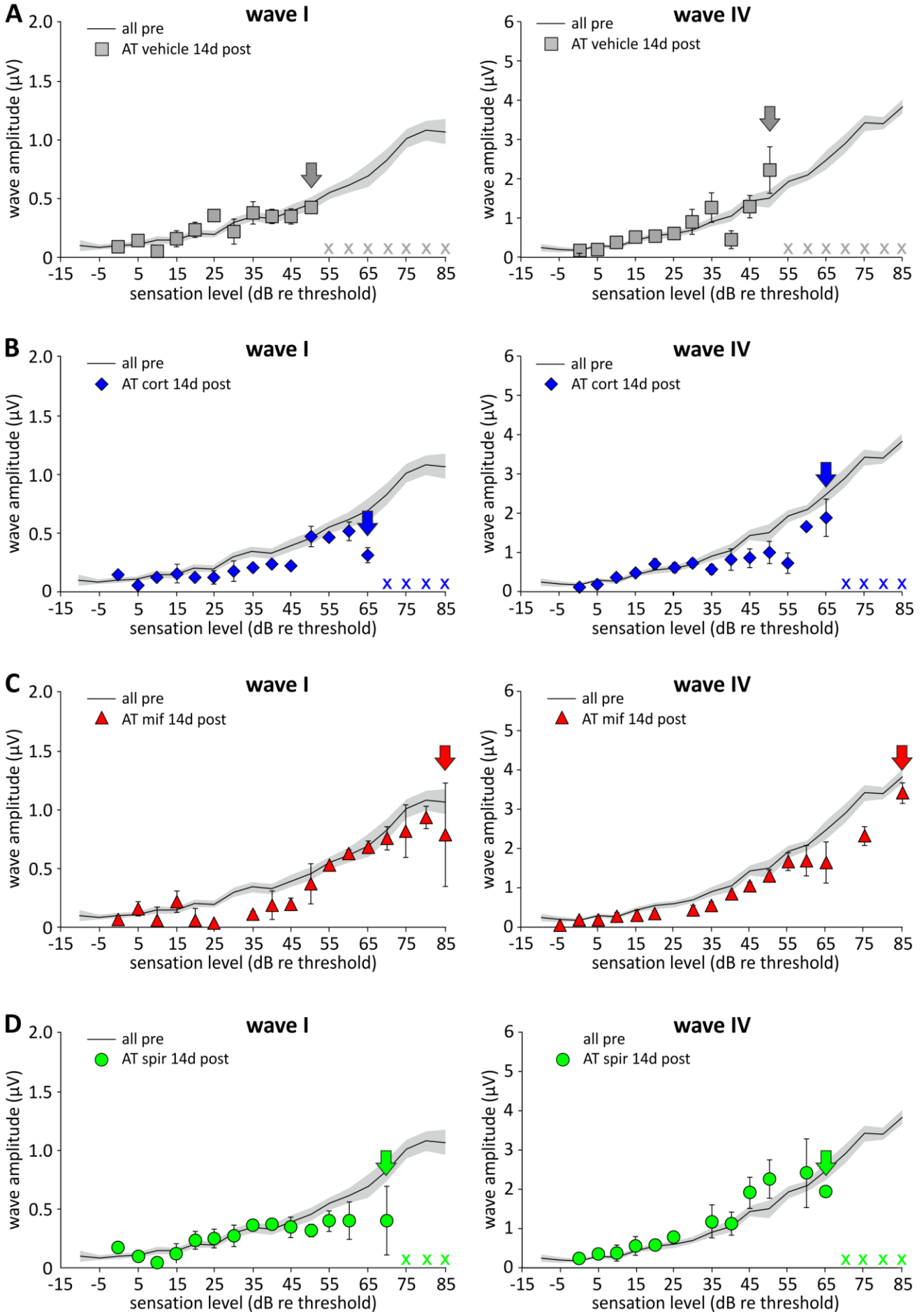
Taking these findings together, one can assume that suppression of GRs, but not MRs, prior to AT maintains ABR thresholds. In a reverse conclusion, GR-mediated signaling elicits disruptive features on ABR thresholds during excessive noise, whereas MR activity may tend to preserve ABR thresholds and the favorable effect of GR-/MR-corticosterone may be exerted through MRs.

### **3.3.3 GR blockage with mifepristone (GR antagonist) maintains supra-threshold responses of a 16 kHz stimulus best after AT**

The last pillar of analysis was the assessment of the activation and inhibition of stress hormone receptors on auditory nerve processing. Therefore, the effect of GR- and MR-potent drugs on supra-threshold ABR wave characteristics was analyzed. The growth of supra-threshold amplitudes of wave I (early ABR) and wave IV (late ABR) to increasing intensities of pure tones was analyzed before and 14 days after acoustic trauma. In Fig. 29, supra-threshold wave amplitudes of post values were plotted and compared to all pre values (*all pre*). As described earlier, pre values were statistically inspected to be non-statistically variant before being merged into one group.

**Figure 29. Treatment with mifepristone (mif, GR antagonist) but not spironolactone (spir, MR antagonist) or corticosterone (cort, GR- and MR-agonist), maintains early (wave I) and late (Wave IV) ABR amplitudes to a wider range at 16 kHz. A-D.** Shown is the effect of vehicle substance, corticosterone, mifepristone and spironolactone application on early and late supra-threshold ABR amplitudes at the level of the AN (wave I) and of the IC (wave IV) in response to 16 kHz pure-tone burst stimuli 14 days after noise exposure. Animals were pre-treated with vehicle (grey squares), corticosterone (blue diamonds) mifepristone (red triangles), or spironolactone (green circles). Baseline responses before drug application (*all pre*) are shown as grey line with shadow (SEM). Arrows in the respective colors indicate highest levels above threshold for which responses could still be determined. Small crosses above the x-axis mark levels that surpass the limits of maximum stimulation levels (usually 110 dB SPL). Data are displayed threshold normalized. Error bars indicate SEM (n = 2-4 ears / 2-4 animals per group). See also (Singer, Kasini et al. 2018), Fig. 6.

16 kHz tone burst stimulus



As anticipated and consistent with previous findings, amplitude increments of noise-treated animals of vehicle-, corticosterone- and spironolactone-treated animals (Fig. 29 A, B, D) stagnated already at moderate levels due to threshold shifts (arrows, Fig. 29 A, B, D) and the maximum amplitude was lower when compared to unimpaired hearing (*all pre*). The ABR wave I (auditory nerve responses) and the ABR wave IV (midbrain responses) were maintained over a broader dynamic range 14 days after acoustic trauma only in animals treated with mifepristone (Fig. 29 C, arrows).

To quantify these observations and to perform statistical analyses, supra-threshold wave responses (wave I and wave IV) of all groups were plotted for ABR amplitude size (Fig. 30 B, D; size) and dynamic response range (Fig. 30 A, C; reach). No effect between groups was noted before the treatment. However, 14 days after noise exposure, differences between groups gained highly significant levels.

Treatment with mifepristone maintained wave I reach better than vehicle- and spironolactone-treated groups, whereas treatment with corticosterone was similarly effective (Fig. 30 A). Also, mifepristone preserved wave I ABR size, while pre-treatment with spironolactone and vehicle resulted in significantly impaired amplitude size. Corticosterone also displays a protective effect on wave I size yet does not gain significance when compared to other drugs (Fig. 30 B).

Late (wave IV) ABR waves exhibited a statistically significant impaired reach when groups were pre-treated with vehicle, corticosterone or spironolactone, whereas mifepristone was the only agent with no wave IV reach impairment when compared to pre-values (Fig. 30 C). For wave IV size, treatment with mifepristone again exhibited highest size values (Fig. 30 D).

Taking these findings for early (auditory nerve response) and late (midbrain response) ABRs into account, it can be inferred that only mifepristone preserved the dynamic range and culmination of the ABR response (reach) for 16 kHz pure-tone generated waves significantly. Corticosterone also exhibited protective features, albeit not reaching significant levels.



dynamic range 16 kHz

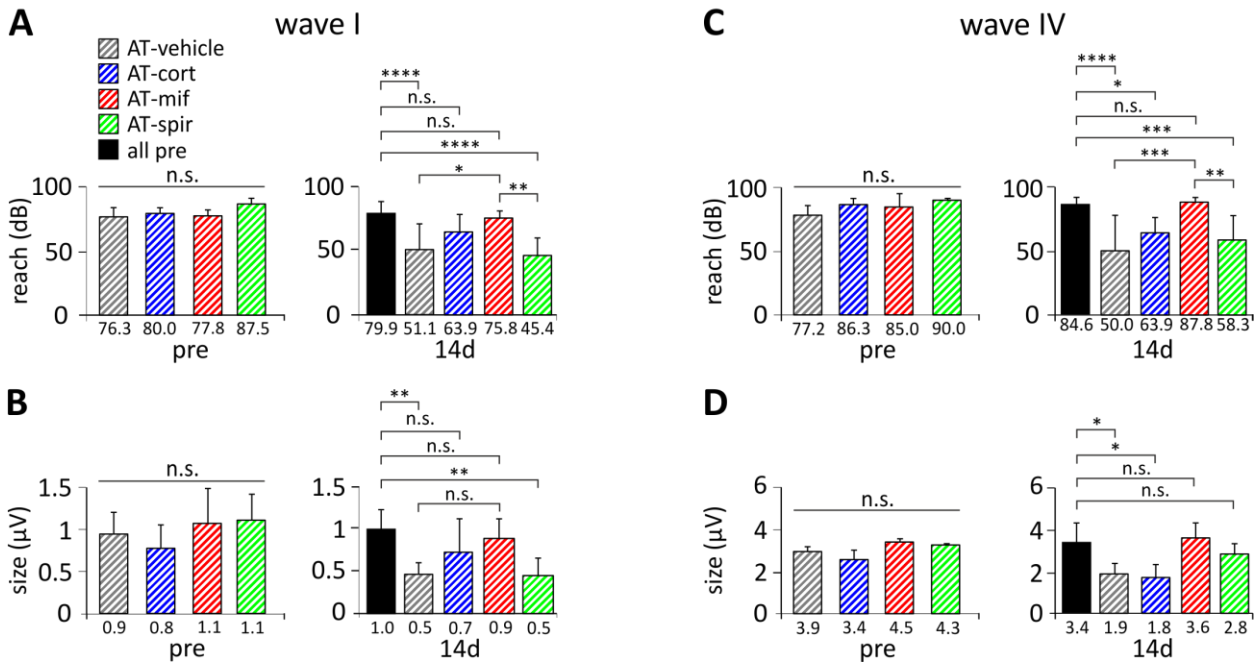


**Figure 30. Pre-treatment with mifepristone (mif, GR antagonist) and corticosterone (cort, MR and GR agonist), but not spironolactone (spir, MR antagonist), maintains the reach for coding high stimulus levels and response size of ABRs to 16 kHz sound stimuli after AT.** The reach of the response range that can be coded is defined as the stimulus level at the maximum response of the wave amplitude. The maximal size of response is defined as the maximal wave amplitude (for further information, see chapter 3.14). **A, B.** Pre-treatment with mifepristone (red bars, GR antagonist), maintains wave I reach and wave I size best. Especially in wave I reach, mifepristone is the only agent that gains significance when compared to vehicle, corticosterone and spironolactone. Corticosterone (blue bars, GR and MR agonist) also displays a protective effect on wave I reach and wave I size yet does not gain significance when compared to other drugs. Spironolactone-treated animals (green bars, MR antagonist) and vehicle-treated animals (grey bars) show a significantly lower wave I reach and size when compared to pre-values (*all pre*, black bars). **C, D.** Wave IV reach and size for 16 kHz stimuli at 14 days after noise exposure is maintained better within the mifepristone-pre-treated group when compared to vehicle, spironolactone and corticosterone. This effect is most prominent in wave IV reach, where corticosterone, spironolactone and vehicle experienced significant losses when compared to the pre-values. Wave IV size was maintained by the mifepristone-group best, exceeding the value of the spironolactone-group. Data displayed as threshold normalized. Error bars represent SD; n.s., not significant. \*  $P < 0.05$ , \*\*  $P < 0.01$ , \*\*\*  $P < 0.001$ , \*\*\*\*  $P < 0.0001$ . See also (Singer, Kasini et al. 2018), Fig. 7. For details of statistical analyses, see Supplemental Table 1.

As observed in Fig. 28 C, high frequency ABR thresholds were gravely affected by acoustic trauma. Therefore, supra-threshold wave responses for 32 kHz were examined thoroughly and results were plotted in Fig. 31. As expected, amplitude increments of post-AT values stagnated earlier (arrows, Fig. 31 A-D) and maximum amplitudes of each group were considerably lower as compared to 16 kHz supra-threshold responses (Fig. 29). Pre-treatment with corticosterone resulted in the lowest levels for which responses could still be determined, closely followed by spironolactone. Solely mifepristone displayed higher levels of maintained supra-threshold responses when compared to vehicle group. The observed effect accounts equally for the growth of supra-threshold early ABR (wave I) and late ABR (wave IV) amplitudes.

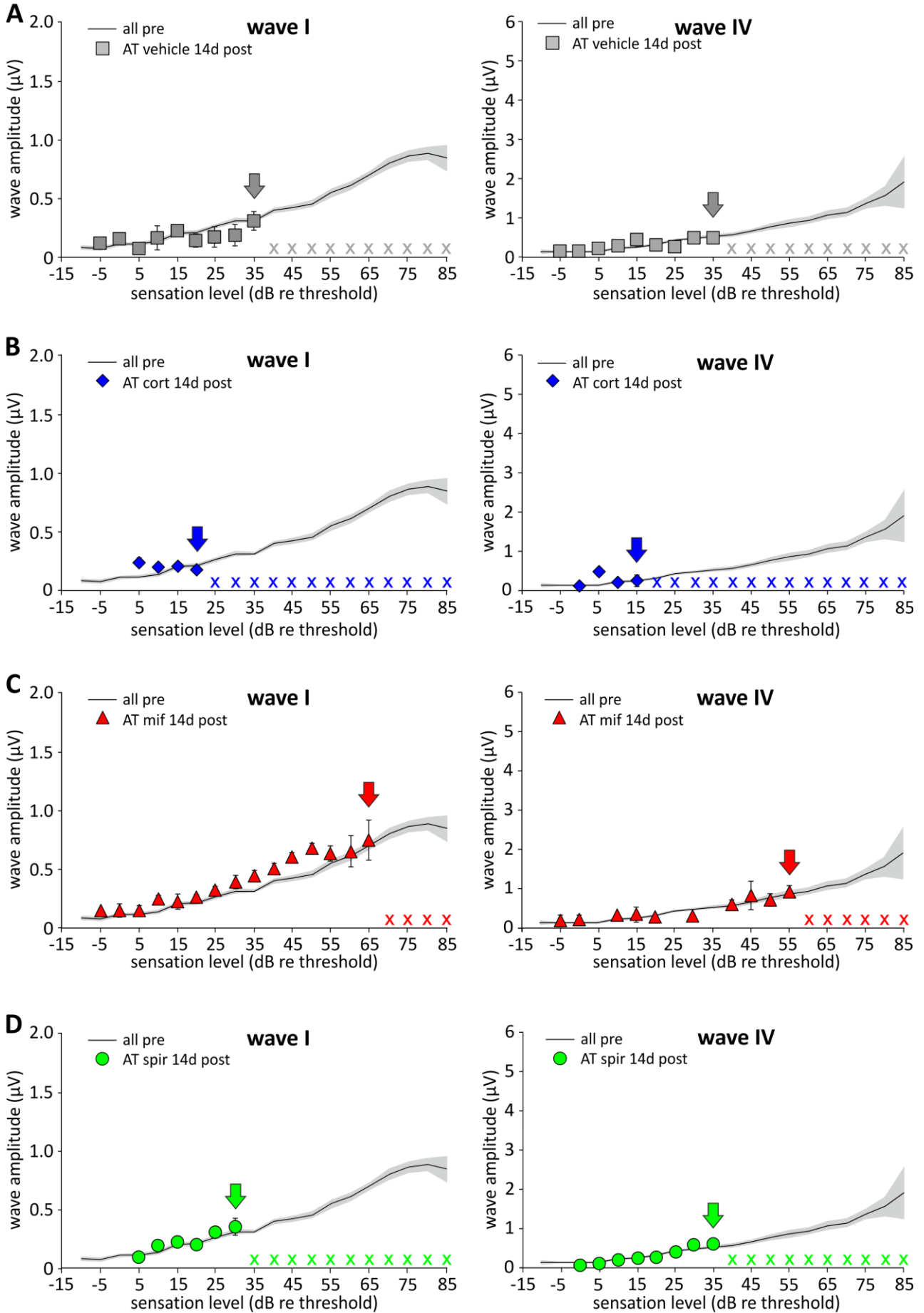
However, to better compare supposed pharmacological effects and for statistical appraisal, maximum reach and maximum size of 32-kHz-evoked ABR signals were calculated individually and results are displayed in Fig. 32. Before acoustic trauma, no significant differences were noted between groups. After trauma, the averaged wave I reach and size was significantly impaired in animals treated with vehicle, corticosterone and spironolactone. Only mifepristone-treated animals displayed no significant loss of amplitude reach and size when compared to pre-measurements (*all pre*, Fig. 32A, B).

When statistical analysis was performed on noise-treated animals only, pharmacological effects of each drug regimen on supra-threshold wave behavior could be appreciated even better (highlighted in red in Fig. 32). Consequently, mifepristone maintained a significantly higher wave I reach and size value as well as wave IV reach when compared to vehicle-treated animals.

---

**Figure 31. Pre-treatment with mifepristone (mif, GR antagonist), but not spironolactone (spir, MR antagonist) or corticosterone (cort, GR- and MR-agonist), maintains early (wave I) and late (Wave IV) ABR amplitudes to a wider range at 32 kHz. A-D.** Animals were pre-treated with vehicle (grey squares), corticosterone (blue diamonds), mifepristone (red triangles) or spironolactone (green dots). Baseline responses before drug application (*all pre*) are shown as grey line with shadow (SEM). The ABR amplitude represents the level of the auditory nerve (wave I) and the level of the inferior colliculus (wave IV) in response to 32 kHz pure-tone burst stimuli 14 days after drug application. Small crosses above x-axis mark levels surpassing the limits of maximum stimulation levels (usually 110 dB SPL). Arrows in the respective colors indicate the highest level above threshold for which responses could still be determined. Data displayed as threshold normalized. Error bars indicate SEM (n = 2-4 ears / 2-4 animals per group). See also (Singer, Kasini et al. 2018), Fig. 6.

32 kHz tone burst stimulus



dynamic range 32 kHz

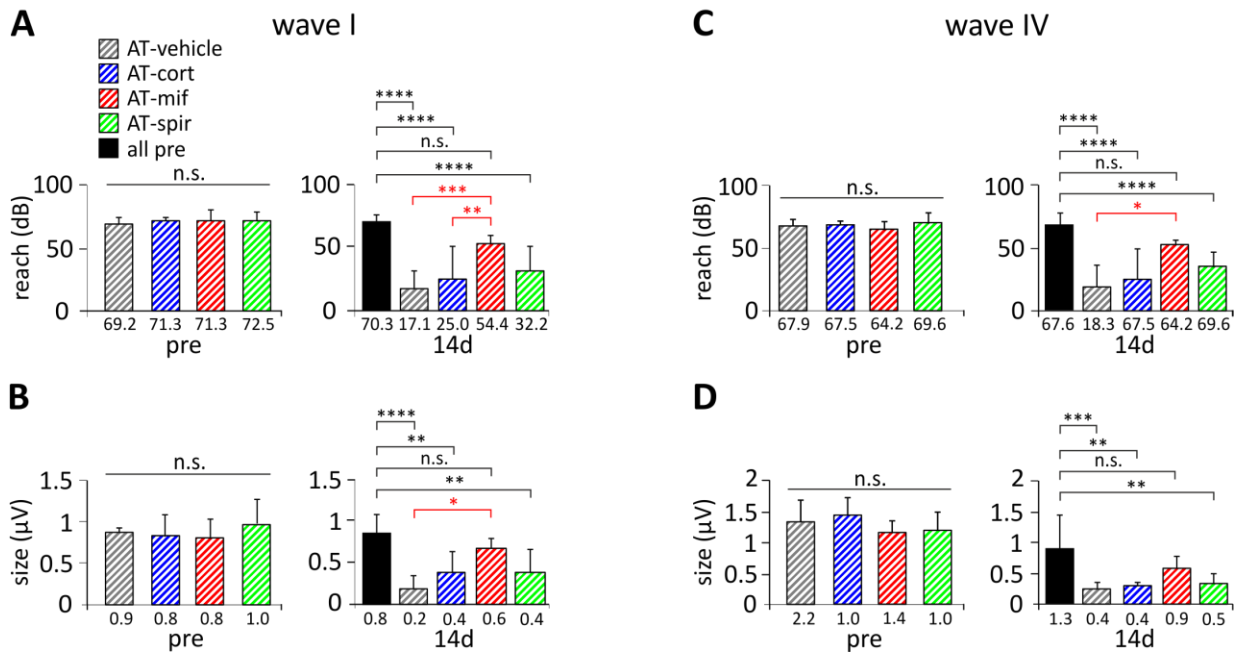


**Figure 32. Pre-treatment with mifepristone (mif, GR antagonist), but not corticosterone (cort, MR and GR agonist) or spironolactone (spir, MR antagonist), maintains amplitude reach and response size of ABRs to 32 kHz after AT.** The reach of the response range is defined as the stimulus level at the maximal response of the wave amplitude. The maximal size of response is defined as the maximal wave amplitude. **A, B.** Excessive noise impairs wave I reach and size in all groups significantly except for pre-treatment with mifepristone (red bars, GR antagonist), which preserved wave I reach and size when compared to baseline (*all pre*, black bars). Mifepristone-treated animals even show a significantly higher wave I reach and size when compared to vehicle- (grey bars) and corticosterone-treated (blue bars) animals (highlighted with red asterisks). **C, D.** Wave IV reach and size for 32 kHz stimuli at 14 days after noise exposure was maintained significantly better within the mifepristone-pre-treated group when compared to vehicle, corticosterone and spironolactone. Again, mifepristone animals display a significantly higher wave IV reach when compared to vehicle (highlighted with red asterisks). Data are displayed threshold normalized. Error bars represent SD; n.s. not significant. \* P < 0.05, \*\* P < 0.01, \*\*\* P < 0.001, \*\*\*\* P < 0.0001. See also (Singer, Kasini et al. 2018), Fig. 7. For details of statistical analyses, see Supplemental Table 1.

*Summarizing GR and MR function on supra-threshold ABR wave characteristics in traumatized animals*

Mifepristone is the only agent that significantly preserved early and late supra-threshold ABR waves of medium (16 kHz) and high (32 kHz) frequencies after excessive noise.

The (non-significant) protective features of corticosterone were limited to supra-threshold ABRs of 16 kHz and could not be reproduced for 32 kHz stimuli. Therefore, treatment with corticosterone or spironolactone displayed no significant protective effect on supra-threshold ABR amplitudes.

This clearly suggests that suppression of GRs, but not MRs, nor GR-/MR-stimulation prior to AT maintains the size and reach of auditory response patterns, emphasizing once more the unfavorable influence of GRs on wave amplitudes.

### 3.3.4 Mifepristone (GR antagonist) and corticosterone (GR/MR agonist) preserve the first synapse of the auditory pathway best after AT

IHC ribbon synapses are essential for the signal transmission along the auditory nerve. The amount of pre-synaptic ribbon synapses is crucial for the amplitude size, the discharge rate and the signal synchronicity of the auditory fiber responses. Therefore, IHC ribbons of treated and untreated animals were counted along the tonotopic axis of the cochlea 14 days after AT (Fig. 33). Counting of CtBP2 positive dots below the IHCs was performed on both ears.

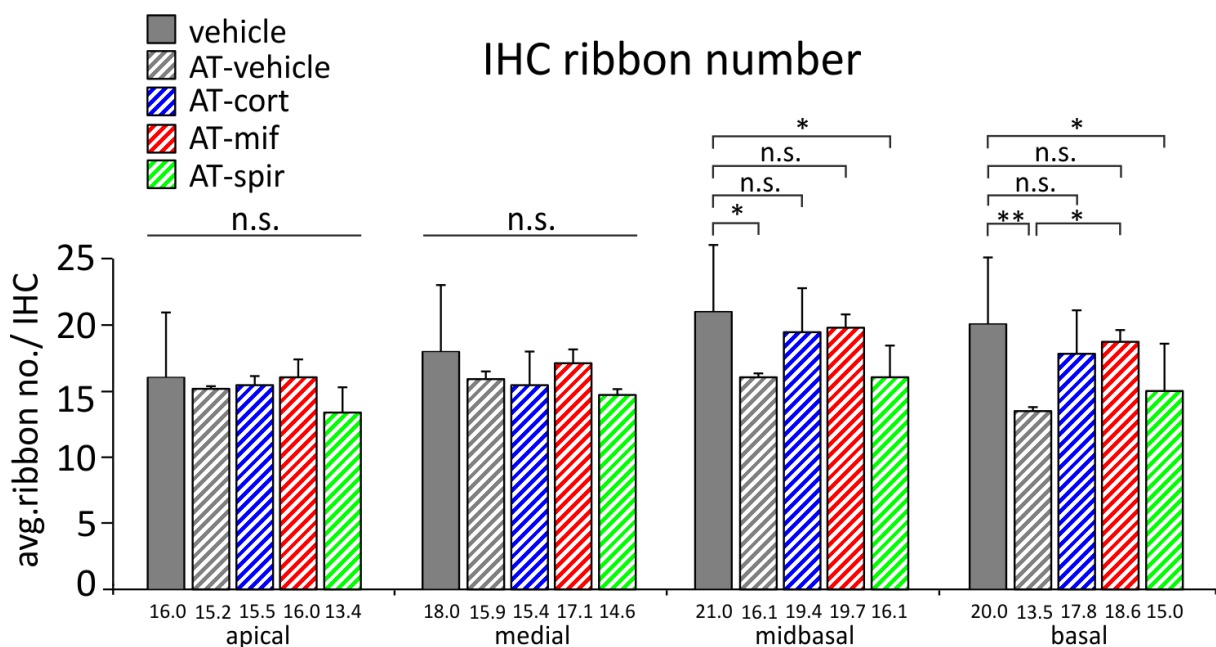


**Figure 33. Mifepristone (mif) and corticosterone (cort), but not spironolactone (spir) or vehicle pre-treatment prevents, in part, IHC ribbon loss in high-frequency cochlear turns. A.** Pre-treatment with mifepristone (GR antagonist; red bars) and corticosterone (MR- and GR- agonist, blue bars), but not spironolactone (MR antagonist; green bars), has a protective effect on IHC ribbon number in midbasal and basal cochlear turns. Error bars represent SD. See also (Singer, Kasini et al. 2018), Fig. 8. For details of statistical analyses, see Supplemental Table 1. \* P < 0.05, \*\* P < 0.01.

The preceding threshold and supra-threshold analysis led to the conclusion that excessive noise of a 10 kHz stimulus mostly affected tonotopic regions of medium to higher frequencies. Adjusted to that, the averaged ribbon number of apical and medial turns (lower frequencies) remained unaffected by AT (Fig. 33), whereas the ribbon number of midbasal and basal turns (higher frequencies) were significantly reduced in the vehicle and spironolactone-treated group after acoustic trauma.

Pre-treatment with mifepristone and corticosterone preserved IHC ribbon quantities in

midbasal and basal turns when compared to the sham-exposed vehicle group. In basal turns, pre-treatment with mifepristone displayed even a significantly higher amount of synaptic ribbons when compared to noise-treated vehicle group. This finding suggests that the prevention of GR receptor activation by mifepristone prior to acoustic trauma as well as GR and MR activation by corticosterone can partly prevent noise-induced IHC ribbon loss and thus avert the decline of auditory nerve fiber responses in high-frequency cochlear turns.

*Summarizing GR and MR function on the synaptic ribbon*

After excessive noise, corticosterone and mifepristone both preserve synaptic ribbons in higher frequencies when compared to unimpaired hearing. This once more underscores the unfavorable influence of GRs and may highlight synaptic preservation mediated by MR.

## 4 Discussion

Today, severe hearing loss is estimated to be a major cause of disability and affects over 5 percent of the world's population (WHO 2015, Cunningham and Tucci 2017). Excessive noise has a profound impact on the recent increase of noise-induced hearing loss (NIHL) prevalence. The lack of successful clinical treatments still renders prevention the best option for limiting the effects of NIHL (Wallhagen, Strawbridge et al. 1997, Folmer, Griest et al. 2002, Health 2012, Le, Straatman et al. 2017).

However, the protective features of social stressors and elevated stress levels are well known (Meltser and Canlon 2011, Canlon, Theorell et al. 2013) and stress hormones (glucocorticoids, GCs) represent a mainstay of treatment for NIHL by inhibiting several inflammatory mediators and preventing cochlear damage caused by noise-induced ischemia and inflammation (Lee, Lyu et al. 2019).

Likewise, earlier studies attributed protective features to acute stress responses. Treatments with heat-shock (Yoshida and Liberman 1999) and restraint stress (Rarey, Gerhardt et al. 1995, Wang and Liberman 2002, Tahera, Meltser et al. 2006, Canlon, Meltser et al. 2007, Tahera, Meltser et al. 2007, Meltser and Canlon 2011) were found to exert protective features for the injured cochlea, specifically targeting cochlear mechanics in the tonotopically most affected high frequency regions by noise exposure (Wang and Liberman 2002). Equally, a lack of CRH and a disruption of the HPA axis lead to a loss of protection against NIHL and create an increased susceptibility to acoustic over-stimulation (Graham, Basappa et al. 2010). Other studies even suggest that elevated GC levels act as upstream protector of noise-induced OHC damage with reduced oxidative stress playing a major role (Fetoni, Rolesi et al. 2016, Kurabi, Keithley et al. 2016, Sha and Schacht 2017).

The abundance of glucocorticoid receptors (GRs) in every single cell, as well as the occurrence of mineralocorticoid receptors (MRs) in hair cells, stria vascularis and the spiral ganglion neurons (Yao and Rarey 1996), make both receptors an important target for hearing loss (Gross, Kempton et al. 2002). This raised the question for the specific role of GRs and MRs on hearing in the first place and required a closer investigation. The main goal of this thesis was to identify the role of GRs and MRs in the cochlea the auditory pathway. The findings presented here together with the current knowledge on this topic provide the basis to discuss this leading question.

## 4.1 The role of corticosterone (GR/ MR agonist) on hearing function

It is known that MRs, under baseline conditions, are already >80% bound to endogenous glucocorticoids (GCs), whereas GRs only become activated with rising GC levels (Reul and de Kloet 1985). This is due to the higher affinity of cortisol and corticosterone for MRs than for GRs (Korte, de Boer et al. 1995, Joels and de Kloet 2017). Until recently, this higher reserve binding capacity of GRs was the basis to attribute stress-related changes of hearing qualities to GR-related effects and the much lower levels of mineralocorticoids (e.g. aldosterone) released by stress (>1000-fold) were considered not to be critical in the acute systemic stress response (Tasker and Herman 2011). It was thought that MRs exert a tonic influence on hippocampal function, neuronal excitability, hypothalamic–pituitary–adrenal (HPA) axis activity, sympathetic outflow and cognitive behavior, but play no important role in acute stress response (Reul and de Kloet 1985, De Kloet and Reul 1987).

Yet, recent findings revealed that although MRs are highly occupied by GCs per default, cytosolic binding of GCs with hormone response elements (HREs) remains at a low binding rate. HREs are short DNA sequences with the ability to regulate gene transcriptions which are responsible for the delayed genomic response of GRs and MRs (Mifsud and Reul 2016). It was discovered that rats reacted to stress responses with similar increases in both MR- and GR-binding to HREs. Additionally, DNA binding of MRs was low in the absence of activated GRs and drastically increased after GR activation. These findings combined underline the premise that high occupancy of MRs does not predict binding to HREs to the same degree and highlights the importance of co-transfected receptors that scale with GR activity (Trapp and Holsboer 1996, Mifsud and Reul 2016). This discovery may hint that MRs play a greater role in genomic stress responses than previously thought.

In contrast to the well-known beneficial effects of stress, earlier experiments demonstrated that higher endogenous corticosterone levels during acoustic trauma led to impaired auditory nerve processing (Singer, Kasini et al. 2018). This appears contradictory to the beneficial features of corticosterone found in this thesis where a short- and long-term stimulation with different corticosterone concentrations (3 mg/kg BW and 30 mg/kg BW) did not impair electrophysiological or subcellular hearing function (Fig. 8 – 25) and pre-treatment with a high dosage of corticosterone attenuated trauma-induced effects.



This discrepancy arises from the complexity of the HPA axis and subsequent activity of glucocorticoid-responsive cytosolic HRE elements. Here, it could be demonstrated that a consecutive corticosterone treatment entailed lower c/c ratios after the treatment period (c/c of 93, Fig. 19) than a single application of the same corticosterone concentration (c/c of 104.4, Fig. 8). Corticosterone acts as an upstream inhibitor due to its rapid and effective feedback on the hypothalamic periventricular nucleus (PVN), the amygdala, and the pituitary gland limiting the endocrine output of the stress axis to a minimum by inhibiting CRH releasing neurons (Di, Malcher-Lopes et al. 2003, Tasker and Herman 2011). This negative feedback curbs the organism's stress response and prevents the stress system from overreacting.

Consequently, the attenuated trauma-induced effects caused by pre-treatment with corticosterone (slightly reduced OHC vulnerability, sustained OHC recovery (Fig. 26), mitigated transient as well as permanent threshold loss (Fig. 27 and 28), preserved supra-threshold wave responses (Fig. 29, 32), and IHC synaptic ribbon preservation (Fig. 33)) paired with the negative feedback response and the fast metabolism of corticosterone underlines the beneficial acute effect of administered, exogenous corticosterone. Here, rapid effects through secondary cell signaling pathways may cause the beneficial corticosterone-related effect. The disruptive effect of spontaneous elevated corticosterone levels during noise exposure however may be based on a HPA-modulated endogenous chronic stress response that highlights a detrimental effect of long-term chronic stress (e.g. HRE-mediated genomic effects via gene transcription) and must be addressed differently than external corticosterone application.

Taken together, the clinical use of GCs as therapy, especially after noise-induced hearing loss, may be based on beneficial acute anti-inflammatory effects of corticosteroids (Meltser and Canlon 2011, Niedermeier, Braun et al. 2012, O'Leary, Monksfield et al. 2013) and not on long-term genomic stress responses. A prolonged stress exposure followed by a long-term HRE-related genomic response may even interfere negatively with the vulnerability of the auditory system.

## 4.2 The role of spironolactone (MR antagonist) on hearing function

The next logical step was to investigate the effect of MRs and GRs on hearing separately by blocking one receptor at a time. Doing so, the described corticosterone-related effects could be attributed to either receptor.

When rats underwent noise treatment, premedication with spironolactone (MR antagonist) revealed a tendency to increase OHC vulnerability for acoustic overstimulation and thus impaired OHC functionality directly after acoustic trauma (Fig. 26). 14 days after noise exposure, however, this decline in DPOAE thresholds and amplitudes was restored with OHC functionality almost reaching its initial performance. The same effect was observed for ABR thresholds, especially for medium to high frequencies (Fig. 28). Paired with the higher affinity of cortisol and corticosterone for MRs than for GRs (Korte, de Boer et al. 1995, Joels and de Kloet 2017), it can be inferred that stimulation of MRs by GCs play a crucial role in OHC and IHC noise vulnerability during and immediately after AT. In other words, spironolactone hampered MR activity, resulting in transient threshold shifts of DPOAEs (TTS), albeit granting an ample IHC and OHC recovery. The latter, favorable effect may be exerted through enhanced GC activity long after drug injection since a single dose of spironolactone is able to increase plasma cortisol by sensitizing the adrenal gland to ACTH as shown here (Fig. 8) and elsewhere (Young, Lopez et al. 1998). The increased plasma cortisol ultimately results in the above-described beneficial effects of corticosteroids which are widely acknowledged (Meltser and Canlon 2011, Niedermeier, Braun et al. 2012, O'Leary, Monksfield et al. 2013).

Further on, early supra-threshold waves (wave I) experienced a severe amplitude loss (Fig. 30, 32), which is heavily dependent on the functionality of the first synapse of the auditory pathway. The number of synaptic ribbons, visualized in Fig. 33, confirmed this observation with lowest values for pre-treatment with spironolactone. In other terms, the present findings suggest that stimulation of MRs by GCs protects the first synapse of the auditory pathway and subsequent low-spontaneous rate (SR) high-threshold auditory fibers. Other authors support the claim that aldosterone (MR agonist) is as effective as the GC prednisolone when controlling cochlear dysfunction. This is due to aldosterone's ability to regulate endolymphatic homeostasis in the inner ear via MR activation which is of paramount importance to ion homeostasis and cochlear ion transport, particularly in the stria vascularis. It is even suggested that the main target of GC-induced hearing preservation is indeed mediated through MRs in the inner ear

(Trune, Kempton et al. 2006). This challenges the assumption that reduction of central auditory acuity in response to chronic stress was attributed to corticosteroids acting first at the level of the IHC synapse via MR (Dagnino-Subiabre, Munoz-Llancao et al. 2009, Felmingham, Rennie et al. 2012, Pérez, Pérez-Valenzuela et al. 2013, Ma, Li et al. 2017, Singer, Kasini et al. 2018).

### **4.3 The role of mifepristone (GR antagonist) on hearing function**

Mifepristone is known to reduce the ACTH response in rats (Wulsin, Herman et al. 2010). Therefore, GR binding sites were blocked in sham-treated rats to observe this putative mifepristone-related change in hearing and its presumably dampening effect on the stress cascade. Interestingly, this premise could not be confirmed as *c/c* levels in urine did not alter 90 minutes after drug injection nor in the following days (Fig. 8). The subsequent assessment of hearing function and the integrity of the auditory pathway (Fig. 14-17) finally led to the conclusion that a single injection of GR antagonist mifepristone elicits no effect on hearing in the healthy rat.

When challenging the rat's ear with traumatizing noise however, the role of GRs during acoustic trauma and hearing recovery reveals its actual importance. After carefully analyzing threshold data and supra-threshold waves, it could be demonstrated for the rat animal model that mifepristone significantly protects the first synapse of the auditory system. IHC synapses, required for response reliability in the auditory system (Buran, Strenzke et al. 2010), contain stress-sensitive components in medial and basal cochlear turns which code for high pitched audio stimulation (Singer, Kasini et al. 2018). The better preservation of these ribbon structures after mifepristone injection and subsequent acoustic trauma (Fig. 33) endorses the stress-sensitivity of said structures.

Likewise, pre-treatment with mifepristone attenuated trauma-related short- and long-term effects on hearing thresholds, noise-induced cochlear synaptopathic injury, auditory nerve responses, and central auditory processing by disrupting glucocorticoid-mediated stress hormone signaling (Singer, Kasini et al. 2018). Mifepristone preserved dynamic range and size of supra-threshold waves and thus protected the ability of auditory nerve fibers to respond along a larger range of higher sound intensities. This finding indicates a GR-mediated disruption of low-spontaneous rate (SR) high-threshold auditory fibers that are sensitive to moderate and higher sound intensities

and accountable for ca. 40% of auditory fibers in the auditory nerve. This fiber type specializes in speech understanding (Bharadwaj, Masud et al. 2015) and is known to be vulnerable to acoustic over-exposure (Furman, Kujawa et al. 2013) and aging (Schmiedt, Mills et al. 1996, Sergeyenko, Lall et al. 2013). Previous studies on this topic similarly revealed unfavorable features of elevated activated GRs on low SR high-threshold auditory nerve fibers in midbasal and basal cochlear turns (McLean, Smith et al. 2009, Singer, Kasini et al. 2018).

This observation complements several other studies where elevated GR activity diminished central auditory capacity in tone perception (Felmingham, Rennie et al. 2012), plasticity of dendritic structures in auditory nuclei (Dagnino-Subiabre, Muñoz-Llanca et al. 2009) or cortical responsiveness (Pérez, Pérez-Valenzuela et al. 2013). Taken together, these data provide a comprehensive picture of GR-mediated stress signaling corrupting the auditory function during or after excessive noise stimuli.

#### **4.4 Summarizing the role of stress on hearing**

The present data exhibit a significant detrimental influence of endogenous stress on the vulnerability of OHC electromechanical properties, the IHC synapse, auditory nerve fibers, and central auditory processing (see also (Singer, Kasini et al. 2018)). Antagonizing endogenous stress hormone signaling with GR-, but not MR-inhibition, entails attenuated hearing vulnerability towards excessive noise. These observations coupled with the abundance of GRs in the stria vascularis, the spiral ganglion and IHCs (Yao and Rarey 1996, Terakado, Kumagami et al. 2011, Kil and Kalinec 2013) create a scenario where elevated GR activity plays a crucial role in hearing vulnerability and recovery.

Interestingly, systemic application of corticosterone correlated with attenuated trauma-related vulnerability and ample hearing recovery as well. Other studies likewise endorse the positive traits of corticosterone and claim that steroids given before, during, or after AT exhibit a beneficial therapeutic effect with higher dosages being more potent (Le, Straatman et al. 2017). This assumption was recently confirmed as a repeated treatment with the GC dexamethasone displayed lowest cochlear inflammatory cytokine levels and reduced noise vulnerability during AT best (Lee, Lyu et al. 2019).

The role of GCs in hearing recovery is a widely discussed controversial topic and the described adverse effects of GR-mediated stress hormone signaling most likely coexist to several known beneficial functions of stressors on hearing (Meltser and Canlon 2011, Trune and Canlon 2012, El Sabbagh, Sewitch et al. 2017, Hickox, Larsen et al. 2017, Kobel, Le Prell et al. 2017, Lee, Kim et al. 2017, Muller, Tisch et al. 2017). However, the role of GRs and MRs cannot be predicted solely on the basis of hormone concentration or receptor saturation levels and gene-dependent and receptor-specific modes of genomic interactions add another layer of complexity to stress response (Mifsud and Reul 2016). The newly found dependence of MRs on GRs may help to understand the importance of MRs and its HRE-related genomic effects on hearing preservation in future research.

The earlier mentioned model of endogenous stress vs. exogenous stress attempts to explain the diverging effect of the detrimental endogenous corticosterone (elevated serum corticosterone via activated HPA axis) on the one hand and the beneficial exogenous corticosterone (elevated serum corticosterone via systemic application) on the other hand: Exogenous corticosterone application induces anti-inflammatory effects via fast secondary cell signaling followed by a negative feedback response whereas the effects of HPA-mediated stress signaling may be strongly associated with disruptive HRE-related delayed effects on DNA transcription. The prolonged and simultaneous activity of GRs and MRs during stress are accountable for the surge of activated cytosolic HREs in chronic endogenous stress and the resulting genomic effects may increase cochlear vulnerability towards excessive noise.

A more recent approach for the opposing role between endogenous and exogenous stress suggests that noise trauma increases serum corticosterone via HPA stress response and simultaneously decreases cochlear GR expression. This leads to the assumption that GR expression may be inversely correlated to the level of stress (Lee, Lyu et al. 2019). Consequently, the systemic application of corticosterone as demonstrated here mimics a strong stress response which may ultimately result in lower cochlear GR expression. Hence, the beneficial effect of both exogenous corticosterone and mifepristone during AT may be based on the same cellular response: minimizing the HRE-related detrimental effect of GRs in the cochlea and the subsequent auditory pathway.

## 4.5 Perspectives

Today, GCs still represent the only proven treatment for hearing loss (Lee, Lyu et al. 2019) and the results as presented here confirm once more that GCs are suitable drugs for an effective clinical therapeutic intervention. Consecutively, a preemptive GC treatment for occupations with high acoustic loads (e.g. construction workers, nightclub workers, soldiers) is inherently possible to minimize anticipated NIHL. However, currently the best option remains prevention considering the side effects of sustained GC treatments. Hearing conservation programs effectively spread awareness about the health risks of noise exposure during early age and child development resulting in noise reduction and hearing protection (Neufeld, Westerberg et al. 2011). Paired with a reduction of industrial and occupational noise through engineering, administrative tools or proper hearing protection, this strategy can effectively regulate noise exposure on a large scale (Joy and Middendorf 2007).

As demonstrated here for the rat animal model, the favorable effect of GR antagonist mifepristone on hearing vulnerability may reveal similar effects in human hearing function. However, mifepristone influences a variety of bodily functions and is most commonly used for medical abortion and for the treatment of Cushing syndrome. Due to severe endocrine interactions with other hormone systems, a systemic clinical trial with mifepristone in order to reiterate observed drug effects is highly unlikely at this time. Other studies first have to further investigate the role of MRs in the auditory system in animal models to ensure drug efficacy and to test and develop topical application of MR antagonists in the cochlea to prevent systemic side effects as already suggested in (Singer, Kasini et al. 2018).

Most importantly, it has been shown that chronic endogenous stress is a main risk factor for noise vulnerability towards excessive noise in rats. Similarly, stress is a predisposing factor in the development of hearing disorders in humans and correlates with the incidence of tinnitus and sudden hearing loss (Schmitt, Patak et al. 2000). It therefore can be assumed that during stressful events, habitual worrying and daily hassles, noise from recreational activities, traffic or industry may challenge the auditory system beyond the ordinary measure. The increased vulnerability towards hearing pathologies during short- or long-term episodes of moderate to extreme stress calls for appropriate preventive measures until sustained research efforts yield a more effective solution.

## 5 Synopsis

Excessive noise is a global health hazard that leads to noise-induced hearing loss, currently with no successful clinical treatment. Recent evidence suggests that endogenous or environmental stress has differential influence on hearing ability and vulnerability for an acoustic insult. Stressors and stress hormones like glucocorticoids (GC) are part of the primary therapy plan of a variety of hearing disorders as they are considered to have protective effects on auditory function following noise exposure. Conversely, stressors are also risk factors for hearing disorders. How these contrasting actions are compatible remained elusive.

Questioning how stress might influence auditory function, the effect of different drug-induced stress levels on acoustic signal processing was examined in a mature rat animal model. In a next step, the influence of GR and MR activity on hearing function was selectively tested on unimpaired hearing and after an acoustic injury.

Stress levels were determined via urinary corticosterone measurements using ELISA at different time points during the testing periods. The hearing function was monitored by auditory brainstem responses (click-sound and frequency-specific pure tone evoked ABR) and the distortion product of the otoacoustic emissions (DPOAE). The cellular phenotype of the auditory receptor was determined via immunofluorescence microscopy.

Here, it could be demonstrated in a rat animal model that the blocking of GR but not MR exerts permanent effects on reducing acoustic trauma-induced negative effects. This includes preserved hearing thresholds, protection of presynaptic inner hair cell ribbons and mitigated injury of early and late auditory brainstem responses. These findings indicate a profound harmful effect of GR activity on auditory nerve processing as these effects could be prevented by its inhibition using mifepristone.

Interestingly, simultaneous GR and MR activation by the GC corticosterone also reveals a tendency to protect hearing function after exposure to traumatizing noise. Paired with the finding above, this suggests that the well-known protective features of GC signaling may be caused by MR, and not GR, activity. The detrimental effect of GRs paired with the protective effect of MR activity during traumatizing noise may help to identify compounds for a suitable clinical therapeutic intervention for patients suffering from noise-induced hearing loss in the future.

## Zusammenfassung

Lärm stellt weltweit eine große Belastung für das Hörorgan dar und ist der Hauptrisikofaktor für schall-induzierten Hörverlust, welcher bis heute nicht ausreichend therapiert werden kann. Zudem beeinflussen Emotionen wie chronischer Stress und Stresshormone wie Glukokorticoide (GC) die Schallverarbeitung des auditorischen Systems und können sowohl einen protektiven wie auch einen ototoxischen Effekt auf die Hörfunktion ausüben. Wie sich diese gegensätzlichen Aussagen vereinen lassen, ist aktuell noch nicht abschließend geklärt.

Vor dem Hintergrund der Frage, wie Stress das auditorische System beeinflusst, wurden im Rattenmodell unterschiedliche Stressniveaus medikamentös mit Kortikosteron induziert und anschließend auf ihre Wirkung im Hörsystem untersucht. In einem zweiten Experiment wurde die spezifische Rolle von Glukokortikoid- (GR) und Mineralokortikoid-Rezeptoren (MR) sowohl im gesunden als auch im schalltraumatisierten Tier analysiert.

Der Effekt der pharmakologischen Stress-Therapie auf die Tiere wurde mittels ELISA an unterschiedlichen Zeitpunkten ermittelt (Kortikosteron/ Kreatinin-Quotient im Urin). Die Hörfunktion wurde anhand von auditorisch evozierten Potentialen (ABRs) und distorsiv-produzierten otoakustischen Emissionen (DPOAEs) überwacht und der Phänotyp der inneren Haarzellen wurde mittels Immunfluoreszenz dargestellt und anschließend histologisch ausgewertet.

Anhand der vorliegenden Ergebnisse konnte gezeigt werden, dass eine Hemmung der GR, jedoch nicht eine Hemmung der MR, im Rattenmodell zu einer signifikanten und permanenten Reduktion der schall-induzierten Traumafolgen an den Hörschwellen, der ersten Synapse des auditorischen Systems und der nachgeschalteten auditorischen Hörbahn führen konnte. Da Mifepriston als Antagonist am GR wirkt, legt dies nahe, dass die GR-vermittelte Signalkaskade die akustische Signalverarbeitung nach einem schall-induziertem Trauma in hohem Maße beeinträchtigt.

Interessanterweise zeigt die simultane GR- und MR-Aktivierung durch Kortikosteron während einer übermäßigen Schallexposition ebenfalls protektive Eigenschaften. In Kombination mit den obenstehenden Erkenntnissen deutet dies darauf hin, dass die weitgehend anerkannte protektive Wirkung von GCs durch einen MR-abhängigen Signalweg ausgelöst wird. Diese Erkenntnisse könnten in Zukunft helfen, die Pathogenese von schall-induzierter Schwerhörigkeit besser zu verstehen und geeignete Therapeutika zu entwickeln.



# Appendix

Supplementary Table 1 Statistical information of the results If not otherwise indicated with *n.s.*, or asterisks, values are not significant to each other

Figure	Label	Comparison	Statistical test	Test value	<i>p</i> -value	Post-hoc test with <i>p</i> -value	<i>n</i> -number
Fig. 8 <i>c/c ratio</i>	pre	AT-veh vs. AT-cort	1-way ANOVA	F (3, 28) = 1.5	P = 0.2361		n = 8 rats per group
	AT	AT-veh vs. AT-mif	1-way ANOVA	F (3, 27) = 13.08	P < 0.0001	Tukey's multiple comparisons test	n = 7-8 rats per group
		AT-cort vs. AT-mif	1-way ANOVA	F (3, 27) = 13.08	P < 0.0001	Tukey's multiple comparisons test	n = 7-8 rats per group
	3d	AT-cort vs. AT-spir	1-way ANOVA	F (3, 28) = 1.073	P = 0.3765	Tukey's multiple comparisons test	n = 8 rats per group
	7d		1-way ANOVA	F (3, 27) = 1.483	P = 0.2415		n = 7-8 rats per group
	14d		F (3, 25) = 0.2356	P = 0.8707		n = 6-8 rats per group	
Fig. 9A <i>max. 2/f1-f2 amplitude</i>	pre		1-way ANOVA	F (3, 60) = 0.6820	P = 0.5665		n = 16 ears/ 8 animals per group
	3d		1-way ANOVA	F (3, 28) = 2.916	P = 0.0516		n = 8 ears/ 4 animals per group
	7d		1-way ANOVA	F (3, 28) = 0.2091	P = 0.8892		n = 8 ears/ 4 animals per group
	14d		1-way ANOVA	F (3, 28) = 1.140	P = 0.3499		n = 8 ears/ 4 animals per group
	vehicle over time		1-way ANOVA	F (3, 28) = 2.582	P = 0.0733		n = 8 ears/ 4 animals per group
Fig. 9B <i>DPOAE thresholds</i>	cort over time		1-way ANOVA	F (3, 28) = 0.7399	P = 0.5372		n = 8 ears/ 4 animals per group
	mif over time		1-way ANOVA	F (3, 28) = 0.3065	P = 0.8205		n = 8 ears/ 4 animals per group
	spir over time		1-way ANOVA	F (3, 28) = 0.8354	P = 0.4858		n = 8 ears/ 4 animals per group
	pre	11.3 kHz; veh vs. spir	2-way ANOVA	F (3, 137) = 6.482	P = 0.0004	Tukey's multiple comparisons test	n = 8 ears/ 4 animals per group
	3d - pre	11.3 kHz; mif vs. spir	2-way ANOVA	F (3, 160) = 0.1713	P = 0.9157	Tukey's multiple comparisons test	n = 8 ears/ 4 animals per group
Fig. 9C <i>DPOAE thresholds delta</i>	7d - pre	32 kHz; veh vs. spir	2-way ANOVA	F (3, 161) = 6.465	P = 0.0004		n = 8 ears/ 4 animals per group
	14d - pre		2-way ANOVA	F (3, 161) = 2.6	P = 0.0541		n = 8 ears/ 4 animals per group
	veh pre vs. veh 14d		2-way matched RM ANOVA (10 - 65 dB SPL)	F (1, 7) = 1.529	P = 0.2362		n = 8 ears/ 4 animals per group
	cort pre vs. cort 14d		2-way matched RM ANOVA (10 - 65 dB SPL)	F (1, 7) = 2.708	P = 0.1439		n = 8 ears/ 4 animals per group
	mifpre vs. mif 14d		2-way matched RM ANOVA (10 - 65 dB SPL)	F (1, 7) = 0.0008289	P = 0.9778		n = 8 ears/ 4 animals per group
Fig. 10A <i>click stimulus</i>	spir pre vs. S pir 14d		2-way matched RM ANOVA (10 - 65 dB SPL)	F (1, 7) = 0.6819	P = 0.4362		n = 8 ears/ 4 animals per group
	pre		1-way ANOVA	F (3, 60) = 1.776	P = 0.1614		n = 16 ears/ 8 animals per group
	day 0		1-way ANOVA	F (3, 28) = 1.453	P = 0.2486		n = 8 ears/ 4 animals per group
	3d		1-way ANOVA	F (3, 28) = 0.8585	P = 0.4740		n = 8 ears/ 4 animals per group
	7d		1-way ANOVA	F (3, 28) = 1.593	P = 0.2132		n = 8 ears/ 4 animals per group
Fig. 10B <i>noise stimulus</i>	14d		1-way ANOVA	F (3, 28) = 0.1035	P = 0.9573		n = 8 ears/ 4 animals per group
	pre		1-way ANOVA	F (3, 60) = 2.5	P = 0.0680		n = 16 ears/ 8 animals per group
	day 0		1-way ANOVA	F (3, 28) = 1.303	P = 0.2931		n = 8 ears/ 4 animals per group
	3d		1-way ANOVA	F (3, 28) = 1.853	P = 0.1606		n = 8 ears/ 4 animals per group
	7d		1-way ANOVA	F (3, 28) = 1.659	P = 0.1984		n = 8 ears/ 4 animals per group
Fig. 10C <i>tone burst stimulus</i>	14d		1-way ANOVA	F (3, 28) = 2.118	P = 0.1204		n = 8 ears/ 4 animals per group
	pre		2-way ANOVA	F (3, 120) = 7.704	P < 0.0001	Tukey's multiple comparisons test	n = 4 ears/ 4 animals per group
	cort vs. spir	1.41 kHz; cort vs. spir	2-way ANOVA	F (3, 120) = 7.704	P < 0.0001	Tukey's multiple comparisons test	n = 4 ears/ 4 animals per group
	1.41 kHz; mif vs. spir	1.41 kHz; mif vs. spir	2-way ANOVA	F (3, 120) = 7.704	P < 0.0001	Tukey's multiple comparisons test	n = 4 ears/ 4 animals per group
	32 kHz; cort vs. mif	32 kHz; cort vs. mif	2-way ANOVA	F (3, 120) = 2.548	P = 0.0591		n = 4 ears/ 4 animals per group
Fig. 10D <i>tone burst stimulus delta</i>	3d - pre		2-way ANOVA	F (3, 120) = 0.0487	P = 0.9857		n = 4 ears/ 4 animals per group
	7d - pre		2-way ANOVA	F (3, 120) = 1.336	P = 0.2659		n = 4 ears/ 4 animals per group
	14d - pre		2-way ANOVA	F (7, 24) = 0.8241	P = 0.5772		n = 8 ears/ 8 animals per group
	pre		1-way ANOVA	F (3, 12) = 0.438	P = 0.7299		n = 4 ears/ 4 animals per group
	3d		1-way ANOVA	F (3, 12) = 1.484	P = 0.2686		n = 4 ears/ 4 animals per group
Fig. 11A <i>1kHz tone burst</i>	7d		1-way ANOVA	F (3, 12) = 0.5511	P = 0.6570		n = 4 ears/ 4 animals per group
	14d		1-way ANOVA	F (3, 12) = 3.052	P = 0.08211		n = 4 ears/ 4 animals per group
	vehicle over time		1-way ANOVA	F (3, 12) = 1.316	P = 0.3146		n = 4 ears/ 4 animals per group
	cort over time		1-way ANOVA	F (3, 12) = 1.581	P = 0.2454		n = 4 ears/ 4 animals per group
	mif over time		1-way ANOVA	F (3, 12) = 0.2776	P = 0.8405		n = 4 ears/ 4 animals per group
Fig. 11B <i>16kHz tone burst</i>	spir over time		1-way ANOVA	F (3, 12) = 0.5511	P = 0.6570		n = 8 ears/ 8 animals per group
	pre		1-way ANOVA	F (3, 12) = 0.618	P = 0.6165		n = 4 ears/ 4 animals per group
	3d		1-way ANOVA	F (3, 12) = 0.4468	P = 0.7241		n = 4 ears/ 4 animals per group
	7d		1-way ANOVA	F (3, 12) = 1.589	P = 0.2435		n = 4 ears/ 4 animals per group
	14d		1-way ANOVA	F (3, 12) = 0.6262	P = 0.6117		n = 4 ears/ 4 animals per group
Fig. 11C <i>32 kHz noise burst</i>	vehicle over time		1-way ANOVA	F (3, 12) = 1.546	P = 0.2534		n = 4 ears/ 4 animals per group
	cort over time		1-way ANOVA	F (3, 12) = 0.8652	P = 0.4857		n = 4 ears/ 4 animals per group
	mif over time		1-way ANOVA	F (3, 12) = 0.5422	P = 0.6625		n = 4 ears/ 4 animals per group
	spir over time		1-way ANOVA	F (3, 12) = 0.6989	P = 0.5705		n = 4 ears/ 4 animals per group
	pre		1-way ANOVA	F (7, 24) = 0.2439	P = 0.9694		n = 8 ears/ 8 animals per group
Fig. 14A <i>16 kHz wave 1 reach</i>	3d		1-way ANOVA	F (3, 12) = 1.158	P = 0.3660		n = 4 ears/ 4 animals per group
	7d		1-way ANOVA	F (3, 12) = 1.589	P = 0.2435		n = 4 ears/ 4 animals per group
	14d		1-way ANOVA	F (3, 12) = 0.6262	P = 0.6117		n = 4 ears/ 4 animals per group
	vehicle over time		1-way ANOVA	F (3, 12) = 1.018	P = 0.4187		n = 4 ears/ 4 animals per group
	cort over time		1-way ANOVA	F (3, 12) = 0.2704	P = 0.8456		n = 4 ears/ 4 animals per group
Fig. 14B <i>16 kHz wave 1 size</i>	mif over time		1-way ANOVA	F (3, 12) = 3.007	P = 0.08243		n = 4 ears/ 4 animals per group
	spir over time		1-way ANOVA	F (3, 12) = 0.1753	P = 0.9111		n = 4 ears/ 4 animals per group
	reach wave 1 pre		1-way ANOVA	F (3, 9) = 0.3341	P = 0.8012		n = 3-4 ears/ 3-4 rats per group
	reach wave 1 14d		1-way ANOVA	F (3, 12) = 0.8391	P = 0.4982		n = 4 ears/ 4 animals per group
	size wave 1 pre		1-way ANOVA	F (3, 9) = 3.521	P = 0.0620		n = 3-4 ears/ 3-4 rats per group
	size wave 1 14d		1-way ANOVA	F (3, 12) = 1.517	P = 0.2604		n = 4 ears/ 4 animals per group

Figure	Label	Comparison	Statistical test	Test value	p-value	Post-hoc test with p-value	n-number
Fig. 14C 16 KHz wave IV reach	reach wave IV pre reach wave IV 14d		1-way ANOVA	F(3, 10) = 0.3783	P = 0.7708		n = 3-4 ears/ 3-4 rats per group
Fig. 14D 16 KHz wave IV size	size wave IV pre size wave IV 14d		1-way ANOVA	F(3, 11) = 1.402	P = 0.2940		n = 3-4 ears/ 3-4 rats per group
Fig. 16A 32 KHz wave I reach	reach wave I pre reach wave I 14d		1-way ANOVA	F(3, 10) = 0.2671	P = 0.8477		n = 3-4 ears/ 3-4 rats per group
Fig. 16B 32 KHz wave I size	size wave I pre size wave I 14d		1-way ANOVA	F(3, 11) = 0.9223	P = 0.4620		n = 3-4 ears/ 3-4 rats per group
Fig. 16C 32 KHz wave IV reach	reach wave IV pre reach wave IV 14d		1-way ANOVA	F(3, 12) = 1.395	P = 0.2919		n = 4 ears/ 4 rats per group
Fig. 16D 32 KHz wave IV size	size wave IV pre size wave IV 14d		1-way ANOVA	F(3, 12) = 1.658	P = 0.2287		n = 4 ears/ 4 rats per group
Fig. 17 HIC ribbon number	apical medial nihilbasal		1-way ANOVA	F(3, 12) = 1.27	P = 0.3287		n = 4 ears/ 4 rats per group
Fig. 19 c/c ratio	pre post	veh post vs. 30mg post 3mg post vs. 30mg post	1-way ANOVA 1-way ANOVA	F(3, 12) = 0.4024 F(3, 11) = 1.914	P = 0.7542 P = 0.1812		n = 4 ears/ 4 rats per group
Fig. 20A max. $\Delta T_{f2}$ amplitude	pre post	1-way ANOVA	1-way ANOVA	F(3, 11) = 1.04 F(3, 12) = 1.502	P = 0.4130 P = 0.2641		n = 3-4 ears/ 3-4 rats per group
Fig. 20C DPOAE I/O function 11KHz	veh pre vs. veh post 3mg pre vs. 3mg post 30mg pre vs. 30mg post	2-way matched RM ANOVA (0 - 65 dB SPL) 2-way matched RM ANOVA (0 - 65 dB SPL) 2-way matched RM ANOVA (0 - 65 dB SPL)	1-way ANOVA 1-way ANOVA 1-way ANOVA	F(2, 32) = 0.6501 F(2, 28) = 0.8459 F(2, 28) = 0.8459	P = 0.5390 P = 0.4399 P = 0.4399		n = 12-14 ears/ 6 animals per group
Fig. 21A c/c/c stimulus	pre post	1-way ANOVA	1-way ANOVA	F(1, 8) = 1.866 F(1, 8) = 1.057	P = 0.2051 P = 0.3340		n = 9 ears/ 6 animals per group
Fig. 21B noise stimulus	pre post	1-way ANOVA	1-way ANOVA	F(1, 8) = 1.662 F(2, 33) = 1.108	P = 0.2533 P = 0.3422		n = 12 ears/ 6 animals per group
Fig. 21C tone burst stimulus	pre post	5.66KHz; veh vs. 30mg	2-way ANOVA	F(2, 33) = 0.9236 F(2, 33) = 0.9236	P = 0.4071 P = 0.4071		n = 12 ears/ 6 animals per group
Fig. 22A 4 KHz	pre post	1-way ANOVA	1-way ANOVA	F(2, 33) = 4.66 F(2, 33) = 4.66	P = 0.0165 P = 0.0165		n = 12 ears/ 6 animals per group
Fig. 22B 11 KHz	pre post	1-way ANOVA	1-way ANOVA	F(2, 15) = 1.779 F(2, 13) = 5.535	P = 0.1722 P = 0.0045		n = 3-6 ears/ 3-6 animals per group
Fig. 22A 4 KHz	veh pre vs. veh post 3mg pre vs. 3mg post 30mg pre vs. 30mg post	2-way ANOVA 2-way ANOVA 2-way ANOVA	2-way ANOVA 2-way ANOVA 2-way ANOVA	F(1, 96) = 2.369 F(1, 89) = 0.08692 F(1, 106) = 0.7642	P = 0.1271 P = 0.7688 P = 0.3840		n = 3-6 ears/ 3-6 animals per group
Fig. 22A 4 KHz	pre post	1-way ANOVA	1-way ANOVA	F(2, 17) = 1.535 F(2, 17) = 1.535	P = 0.2459 P = 0.2459		n = 6-8 ears/ 6 animals per group
Fig. 22A 4 KHz	veh pre vs. veh post 3mg pre vs. 3mg post 30mg pre vs. 30mg post	two-tailed paired t-test two-tailed paired t-test two-tailed paired t-test	two-tailed paired t-test two-tailed paired t-test two-tailed paired t-test	F(2, 17) = 0.1223 F(2, 17) = 0.1223 F(2, 17) = 0.1223	P = 0.9072 P = 0.9072 P = 0.9072		n = 6-8 ears/ 6 animals per group
Fig. 22C 32 KHz	pre post	1-way ANOVA	1-way ANOVA	F(2, 16) = 0.848 F(2, 16) = 0.848	P = 0.4466 P = 0.4466		n = 6-8 ears/ 6 animals per group
Fig. 24A wave I reach	reach wave I pre reach wave I 14d	1-way ANOVA	1-way ANOVA	F(2, 17) = 0.3504 F(2, 17) = 0.3504	P = 0.7094 P = 0.7094		n = 6-8 ears/ 6 animals per group
Fig. 24B wave I size	size wave I pre size wave I 14d	1-way ANOVA	1-way ANOVA	F(2, 17) = 0.3504 F(2, 17) = 0.3504	P = 0.7094 P = 0.7094		n = 6-8 ears/ 6 animals per group
Fig. 24C wave IV reach	reach wave IV pre reach wave IV 14d	1-way ANOVA	1-way ANOVA	F(2, 13) = 2.374 F(2, 13) = 2.374	P = 0.1322 P = 0.1322		n = 5-6 ears/ 5-6 rats per group
Fig. 24D wave IV size	size wave IV pre size wave IV 14d	1-way ANOVA	1-way ANOVA	F(2, 14) = 1.458 F(2, 14) = 1.458	P = 0.2729 P = 0.2729		n = 4-6 ears/ 4-6 rats per group
Fig. 25 HIC ribbon number	apical medial nihilbasal	1-way ANOVA	1-way ANOVA	F(2, 13) = 0.6848 F(2, 13) = 0.6848	P = 0.5248 P = 0.5248		n = 4-6 ears/ 4-6 rats per group
Fig. 26A DPOAE max. amplitude	pre 3d	all pre vs. AT-veh all pre vs. AT-cont all pre vs. AT-cont all pre vs. AT-spr all pre vs. veh-AT all pre vs. AT-cont	1-way ANOVA 1-way ANOVA 1-way ANOVA 1-way ANOVA 1-way ANOVA 1-way ANOVA	F(4, 9) = 17.87 F(4, 9) = 17.87 F(4, 9) = 17.87 F(4, 9) = 17.87 F(4, 8) = 17.26 F(4, 8) = 17.26	P = 0.0001 P = 0.0001 P = 0.0001 P = 0.0001 P < 0.0001 P < 0.0001	<p>Tukey's multiple comparisons test</p> <p>Tukey's multiple comparisons test</p> <p>Tukey's multiple comparisons test</p> <p>Tukey's multiple comparisons test</p> <p>Tukey's multiple comparisons test</p> <p>Tukey's multiple comparisons test</p>	<p>n = 8-64 ears/ 4-32 animals per group</p> <p>n = 8-64 ears/ 4-32 animals per group</p> <p>n = 8-64 ears/ 4-32 animals per group</p> <p>n = 8-64 ears/ 4-32 animals per group</p> <p>n = 8-64 ears/ 4-32 animals per group</p> <p>n = 6-64 ears/ 3-32 animals per group</p>





Supplementary Table 2 Cortisol and creatinine raw data

probe number	Number of animal	Treatment	Time point	Lab number	Test	Result	Unit
1	Cort010	Control	pre	BR702069	c/c ratio	10.1	n/a
1	Cort010	Control	pre	BR702069	urine cortisol (CIA)	3.6	µg/l
1	Cort010	Control	pre	BR702069	urine creatinine	11.0	mg/dl
2	Cort010	Control	post	BR702070	c/c ratio	9.3	n/a
2	Cort010	Control	post	BR702070	urine cortisol (CIA)	4.2	µg/l
2	Cort010	Control	post	BR702070	urine creatinine	14.2	mg/dl
3	Cort019	Control	pre	BR702071	c/c ratio	11.5	n/a
3	Cort019	Control	pre	BR702071	urine cortisol (CIA)	4.0	µg/l
3	Cort019	Control	pre	BR702071	urine creatinine	10.9	mg/dl
4	Cort019	Control	post	BR702072	c/c ratio	4.7	n/a
4	Cort019	Control	post	BR702072	urine cortisol (CIA)	10.3	µg/l
4	Cort019	Control	post	BR702072	urine creatinine	68.5	mg/dl
5	Cort011	3mg	pre	BR702073	c/c ratio	12.5	n/a
5	Cort011	3mg	pre	BR702073	urine cortisol (CIA)	2.3	µg/l
5	Cort011	3mg	pre	BR702073	urine creatinine	5.7	mg/dl
6	Cort011	3mg	post	BR702074	c/c ratio	12.9	n/a
6	Cort011	3mg	post	BR702074	urine cortisol (CIA)	13.4	µg/l
6	Cort011	3mg	post	BR702074	urine creatinine	32.3	mg/dl
7	Cort016	3mg	pre	BR702075	c/c ratio	2.6	n/a
7	Cort016	3mg	pre	BR702075	urine cortisol (CIA)	3.6	µg/l
7	Cort016	3mg	pre	BR702075	urine creatinine	43.0	mg/dl
8	Cort016	3mg	post	BR702076	c/c ratio	8.9	n/a
8	Cort016	3mg	post	BR702076	urine cortisol (CIA)	9.6	µg/l
8	Cort016	3mg	post	BR702076	urine creatinine	33.5	mg/dl
9	Cort008	30mg	pre	BR702077	c/c ratio	1.9	n/a
9	Cort008	30mg	pre	BR702077	urine cortisol (CIA)	5.0	µg/l
9	Cort008	30mg	pre	BR702077	urine creatinine	79.4	mg/dl
10	Cort008	30mg	post	BR702078	c/c ratio	125.6	n/a
10	Cort008	30mg	post	BR702078	urine cortisol (CIA)	158.0	µg/l
10	Cort008	30mg	post	BR702078	urine creatinine	39.3	mg/dl
11	Cort018	30mg	pre	BR702079	c/c ratio	16.1	n/a
11	Cort018	30mg	pre	BR702079	urine cortisol (CIA)	3.8	µg/l
11	Cort018	30mg	pre	BR702079	urine creatinine	7.4	mg/dl
12	Cort018	30mg	post	BR702080	c/c ratio	186.7	n/a
12	Cort018	30mg	post	BR702080	urine cortisol (CIA)	52.2	µg/l
12	Cort018	30mg	post	BR702080	urine creatinine	8.7	mg/dl
13	Cort021	Vehicle+sham	pre	BR702081	c/c ratio	0.8	n/a
13	Cort021	Vehicle+sham	pre	BR702081	urine cortisol (CIA)	0.2	µg/l
13	Cort021	Vehicle+sham	pre	BR702081	urine creatinine	8.0	mg/dl
14	Cort021	Veh.+sham	AT	BR702082	c/c ratio	5.5	n/a
14	Cort021	Veh.+sham	AT	BR702082	urine cortisol (CIA)	4.3	µg/l
14	Cort021	Veh.+sham	AT	BR702082	urine creatinine	24.5	mg/dl
15	Cort021	Veh.+sham	3dpost	BR702083	c/c ratio	1.9	n/a
15	Cort021	Veh.+sham	3dpost	BR702083	urine cortisol (CIA)	0.2	µg/l

15	Cort021	Veh.+sham	3dpost	BR702083	urine creatinine	3.4	mg/dl
16	Cort021	Veh.+sham	7dpost	BR702084	c/c ratio	5.7	n/a
16	Cort021	Veh.+sham	7dpost	BR702084	urine cortisol (CIA)	2.1	µg/l
16	Cort021	Veh.+sham	7dpost	BR702084	urine creatinine	11.3	mg/dl
17	Cort021	Veh.shamA	14dpost	BR702085	c/c ratio	2.9	n/a
17	Cort021	Veh.shamA	14dpost	BR702085	urine cortisol (CIA)	0.2	µg/l
17	Cort021	Veh.shamA	14dpost	BR702085	urine creatinine	2.2	mg/dl
18	Cort022	VehicleAT	pre	BR702086	c/c ratio	29.6	n/a
18	Cort022	VehicleAT	pre	BR702086	urine cortisol (CIA)	3.4	µg/l
18	Cort022	VehicleAT	pre	BR702086	urine creatinine	3.6	mg/dl
19	Cort022	Veh.AT	AT	BR702087	c/c ratio	16.5	n/a
19	Cort022	Veh.AT	AT	BR702087	urine cortisol (CIA)	10.1	µg/l
19	Cort022	Veh.AT	AT	BR702087	urine creatinine	19.1	mg/dl
20	Cort022	VehicleAT	3dpost	BR702088	c/c ratio	1.4	n/a
20	Cort022	VehicleAT	3dpost	BR702088	urine cortisol (CIA)	0.2	µg/l
20	Cort022	VehicleAT	3dpost	BR702088	urine creatinine	4.5	mg/dl
19	Cort022	VehicleAT	7dpost	BR702089	c/c ratio	1.4	n/a
19	Cort022	VehicleAT	7dpost	BR702089	urine cortisol (CIA)	0.2	µg/l
19	Cort022	VehicleAT	7dpost	BR702089	urine creatinine	4.5	mg/dl
22	Cort022	VehicleAT	14dpost	BR702090	c/c ratio	2.5	n/a
22	Cort022	VehicleAT	14dpost	BR702090	urine cortisol (CIA)	0.2	µg/l
22	Cort022	VehicleAT	14dpost	BR702090	urine creatinine	2.5	mg/dl
23	Cort037	Mife.sham	pre	BR702091	c/c ratio	25.8	n/a
23	Cort037	Mife.sham	pre	BR702091	urine cortisol (CIA)	5.0	µg/l
23	Cort037	Mife.sham	pre	BR702091	urine creatinine	6.0	mg/dl
24	Cort037	Mife.sham	AT	BR702092	c/c ratio	8.2	n/a
24	Cort037	Mife.sham	AT	BR702092	urine cortisol (CIA)	3.7	µg/l
24	Cort037	Mife.sham	AT	BR702092	urine creatinine	14.1	mg/dl
25	Cort037	Mife.sham	3dpost	BR702093	c/c ratio	14.7	n/a
25	Cort037	Mife.sham	3dpost	BR702093	urine cortisol (CIA)	6.3	µg/l
25	Cort037	Mife.sham	3dpost	BR702093	urine creatinine	13.5	mg/dl
26	Cort037	Mife.sham	7dpost	BR702094	c/c ratio	0.3	n/a
26	Cort037	Mife.sham	7dpost	BR702094	urine cortisol (CIA)	0.2	µg/l
26	Cort037	Mife.sham	7dpost	BR702094	urine creatinine	21.7	mg/dl
27	Cort037	Mife.sham	14dpost	BR702095	c/c ratio	0.3	n/a
27	Cort037	Mife.sham	14dpost	BR702095	urine cortisol (CIA)	0.2	µg/l
27	Cort037	Mife.sham	14dpost	BR702095	urine creatinine	18.6	mg/dl
28	Cort024	Mife.AT	pre	BR702096	c/c ratio	0.6	n/a
28	Cort024	Mife.AT	pre	BR702096	urine cortisol (CIA)	0.2	µg/l
28	Cort024	Mife.AT	pre	BR702096	urine creatinine	11.0	mg/dl
29	Cort024	Mife.AT	AT	BR702097	c/c ratio	6.0	n/a
29	Cort024	Mife.AT	AT	BR702097	urine cortisol (CIA)	3.7	µg/l
29	Cort024	Mife.AT	AT	BR702097	urine creatinine	19.0	mg/dl
30	Cort024	Mife.AT	3dpost	BR702098	c/c ratio	2.6	n/a
30	Cort024	Mife.AT	3dpost	BR702098	urine cortisol (CIA)	4.8	µg/l
30	Cort024	Mife.AT	3dpost	BR702098	urine creatinine	58.4	mg/dl
31	Cort024	Mife.AT	7dpost	BR702099	c/c ratio	2.6	n/a
31	Cort024	Mife.AT	7dpost	BR702099	urine cortisol (CIA)	2.7	µg/l
31	Cort024	Mife.AT	7dpost	BR702099	urine creatinine	32.1	mg/dl
32	Cort024	Mife.AT	14dpost	BR702100	c/c ratio	8.0	n/a

32	Cort024	Mife.AT	14dpost	BR702100	urine cortisol (CLIA)	4.2	µg/l
32	Cort024	Mife.AT	14dpost	BR702100	urine creatinine	16.4	mg/dl
33	Cort025	Spiro.sham	pre	BR702101	c/c ratio	7.1	n/a
33	Cort025	Spiro.sham	pre	BR702101	urine cortisol (CLIA)	2.7	µg/l
33	Cort025	Spiro.sham	pre	BR702101	urine creatinine	11.9	mg/dl
34	Cort025	Spiro.sham	At	BR702102	c/c ratio	8.5	n/a
34	Cort025	Spiro.sham	At	BR702102	urine cortisol (CLIA)	7.4	µg/l
34	Cort025	Spiro.sham	At	BR702102	urine creatinine	26.9	mg/dl
35	Cort025	Spiro	shamAT 3	BR702103	c/c ratio	3.8	n/a
35	Cort025	Spiro	shamAT 3	BR702103	urine cortisol (CLIA)	4.7	µg/l
35	Cort025	Spiro	shamAT 3	BR702103	urine creatinine	38.2	mg/dl
36	Cort025	Spiro.sham	7dpo.	BR702104	c/c ratio	10.0	n/a
36	Cort025	Spiro.sham	7dpo.	BR702104	urine cortisol (CLIA)	5.4	µg/l
36	Cort025	Spiro.sham	7dpo.	BR702104	urine creatinine	16.8	mg/dl
37	Cort025	Spiro.sham	14dpo	BR702105	c/c ratio	4.7	n/a
37	Cort025	Spiro.sham	14dpo	BR702105	urine cortisol (CLIA)	4.3	µg/l
37	Cort025	Spiro.sham	14dpo	BR702105	urine creatinine	28.9	mg/dl
38	Cort026	Spiro.At	pre	BR702106	c/c ratio	3.7	n/a
38	Cort026	Spiro.At	pre	BR702106	urine cortisol (CLIA)	3.5	µg/l
38	Cort026	Spiro.At	pre	BR702106	urine creatinine	29.5	mg/dl
39	Cort026	Spiro.AT	AT	BR702107	c/c ratio	9.7	n/a
39	Cort026	Spiro.AT	AT	BR702107	urine cortisol (CLIA)	5.9	µg/l
39	Cort026	Spiro.AT	AT	BR702107	urine creatinine	18.9	mg/dl
40	Cort026	Spiro.AT	3dpost	BR702108	c/c ratio	3.4	n/a
40	Cort026	Spiro.AT	3dpost	BR702108	urine cortisol (CLIA)	4.5	µg/l
40	Cort026	Spiro.AT	3dpost	BR702108	urine creatinine	41.5	mg/dl
41	Cort026	Spiro.AT	7dpost	BR702109	c/c ratio	12.8	n/a
41	Cort026	Spiro.AT	7dpost	BR702109	urine cortisol (CLIA)	2.2	µg/l
41	Cort026	Spiro.AT	7dpost	BR702109	urine creatinine	5.4	mg/dl
42	Cort026	Spiro.AT	14dpost	BR702110	c/c ratio	2.3	n/a
42	Cort026	Spiro.AT	14dpost	BR702110	urine cortisol (CLIA)	0.2	µg/l
42	Cort026	Spiro.AT	14dpost	BR702110	urine creatinine	2.7	mg/dl
43	Cort028	Cort.sham	pre	BR702111	c/c ratio	1.2	n/a
43	Cort028	Cort.sham	pre	BR702111	urine cortisol (CLIA)	0.2	µg/l
43	Cort028	Cort.sham	pre	BR702111	urine creatinine	5.2	mg/dl
44	Cort028	Cort.sham	AT	BR702112	c/c ratio	24138.	n/a
44	Cort028	Cort.sham	AT	BR702112	urine cortisol (CLIA)	3510.0	µg/l
44	Cort028	Cort.sham	AT	BR702112	urine creatinine	4.5	mg/dl
45	Cort028	Cort.sham	3dpost	BR702113	c/c ratio	20.3	n/a
45	Cort028	Cort.sham	3dpost	BR702113	urine cortisol (CLIA)	3.0	µg/l
45	Cort028	Cort.sham	3dpost	BR702113	urine creatinine	4.5	mg/dl
46	Cort028	Cort.sham	7dpost	BR702114	c/c ratio	16.9	n/a
46	Cort028	Cort.sham	7dpost	BR702114	urine cortisol (CLIA)	3.1	µg/l
46	Cort028	Cort.sham	7dpost	BR702114	urine creatinine	5.8	mg/dl
47	Cort028	Cort.sham	14dpo.	BR702115	c/c ratio	19.3	n/a
47	Cort028	Cort.sham	14dpo.	BR702115	urine cortisol (CLIA)	2.6	µg/l
47	Cort028	Cort.sham	14dpo.	BR702115	urine creatinine	4.3	mg/dl
48	Cort027	Cort.AT	pre	BR702116	c/c ratio	16.1	n/a
48	Cort027	Cort.AT	pre	BR702116	urine cortisol (CLIA)	9.2	µg/l
48	Cort027	Cort.AT	pre	BR702116	urine creatinine	17.9	mg/dl

49	Cort027	Cort.AT	AT	BR702117	c/c ratio	145.6	n/a
49	Cort027	Cort.AT	AT	BR702117	urine cortisol (CIA)	82.3	µg/l
49	Cort027	Cort.AT	AT	BR702117	urine creatinine	17.7	mg/dl
50	Cort027	Cort.AT	3dpost	BR702118	c/c ratio	22.2	n/a
50	Cort027	Cort.AT	3dpost	BR702118	urine cortisol (CIA)	2.9	µg/l
50	Cort027	Cort.AT	3dpost	BR702118	urine creatinine	4.1	mg/dl
51	Cort027	Cort.AT	7dpost	BR702119	c/c ratio	16.0	n/a
51	Cort027	Cort.AT	7dpost	BR702119	urine cortisol (CIA)	3.1	µg/l
51	Cort027	Cort.AT	7dpost	BR702119	urine creatinine	6.0	mg/dl
52	Cort027	Cort.AT	14dpost	BR702120	c/c ratio	836.0	n/a
52	Cort027	Cort.AT	14dpost	BR702120	urine cortisol (CIA)	792.0	µg/l
52	Cort027	Cort.AT	14dpost	BR702120	urine creatinine	29.6	mg/dl
53	Cort029	Mife.sham	pre	BR702121	c/c ratio	2.3	n/a
53	Cort029	Mife.sham	pre	BR702121	urine cortisol (CIA)	0.2	µg/l
53	Cort029	Mife.sham	pre	BR702121	urine creatinine	2.8	mg/dl
54	Cort029	Mife.sham	AT	BR702122	c/c ratio	13.0	n/a
54	Cort029	Mife.sham	AT	BR702122	urine cortisol (CIA)	8.8	µg/l
54	Cort029	Mife.sham	AT	BR702122	urine creatinine	21.2	mg/dl
55	Cort029	Mife.sham	3dpost	BR702123	c/c ratio	1.8	n/a
55	Cort029	Mife.sham	3dpost	BR702123	urine cortisol (CIA)	0.2	µg/l
55	Cort029	Mife.sham	3dpost	BR702123	urine creatinine	3.6	mg/dl
56	Cort029	Mife.sham	7dpost	BR702124	c/c ratio	8.7	n/a
56	Cort029	Mife.sham	7dpost	BR702124	urine cortisol (CIA)	2.3	µg/l
56	Cort029	Mife.sham	7dpost	BR702124	urine creatinine	8.3	mg/dl
57	Cort029	Mife.sham	14dpo.	BR702125	c/c ratio	9.4	n/a
57	Cort029	Mife.sham	14dpo.	BR702125	urine cortisol (CIA)	3.9	µg/l
57	Cort029	Mife.sham	14dpo.	BR702125	urine creatinine	12.8	mg/dl
58	Cort030	Mife.AT	pre	BR702126	c/c ratio	0.3	n/a
58	Cort030	Mife.AT	pre	BR702126	urine cortisol (CIA)	0.2	µg/l
58	Cort030	Mife.AT	pre	BR702126	urine creatinine	22.5	mg/dl
59	Cort030	Mife.AT	AT	BR702127	c/c ratio	6.2	n/a
59	Cort030	Mife.AT	AT	BR702127	urine cortisol (CIA)	3.5	µg/l
59	Cort030	Mife.AT	AT	BR702127	urine creatinine	17.6	mg/dl
60	Cort030	Mife.AT	3dpost	BR702128	c/c ratio	0.4	n/a
60	Cort030	Mife.AT	3dpost	BR702128	urine cortisol (CIA)	0.2	µg/l
60	Cort030	Mife.AT	3dpost	BR702128	urine creatinine	17.2	mg/dl
61	Cort030	Mife.AT	7dpost	BR702129	c/c ratio	13.0	n/a
61	Cort030	Mife.AT	7dpost	BR702129	urine cortisol (CIA)	2.1	µg/l
61	Cort030	Mife.AT	7dpost	BR702129	urine creatinine	5.0	mg/dl
62	Cort030	Mife.AT	14dpost	BR702130	c/c ratio	0.9	n/a
62	Cort030	Mife.AT	14dpost	BR702130	urine cortisol (CIA)	0.2	µg/l
62	Cort030	Mife.AT	14dpost	BR702130	urine creatinine	6.9	mg/dl
63	Cort031	Spiro.sham	pre	BR702131	c/c ratio	6.1	n/a
63	Cort031	Spiro.sham	pre	BR702131	urine cortisol (CIA)	2.6	µg/l
63	Cort031	Spiro.sham	pre	BR702131	urine creatinine	13.3	mg/dl
64	Cort031	Spiro.sham	AT	BR702132	c/c ratio	14.9	n/a
64	Cort031	Spiro.sham	AT	BR702132	urine cortisol (CIA)	8.2	µg/l
64	Cort031	Spiro.sham	AT	BR702132	urine creatinine	17.1	mg/dl
65	Cort031	Spiro.sham	3dpo.	BR702133	c/c ratio	1.4	n/a
65	Cort031	Spiro.sham	3dpo.	BR702133	urine cortisol (CIA)	0.2	µg/l



65	Cort031	Spiro.sham	3dpo.	BR702133	urine creatinine	4.4	mg/dl
66	Cort031	Spiro.sham	7dpo.	BR702134	c/c ratio	2.2	n/a
66	Cort031	Spiro.sham	7dpo.	BR702134	urine cortisol (CLIA)	0.2	µg/l
66	Cort031	Spiro.sham	7dpo.	BR702134	urine creatinine	2.9	mg/dl
67	Cort032	Spiro.sham	14dpo	BR702135	c/c ratio	2.0	n/a
67	Cort032	Spiro.sham	14dpo	BR702135	urine cortisol (CLIA)	0.2	µg/l
67	Cort032	Spiro.sham	14dpo	BR702135	urine creatinine	3.1	mg/dl
68	Cort032	Spiro.AT	pre	BR702136	c/c ratio	3.7	n/a
68	Cort032	Spiro.AT	pre	BR702136	urine cortisol (CLIA)	4.6	µg/l
68	Cort032	Spiro.AT	pre	BR702136	urine creatinine	39.6	mg/dl
69	Cort032	Spiro.AT	AT	BR702137	c/c ratio	18.1	n/a
69	Cort032	Spiro.AT	AT	BR702137	urine cortisol (CLIA)	11.9	µg/l
69	Cort032	Spiro.AT	AT	BR702137	urine creatinine	20.5	mg/dl
70	Cort032	Spiro.AT	3dpost	BR702138	c/c ratio	19.7	n/a
70	Cort032	Spiro.AT	3dpost	BR702138	urine cortisol (CLIA)	3.8	µg/l
70	Cort032	Spiro.AT	3dpost	BR702138	urine creatinine	6.1	mg/dl
71	Cort032	Spiro.AT	7dpost	BR702139	c/c ratio	3.7	n/a
71	Cort032	Spiro.AT	7dpost	BR702139	urine cortisol (CLIA)	3.4	µg/l
71	Cort032	Spiro.AT	7dpost	BR702139	urine creatinine	29.0	mg/dl
72	Cort032	Spiro.At	14dpost	BR702140	c/c ratio	1.8	n/a
72	Cort032	Spiro.At	14dpost	BR702140	urine cortisol (CLIA)	0.2	µg/l
72	Cort032	Spiro.At	14dpost	BR702140	urine creatinine	3.4	mg/dl
73	Cort033	Cort.sham	pre	BR702141	c/c ratio	1.4	n/a
73	Cort033	Cort.sham	pre	BR702141	urine cortisol (CLIA)	0.2	µg/l
73	Cort033	Cort.sham	pre	BR702141	urine creatinine	4.6	mg/dl
74	Cort033	Cort.sham	AT	BR702142	c/c ratio	74.4	n/a
74	Cort033	Cort.sham	AT	BR702142	urine cortisol (CLIA)	64.1	µg/l
74	Cort033	Cort.sham	AT	BR702142	urine creatinine	26.9	mg/dl
75	Cort033	Cort.sham	3dpost	BR702143	c/c ratio	0.5	n/a
75	Cort033	Cort.sham	3dpost	BR702143	urine cortisol (CLIA)	0.2	µg/l
75	Cort033	Cort.sham	3dpost	BR702143	urine creatinine	12.8	mg/dl
76	Cort033	Cort.sham	7dpost	BR702144	c/c ratio	3.6	n/a
76	Cort033	Cort.sham	7dpost	BR702144	urine cortisol (CLIA)	4.0	µg/l
76	Cort033	Cort.sham	7dpost	BR702144	urine creatinine	34.8	mg/dl
77	Cort033	Cort.sham	14dpo.	BR702145	c/c ratio	7.3	n/a
77	Cort033	Cort.sham	14dpo.	BR702145	urine cortisol (CLIA)	3.2	µg/l
77	Cort033	Cort.sham	14dpo.	BR702145	urine creatinine	13.7	mg/dl
78	Cort034	Cort.AT	pre	BR702146	c/c ratio	20.8	n/a
78	Cort034	Cort.AT	pre	BR702146	urine cortisol (CLIA)	2.2	µg/l
78	Cort034	Cort.AT	pre	BR702146	urine creatinine	3.3	mg/dl
79	Cort034	Cort.AT	AT	BR702147	c/c ratio	56.4	n/a
79	Cort034	Cort.AT	AT	BR702147	urine cortisol (CLIA)	54.7	µg/l
79	Cort034	Cort.AT	AT	BR702147	urine creatinine	30.3	mg/dl
80	Cort034	Cort.AT	3dpost	BR702148	c/c ratio	31.0	n/a
80	Cort034	Cort.AT	3dpost	BR702148	urine cortisol (CLIA)	5.2	µg/l
80	Cort034	Cort.AT	3dpost	BR702148	urine creatinine	5.2	mg/dl
81	Cort034	Cort.AT	7dpost	BR702149	c/c ratio	1.3	n/a
81	Cort034	Cort.AT	7dpost	BR702149	urine cortisol (CLIA)	0.2	µg/l
81	Cort034	Cort.AT	7dpost	BR702149	urine creatinine	4.9	mg/dl
82	Cort034	Cort.AT	14dpost	BR702150	c/c ratio	2949.7	n/a

## References

- Ackermann, D., N. Gresko, M. Carrel, D. Loffing-Cueni, D. Habermehl, C. Gomez-Sanchez, B. C. Rossier and J. Loffing (2010). "In vivo nuclear translocation of mineralocorticoid and glucocorticoid receptors in rat kidney: differential effect of corticosteroids along the distal tubule." Am J Physiol Renal Physiol **299**(6): F1473-1485.
- Agarwal, M. K. and M. Mirshahi (1999). "General overview of mineralocorticoid hormone action." Pharmacol Ther **84**(3): 273-326.
- Arriza, J. L., R. B. Simerly, L. W. Swanson and R. M. Evans (1988). "The neuronal mineralocorticoid receptor as a mediator of glucocorticoid response." Neuron **1**(9): 887-900.
- Bao, A. M. and D. F. Swaab (2010). "Corticotropin-releasing hormone and arginine vasopressin in depression focus on the human postmortem hypothalamus." Vitam Horm **82**: 339-365.
- Barry, T. J., L. Murray, P. Fearon, C. Moutsiana, T. Johnstone and S. L. Halligan (2017). "Amygdala volume and hypothalamic-pituitary-adrenal axis reactivity to social stress." Psychoneuroendocrinology **85**: 96-99.
- Basner, M., W. Babisch, A. Davis, M. Brink, C. Clark, S. Janssen and S. Stansfeld (2014). "Auditory and non-auditory effects of noise on health." Lancet **383**(9925): 1325-1332.
- Bharadwaj, H. M., S. Masud, G. Mehraei, S. Verhulst and B. G. Shinn-Cunningham (2015). "Individual differences reveal correlates of hidden hearing deficits." J Neurosci **35**(5): 2161-2172.
- Bing, D., S. C. Lee, D. Campanelli, H. Xiong, M. Matsumoto, R. Panford-Walsh, S. Wolpert, M. Praetorius, U. Zimmermann, H. Chu, M. Knipper, L. Ruttiger and W. Singer (2015). "Cochlear NMDA receptors as a therapeutic target of noise-induced tinnitus." Cell Physiol Biochem **35**(5): 1905-1923.
- Buijs, R. M., C. G. van Eden, V. D. Goncharuk and A. Kalsbeek (2003). "The biological clock tunes the organs of the body: timing by hormones and the autonomic nervous system." J Endocrinol **177**(1): 17-26.
- Buran, B. N., N. Strenzke, A. Neef, E. D. Gundelfinger, T. Moser and M. C. Liberman (2010). "Onset coding is degraded in auditory nerve fibers from mutant mice lacking synaptic ribbons." J Neurosci **30**(22): 7587-7597.
- Canlon, B., I. Meltser, P. Johansson and Y. Tahera (2007). "Glucocorticoid receptors modulate auditory sensitivity to acoustic trauma." Hear Res **226**(1-2): 61-69.
- Canlon, B., T. Theorell and D. Hasson (2013). "Associations between stress and hearing problems in humans." Hear Res **295**: 9-15.
- Cannon, W. B. (1929). "Bodily changes in pain, hunger, fear, and rage."
- Cannon, W. B. (1932). "The wisdom of the body."

- Chumak, T., L. Rüttiger, S. C. Lee, D. Campanelli, A. Zuccotti, W. Singer, J. Popelar, K. Gutsche, H. S. Geisler, S. P. Schraven, M. Jaumann, R. Panford-Walsh, J. Hu, T. Schimmang, U. Zimmermann, J. Syka and M. Knipper (2015). "BDNF in lower brain parts modifies auditory fiber activity to gain fidelity but increases the risk for generation of central noise after injury." Mol Neurobiol.
- Cole, M. A., B. A. Kalman, T. W. Pace, F. Topczewski, M. J. Lowrey and R. L. Spencer (2000). "Selective blockade of the mineralocorticoid receptor impairs hypothalamic-pituitary-adrenal axis expression of habituation." J Neuroendocrinol **12**(10): 1034-1042.
- Cunningham, L. L. and D. L. Tucci (2017). "Hearing Loss in Adults." N Engl J Med **377**(25): 2465-2473.
- Dagnino-Subiabre, A., P. Muñoz-Llancao, G. Terreros, U. Wyneken, G. Diaz-Veliz, B. Porter, M. P. Kilgard, M. Atzori and F. Aboitiz (2009). "Chronic stress induces dendritic atrophy in the rat medial geniculate nucleus: effects on auditory conditioning." Behav Brain Res **203**(1): 88-96.
- Dagnino-Subiabre, A., P. Muñoz-Llancao, G. Terreros, U. Wyneken, G. Díaz-Véliz, B. Porter, M. P. Kilgard, M. Atzori and F. Aboitiz (2009). "Chronic stress induces dendritic atrophy in the rat medial geniculate nucleus: effects on auditory conditioning." Behav Brain Res **203**(1): 88-96.
- Dale Purves, G. J. A., David Fitzpatrick, Lawrence C Katz, Anthony-Samuel LaMantia, James O McNamara, and S Mark Williams. (2001). "Neuroscience, 2nd edition."
- De Kloet, E. R. (2004). "Hormones and the stressed brain." Ann N Y Acad Sci **1018**: 1-15.
- De Kloet, E. R. and J. M. Reul (1987). "Feedback action and tonic influence of corticosteroids on brain function: a concept arising from the heterogeneity of brain receptor systems." Psychoneuroendocrinology **12**(2): 83-105.
- Delyani, J. A. (2000). "Mineralocorticoid receptor antagonists: the evolution of utility and pharmacology." Kidney Int **57**(4): 1408-1411.
- Di, S., R. Malcher-Lopes, K. C. Halmos and J. G. Tasker (2003). "Nongenomic glucocorticoid inhibition via endocannabinoid release in the hypothalamus: a fast feedback mechanism." J Neurosci **23**(12): 4850-4857.
- Dixon, S. J. and B. R. Stockwell (2014). "The role of iron and reactive oxygen species in cell death." Nat Chem Biol **10**(1): 9-17.
- Ehret, G. (1978). "Stiffness gradient along the basilar membrane as a basis for spatial frequency analysis within the cochlea." J Acoust Soc Am **64**(6): 1723-1726.
- El Sabbagh, N. G., M. J. Sewitch, A. Bezdjian and S. J. Daniel (2017). "Intratympanic dexamethasone in sudden sensorineural hearing loss: A systematic review and meta-analysis." Laryngoscope **127**(8): 1897-1908.
- Engel, J., C. Braig, L. Rüttiger, S. Kuhn, U. Zimmermann, N. Blin, M. Sausbier, H. Kalbacher, S. Munkner, K. Rohbock, P. Ruth, H. Winter and M. Knipper (2006). "Two classes of outer hair cells along the tonotopic axis of the cochlea." Neuroscience **143**(3): 837-849.

Fejes-Toth, G., D. Pearce and A. Naray-Fejes-Toth (1998). "Subcellular localization of mineralocorticoid receptors in living cells: effects of receptor agonists and antagonists." Proc Natl Acad Sci U S A **95**(6): 2973-2978.

Felmingham, K. L., C. Rennie, E. Gordon and R. A. Bryant (2012). "Autonomic and cortical reactivity in acute and chronic posttraumatic stress." Biol Psychol **90**(3): 224-227.

Fetoni, A. R., R. Rolesi, F. Paciello, S. L. Eramo, C. Grassi, D. Troiani and G. Paludetti (2016). "Styrene enhances the noise induced oxidative stress in the cochlea and affects differently mechanosensory and supporting cells." Free Radic Biol Med **101**: 211-225.

Folmer, R. L., S. E. Griest and W. H. Martin (2002). "Hearing conservation education programs for children: a review." J Sch Health **72**(2): 51-57.

Fries, E., L. Dettenborn and C. Kirschbaum (2009). "The cortisol awakening response (CAR): facts and future directions." Int J Psychophysiol **72**(1): 67-73.

Furman, A. C., S. G. Kujawa and M. C. Liberman (2013). "Noise-induced cochlear neuropathy is selective for fibers with low spontaneous rates." J Neurophysiol **110**(3): 577-586.

Gates, G. A., P. Schmid, S. G. Kujawa, B. Nam and R. D'Agostino (2000). "Longitudinal threshold changes in older men with audiometric notches." Hear Res **141**(1-2): 220-228.

Gilbert, K. C. and N. J. Brown (2010). "Aldosterone and inflammation." Curr Opin Endocrinol Diabetes Obes **17**(3): 199-204.

Goldstein, D. S. and I. J. Kopin (2007). "Evolution of concepts of stress." Stress **10**(2): 109-120.

Gomez-Sanchez, E. and C. E. Gomez-Sanchez (2014). "The multifaceted mineralocorticoid receptor." Compr Physiol **4**(3): 965-994.

Gomez-Sanchez, E. P. and C. E. Gomez-Sanchez (2012). "Central regulation of blood pressure by the mineralocorticoid receptor." Mol Cell Endocrinol **350**(2): 289-298.

Gong, S., Y. L. Miao, G. Z. Jiao, M. J. Sun, H. Li, J. Lin, M. J. Luo and J. H. Tan (2015). "Dynamics and correlation of serum cortisol and corticosterone under different physiological or stressful conditions in mice." PLoS One **10**(2): e0117503.

Graham, C. E., J. Basappa and D. E. Vetter (2010). "A corticotropin-releasing factor system expressed in the cochlea modulates hearing sensitivity and protects against noise-induced hearing loss." Neurobiol Dis **38**(2): 246-258.

Gross, N. D., J. B. Kempton and D. R. Trune (2002). "Spironolactone blocks glucocorticoid-mediated hearing preservation in autoimmune mice." Laryngoscope **112**(2): 298-303.

Han, F., H. Ozawa, K. I. Matsuda, H. Lu, E. R. De Kloet and M. Kawata (2007). "Changes in the expression of corticotrophin-releasing hormone, mineralocorticoid receptor and glucocorticoid receptor mRNAs in the hypothalamic paraventricular nucleus induced by fornix transection and adrenalectomy." J Neuroendocrinol **19**(4): 229-238.

Health, N. I. o. (2012). "Survey: Noise-Induced Hearing Loss Among Adolescents."

- Heeringa, A. N. and P. van Dijk (2014). "The dissimilar time course of temporary threshold shifts and reduction of inhibition in the inferior colliculus following intense sound exposure." Hear Res **312**: 38-47.
- Heidrych, P., U. Zimmermann, S. Kuhn, C. Franz, J. Engel, S. V. Duncker, B. Hirt, C. M. Pusch, P. Ruth, M. Pfister, W. Marcotti, N. Blin and M. Knipper (2009). "Otoferlin interacts with myosin VI: implications for maintenance of the basolateral synaptic structure of the inner hair cell." Hum Mol Genet **18**(15): 2779-2790.
- Heinz, M. G. and E. D. Young (2004). "Response growth with sound level in auditory-nerve fibers after noise-induced hearing loss." J Neurophysiol **91**(2): 784-795.
- Henderson, D., E. C. Bielefeld, K. C. Harris and B. H. Hu (2006). "The role of oxidative stress in noise-induced hearing loss." Ear Hear **27**(1): 1-19.
- Henderson, D. and R. P. Hamernik (1986). "Impulse noise: critical review." J Acoust Soc Am **80**(2): 569-584.
- Hickox, A. E., E. Larsen, M. G. Heinz, L. Shinobu and J. P. Whitton (2017). "Translational issues in cochlear synaptopathy." Hear Res **349**: 164-171.
- Joels, M. and E. R. de Kloet (2017). "30 YEARS OF THE MINERALOCORTICOID RECEPTOR: The brain mineralocorticoid receptor: a saga in three episodes." J Endocrinol **234**(1): T49-T66.
- Joy, G. J. and P. J. Middendorf (2007). "Noise exposure and hearing conservation in U.S. coal mines--a surveillance report." J Occup Environ Hyg **4**(1): 26-35.
- Kil, S. H. and F. Kalinec (2013). "Expression and dexamethasone-induced nuclear translocation of glucocorticoid and mineralocorticoid receptors in guinea pig cochlear cells." Hear Res **299**: 63-78.
- Kim, D. K., Y. Park, S. A. Back, H. L. Kim, H. E. Park, K. H. Park, S. W. Yeo and S. N. Park (2014). "Protective effect of unilateral and bilateral ear plugs on noise-induced hearing loss: functional and morphological evaluation in animal model." Noise Health **16**(70): 149-156.
- Knipper, M., P. Van Dijk, I. Nunes, L. Ruttiger and U. Zimmermann (2013). "Advances in the neurobiology of hearing disorders: recent developments regarding the basis of tinnitus and hyperacusis." Prog Neurobiol **111**: 17-33.
- Knipper, M., C. Zinn, H. Maier, M. Praetorius, K. Rohbock, I. Kopschall and U. Zimmermann (2000). "Thyroid hormone deficiency before the onset of hearing causes irreversible damage to peripheral and central auditory systems." J Neurophysiol **83**(5): 3101-3112.
- Knipper, M., C. Zinn, H. Maier, M. Praetorius, K. Rohbock, I. Köpschall and U. Zimmermann (2000). "Thyroid hormone deficiency before the onset of hearing causes irreversible damage to peripheral and central auditory systems." J Neurophysiol **83**(5): 3101-3112.
- Kobel, M., C. G. Le Prell, J. Liu, J. W. Hawks and J. Bao (2017). "Noise-induced cochlear synaptopathy: Past findings and future studies." Hear Res **349**: 148-154.

- Korte, S. M., S. F. de Boer, E. R. de Kloet and B. Bohus (1995). "Anxiolytic-like effects of selective mineralocorticoid and glucocorticoid antagonists on fear-enhanced behavior in the elevated plus-maze." Psychoneuroendocrinology **20**(4): 385-394.
- Kujawa, S. G. and M. C. Liberman (2006). "Acceleration of age-related hearing loss by early noise exposure: evidence of a missed youth." J Neurosci **26**(7): 2115-2123.
- Kujawa, S. G. and M. C. Liberman (2009). "Adding insult to injury: cochlear nerve degeneration after "temporary" noise-induced hearing loss." J Neurosci **29**(45): 14077-14085.
- Kurabi, A., E. M. Keithley, G. D. Housley, A. F. Ryan and A. C. Wong (2016). "Cellular mechanisms of noise-induced hearing loss." Hear Res.
- Le, T. N., L. V. Straatman, J. Lea and B. Westerberg (2017). "Current insights in noise-induced hearing loss: a literature review of the underlying mechanism, pathophysiology, asymmetry, and management options." J Otolaryngol Head Neck Surg **46**(1): 41.
- Lee, H. Y., D. K. Kim, Y. H. Park, W. W. Cha, G. J. Kim and S. H. Lee (2017). "Prognostic factors for profound sudden idiopathic sensorineural hearing loss: a multicenter retrospective study." Eur Arch Otorhinolaryngol **274**(1): 143-149.
- Lee, S. H., A. R. Lyu, S. A. Shin, S. H. Jeong, S. A. Lee, M. J. Park and Y. H. Park (2019). "Cochlear Glucocorticoid Receptor and Serum Corticosterone Expression in a Rodent Model of Noise-induced Hearing Loss: Comparison of Timing of Dexamethasone Administration." Sci Rep **9**(1): 12646.
- Liberman, M. C. (1978). "Auditory-nerve response from cats raised in a low-noise chamber." J Acoust Soc Am **63**(2): 442-455.
- Liberman, M. C. (2017). "Noise-induced and age-related hearing loss: new perspectives and potential therapies." F1000Res **6**: 927.
- Liberman, M. C., M. J. Epstein, S. S. Cleveland, H. Wang and S. F. Maison (2016). "Toward a Differential Diagnosis of Hidden Hearing Loss in Humans." PLoS One **11**(9): e0162726.
- Ma, L., W. Li, S. Li, X. Wang and L. Qin (2017). "Effect of chronic restraint stress on inhibitory gating in the auditory cortex of rats." Stress **20**(3): 312-319.
- Malmierca, M. S. and M. Merchan (2004). The Rat Nervous System (Third Edition).
- Malmierca, M. S., M. A. Merchan, C. K. Henkel and D. L. Oliver (2002). "Direct projections from cochlear nuclear complex to auditory thalamus in the rat." J Neurosci **22**(24): 10891-10897.
- Mathers, C., D. M. Fat, J. T. Boerma and World Health Organization. (2008). The global burden of disease : 2004 update. Geneva, Switzerland, World Health Organization.
- Matthews, G. and P. Fuchs (2010). "The diverse roles of ribbon synapses in sensory neurotransmission." Nat Rev Neurosci **11**(12): 812-822.
- McLean, W. J., K. A. Smith, E. Glowatzki and S. J. Pyott (2009). "Distribution of the Na,K-ATPase alpha subunit in the rat spiral ganglion and organ of corti." J Assoc Res Otolaryngol **10**(1): 37-49.

Meltser, I. and B. Canlon (2011). "Protecting the auditory system with glucocorticoids." Hear Res **281**(1-2): 47-55.

Mifsud, K. R. and J. M. Reul (2016). "Acute stress enhances heterodimerization and binding of corticosteroid receptors at glucocorticoid target genes in the hippocampus." Proc Natl Acad Sci U S A **113**(40): 11336-11341.

Mosges, R., J. Koberlein, B. Erdtracht and R. Klingel (2008). "Quality of life in patients with idiopathic sudden hearing loss: comparison of different therapies using the Medical Outcome Short Form (36) Health Survey questionnaire." Otol Neurotol **29**(6): 769-775.

Muller, M. (1991). "Frequency representation in the rat cochlea." Hear Res **51**(2): 247-254.

Muller, M., M. Tisch, H. Maier and H. Lowenheim (2017). "Reduction of permanent hearing loss by local glucocorticoid application : Guinea pigs with acute acoustic trauma." HNO **65**(Suppl 1): 59-67.

Nadol, J. B., Jr. (1993). "Hearing loss." N Engl J Med **329**(15): 1092-1102.

Nelson, D. I., R. Y. Nelson, M. Concha-Barrientos and M. Fingerhut (2005). "The global burden of occupational noise-induced hearing loss." American Journal of Industrial Medicine **48**(6): 446-458.

Neufeld, A., B. D. Westerberg, S. Nabi, G. Bryce and Y. Bureau (2011). "Prospective, randomized controlled assessment of the short- and long-term efficacy of a hearing conservation education program in Canadian elementary school children." Laryngoscope **121**(1): 176-181.

Niedermeier, K., S. Braun, C. Fauser, J. Kiefer, R. K. Straubinger and T. Stark (2012). "A safety evaluation of dexamethasone-releasing cochlear implants: comparative study on the risk of otogenic meningitis after implantation." Acta Otolaryngol **132**(12): 1252-1260.

Nishi, M., H. Ogawa, T. Ito, K. I. Matsuda and M. Kawata (2001). "Dynamic changes in subcellular localization of mineralocorticoid receptor in living cells: in comparison with glucocorticoid receptor using dual-color labeling with green fluorescent protein spectral variants." Mol Endocrinol **15**(7): 1077-1092.

Nordmann, A. S., B. A. Bohne and G. W. Harding (2000). "Histopathological differences between temporary and permanent threshold shift." Hear Res **139**(1-2): 13-30.

O'Leary, S. J., P. Monksfield, G. Kel, T. Connolly, M. A. Souter, A. Chang, P. Marovic, J. S. O'Leary, R. Richardson and H. Eastwood (2013). "Relations between cochlear histopathology and hearing loss in experimental cochlear implantation." Hear Res **298**: 27-35.

Pascual-Le Tallec, L. and M. Lombes (2005). "The mineralocorticoid receptor: a journey exploring its diversity and specificity of action." Mol Endocrinol **19**(9): 2211-2221.

Pérez, M. A., C. Pérez-Valenzuela, F. Rojas-Thomas, J. Ahumada, M. Fuenzalida and A. Dagnino-Subiabre (2013). "Repeated restraint stress impairs auditory attention and GABAergic synaptic efficacy in the rat auditory cortex." Neuroscience **246**: 94-107.

Peter Dallos, A. N. P., Richard R. Fay (1996). "The Cochlea."

- Rance, G. and A. Starr (2015). "Pathophysiological mechanisms and functional hearing consequences of auditory neuropathy." Brain **138**(Pt 11): 3141-3158.
- Rarey, K. E., K. J. Gerhardt, L. M. Curtis and W. J. ten Cate (1995). "Effect of stress on cochlear glucocorticoid protein: acoustic stress." Hear Res **82**(2): 135-138.
- Reul, J. M. and E. R. de Kloet (1985). "Two receptor systems for corticosterone in rat brain: microdistribution and differential occupation." Endocrinology **117**(6): 2505-2511.
- Robertson, D. (1983). "Functional significance of dendritic swelling after loud sounds in the guinea pig cochlea." Hear Res **9**(3): 263-278.
- Roosendaal, B., Q. K. Griffith, J. Buranday, D. J. De Quervain and J. L. McGaugh (2003). "The hippocampus mediates glucocorticoid-induced impairment of spatial memory retrieval: dependence on the basolateral amygdala." Proc Natl Acad Sci U S A **100**(3): 1328-1333.
- Rüttiger, L., W. Singer, R. Panford-Walsh, M. Matsumoto, S. C. Lee, A. Zuccotti, U. Zimmermann, M. Jaumann, K. Rohbock, H. Xiong and M. Knipper (2013). "The reduced cochlear output and the failure to adapt the central auditory response causes tinnitus in noise exposed rats." PLoS One **8**(3): e57247.
- Rüttiger, L., W. Singer, R. Panford-Walsh, M. Matsumoto, S. C. Lee, A. Zuccotti, U. Zimmermann, M. Jaumann, K. Rohbock, H. Xiong and M. Knipper (2013). "The reduced cochlear output and the failure to adapt the central auditory response causes tinnitus in noise exposed rats." PLoS One **8**(3): e57247.
- Sachs, M. B. and P. J. Abbas (1974). "Rate versus level functions for auditory-nerve fibers in cats: tone-burst stimuli." J Acoust Soc Am **56**(6): 1835-1847.
- Savory, J. G., G. G. Prefontaine, C. Lamprecht, M. Liao, R. F. Walther, Y. A. Lefebvre and R. J. Hache (2001). "Glucocorticoid receptor homodimers and glucocorticoid-mineralocorticoid receptor heterodimers form in the cytoplasm through alternative dimerization interfaces." Mol Cell Biol **21**(3): 781-793.
- Schmiedt, R. A., J. H. Mills and F. A. Boettcher (1996). "Age-related loss of activity of auditory-nerve fibers." J Neurophysiol **76**(4): 2799-2803.
- Schmitt, C., M. Patak and B. Kroner-Herwig (2000). "Stress and the onset of sudden hearing loss and tinnitus." Int Tinnitus J **6**(1): 41-49.
- Sergeyenko, Y., K. Lall, M. C. Liberman and S. G. Kujawa (2013). "Age-related cochlear synaptopathy: an early-onset contributor to auditory functional decline." J Neurosci **33**(34): 13686-13694.
- Sha, S. H. and J. Schacht (2017). "Emerging therapeutic interventions against noise-induced hearing loss." Expert Opin Investig Drugs **26**(1): 85-96.
- Sheriff, M. J., B. Dantzer, B. Delehanty, R. Palme and R. Boonstra (2011). "Measuring stress in wildlife: techniques for quantifying glucocorticoids." Oecologia **166**(4): 869-887.
- Shi, L., Y. Chang, X. Li, S. Aiken, L. Liu and J. Wang (2016). "Cochlear Synaptopathy and Noise-Induced Hidden Hearing Loss." Neural Plast **2016**: 6143164.



Shield, B. (2006). "Evaluation of the social and economic costs of hearing impairment." Hear-it AISBL.

Singer, W., H. S. Geisler, R. Panford-Walsh and M. Knipper (2016). "Detection of Excitatory and Inhibitory Synapses in the Auditory System Using Fluorescence Immunohistochemistry and High-Resolution Fluorescence Microscopy." Methods Mol Biol **1427**: 263-276.

Singer, W., K. Kasini, M. Manthey, P. Eckert, P. Armbruster, M. A. Vogt, M. Jaumann, M. Dotta, K. Yamahara, C. Harasztosi, U. Zimmermann, M. Knipper and L. Ruttiger (2018). "The glucocorticoid antagonist mifepristone attenuates sound-induced long-term deficits in auditory nerve response and central auditory processing in female rats." FASEB J: fj201701041RRR.

Singer, W., R. Panford-Walsh and M. Knipper (2014). "The function of BDNF in the adult auditory system." Neuropharmacology **76 Pt C**: 719-728.

Singer, W., A. Zuccotti, M. Jaumann, S. C. Lee, R. Panford-Walsh, H. Xiong, U. Zimmermann, C. Franz, H. S. Geisler, I. Kopschall, K. Rohbock, K. Varakina, S. Verpoorten, T. Reinbothe, T. Schimmang, L. Ruttiger and M. Knipper (2013). "Noise-induced inner hair cell ribbon loss disturbs central arc mobilization: a novel molecular paradigm for understanding tinnitus." Mol Neurobiol **47**(1): 261-279.

Spoendlin, H. (1971). "Primary structural changes in the organ of Corti after acoustic overstimulation." Acta Otolaryngol **71**(2): 166-176.

Suvorov, G., E. Denisov, V. Antipin, V. Kharitonov, J. Starck, I. Pyykkö and E. Toppila (2001). "Effects of peak levels and number of impulses to hearing among forge hammering workers." Appl Occup Environ Hyg **16**(8): 816-822.

Tahera, Y., I. Meltser, P. Johansson, Z. Bian, P. Stiernä, A. C. Hansson and B. Canlon (2006). "NF-kappaB mediated glucocorticoid response in the inner ear after acoustic trauma." J Neurosci Res **83**(6): 1066-1076.

Tahera, Y., I. Meltser, P. Johansson, A. C. Hansson and B. Canlon (2006). "Glucocorticoid receptor and nuclear factor-kappa B interactions in restraint stress-mediated protection against acoustic trauma." Endocrinology **147**(9): 4430-4437.

Tahera, Y., I. Meltser, P. Johansson, H. Salman and B. Canlon (2007). "Sound conditioning protects hearing by activating the hypothalamic-pituitary-adrenal axis." Neurobiol Dis **25**(1): 189-197.

Tan, J., L. Ruttiger, R. Panford-Walsh, W. Singer, H. Schulze, S. B. Kilian, S. Hadjab, U. Zimmermann, I. Kopschall, K. Rohbock and M. Knipper (2007). "Tinnitus behavior and hearing function correlate with the reciprocal expression patterns of BDNF and Arg3.1/arc in auditory neurons following acoustic trauma." Neuroscience **145**(2): 715-726.

Tasker, J. G. and J. P. Herman (2011). "Mechanisms of rapid glucocorticoid feedback inhibition of the hypothalamic-pituitary-adrenal axis." Stress **14**(4): 398-406.

Terakado, M., H. Kumagami and H. Takahashi (2011). "Distribution of glucocorticoid receptors and 11 beta-hydroxysteroid dehydrogenase isoforms in the rat inner ear." Hear Res **280**(1-2): 148-156.

- Tikka, C., J. H. Verbeek, E. Kateman, T. C. Morata, W. A. Dreschler and S. Ferrite (2017). "Interventions to prevent occupational noise-induced hearing loss." Cochrane Database Syst Rev **7**: CD006396.
- Trapp, T. and F. Holsboer (1996). "Heterodimerization between mineralocorticoid and glucocorticoid receptors increases the functional diversity of corticosteroid action." Trends Pharmacol Sci **17**(4): 145-149.
- Trune, D. R. and B. Canlon (2012). "Corticosteroid therapy for hearing and balance disorders." Anat Rec (Hoboken) **295**(11): 1928-1943.
- Trune, D. R. and J. B. Kempton (2009). "Blocking the glucocorticoid receptor with RU-486 does not prevent glucocorticoid control of autoimmune mouse hearing loss." Audiol Neurootol **14**(6): 423-431.
- Trune, D. R., J. B. Kempton and N. D. Gross (2006). "Mineralocorticoid receptor mediates glucocorticoid treatment effects in the autoimmune mouse ear." Hear Res **212**(1-2): 22-32.
- Viengchareun, S., D. Le Menuet, L. Martinerie, M. Munier, L. Pascual-Le Tallec and M. Lombes (2007). "The mineralocorticoid receptor: insights into its molecular and (patho)physiological biology." Nucl Recept Signal **5**: e012.
- Vio, M. M. and R. H. Holme (2005). "Hearing loss and tinnitus: 250 million people and a US\$10 billion potential market." Drug Discov Today **10**(19): 1263-1265.
- Wallhagen, M. I., W. J. Strawbridge, R. D. Cohen and G. A. Kaplan (1997). "An increasing prevalence of hearing impairment and associated risk factors over three decades of the Alameda County Study." Am J Public Health **87**(3): 440-442.
- Wang, Y. and M. C. Liberman (2002). "Restraint stress and protection from acoustic injury in mice." Hear Res **165**(1-2): 96-102.
- Waschke, B., Paulsen (2015). "Anatomie, das Lehrbuch." **1. edition.**
- WHO (2015). Global Health Estimates.
- Wichmann, C. and T. Moser (2015). "Relating structure and function of inner hair cell ribbon synapses." Cell Tissue Res **361**(1): 95-114.
- Wolf, O. T. (2009). "Stress and memory in humans: twelve years of progress?" Brain Res **1293**: 142-154.
- Wulsin, A. C., J. P. Herman and M. B. Solomon (2010). "Mifepristone decreases depression-like behavior and modulates neuroendocrine and central hypothalamic-pituitary-adrenocortical axis responsiveness to stress." Psychoneuroendocrinology **35**(7): 1100-1112.
- Yamane, H., Y. Nakai, M. Takayama, H. Iguchi, T. Nakagawa and A. Kojima (1995). "Appearance of free radicals in the guinea pig inner ear after noise-induced acoustic trauma." Eur Arch Otorhinolaryngol **252**(8): 504-508.
- Yamashita, D., H. Y. Jiang, J. Schacht and J. M. Miller (2004). "Delayed production of free radicals following noise exposure." Brain Res **1019**(1-2): 201-209.

- Yao, X. and K. E. Rarey (1996). "Localization of the mineralocorticoid receptor in rat cochlear tissue." Acta Otolaryngol **116**(3): 493-496.
- Yates, G. K. (1991). "Auditory-nerve spontaneous rates vary predictably with threshold." Hear Res **57**(1): 57-62.
- Yoshida, N. and M. C. Liberman (1999). "Stereociliary anomaly in the guinea pig: effects of hair bundle rotation on cochlear sensitivity." Hear Res **131**(1-2): 29-38.
- Young, E. A., J. Abelson and S. L. Lightman (2004). "Cortisol pulsatility and its role in stress regulation and health." Front Neuroendocrinol **25**(2): 69-76.
- Young, E. A., J. F. Lopez, V. Murphy-Weinberg, S. J. Watson and H. Akil (1998). "The role of mineralocorticoid receptors in hypothalamic-pituitary-adrenal axis regulation in humans." J Clin Endocrinol Metab **83**(9): 3339-3345.
- Zhu, X., R. D. Manning, Jr., D. Lu, C. E. Gomez-Sanchez, Y. Fu, L. A. Juncos and R. Liu (2011). "Aldosterone stimulates superoxide production in macula densa cells." Am J Physiol Renal Physiol **301**(3): F529-535.

## Publication list

### Publication in peer-reviewed journals

Singer, W,<sup>1</sup> Kasini, K,<sup>1</sup> Manthey, M,<sup>1</sup> Eckert, P,<sup>1</sup> Armbruster, P,<sup>1</sup> Vogt, M, Jaumann, M, Dotta, M, Yamahara, K, Harasztosi, C, Zimmermann, U, Knipper, M, Rüttiger, L (2018). The glucocorticoid antagonist mifepristone attenuates sound-induced long-term deficits in auditory nerve response and central auditory processing in female rats.

— *FASEB Journal*: 2018 Jun;32(6):3005-3019

<sup>1</sup> These authors contributed equally to this work.

### Oral presentations

Armbruster, P, Singer, W, Rüttiger, L, and Knipper, M.

Stress Hormone Induced Changes Of Auditory Function In The Rat. *Presentations and talks in Bad Liebenzell (Symposium Tübingen Hearing Research Centre, 2014), Rottenburg (Interdisziplinäres Zentrum für klinische Forschung, IZKF, 2015), Tübingen (Zentrum für Neurosensorik, ZfN, 2015)*

### Abstracts/Posters

1. Armbruster, P, Singer, W, Rüttiger, L, and Knipper, M. (2015)

Analysis of acute stress on long-term vulnerability after an acoustic injury in a mature rat model. *Meeting abstract and poster presentation of the annual conference of the German Neuroscience Society 2015 in Göttingen, Germany.*

2. Armbruster, P, Singer, W, Rüttiger, L, and Knipper, M. (2015)

Einfluss von Stresshormon auf das auditorische System der Ratte. *Meeting abstract and poster presentation of the annual conference of the German Society for ENT/Head-and-Neck Surgery (DGHNO) 2015 in Berlin, Germany.*

3. Armbruster, P, Singer, W, Rüttiger, L, and Knipper, M. (2015)

Einfluss von Stresshormon auf das auditorische System der Ratte. *Poster presentation and winner of the poster prize at the annual research colloquium of the Faculty of Medicine 2014 in Tübingen, Germany.*

## Danksagung

Mein Dank gilt all jenen, die mich auf meinem Weg unterstützt und zum guten Gelingen beigetragen haben.

Zuallererst möchte ich mich herzlich bei Frau Prof. Dr. Marlies Knipper für die Überlassung des Dissertationsthemas, die freundliche Aufnahme in ihre Arbeitsgruppe, die inspirierenden Gespräche und die fachliche und persönliche Unterstützung, insbesondere während des intensiven IZKF Promotionskollegs bedanken.

Weiterhin danke ich Frau Dr. Wibke Singer und Herrn PD Dr. Lukas Rüttiger für die einzigartige persönliche Betreuung und unermüdliche Unterstützung. Eure Einsatzbereitschaft, Motivation und Geduld suchen ihresgleichen! Ohne eure konstruktive Kritik, eure zahlreichen Tipps und die regelmäßigen „Laborküchentalks“ wäre diese Arbeit nicht möglich gewesen.

Danken möchte ich ebenfalls meinen Kollegen der Arbeitsgruppe. Frau Karin Rohbock danke ich für ihre Unterstützung bei der Präparation und die Aufbereitung der Cochleae. Ich danke Dr. Ulrike Zimmermann, Dr. Steffen Wolter, Dr. Dorit Möhrle, Dr. Lewis Lee, Dr. Dario Campanelli, Iris Köpschall, Hyun-Soon Geisler, Kerstin Just und Monika Gaus für die gute Zusammenarbeit, die herzliche Atmosphäre im Labor, aber auch die netten Kaffeepausen. Ihr habt meine Zeit im Labor zu etwas ganz Besonderem gemacht.

Außerhalb der Welt des Labors haben meine Freunde maßgeblich zum Gelingen dieser Arbeit beigetragen, indem sie für den nötigen Ausgleich und Ansporn gesorgt haben – auch dafür ein herzliches Dankeschön.

Zuletzt und ganz besonders möchte ich mich an dieser Stelle bei meiner Familie bedanken, die mich auf meinem bisherigen Lebensweg jederzeit und in jeder erdenklichen Form unterstützt hat. Insbesondere bei meinen Eltern und bei Antonia – auf eure Unterstützung konnte ich mich während der gesamten Arbeit verlassen. Ihr standet mir bei der Verwirklichung meiner Ziele stets zur Seite und ihr habt mich in den zehrenden Zeiten angespornt. Ohne euren starken Rückhalt, euer Verständnis, eure Motivation und eure moralische Unterstützung wäre all dies nicht möglich gewesen.

Danke!